THE MULTIPART COPOLYELECTROLYTE ADHESIVE SYSTEM OF THE SANDCASTLE WORM: THE BIOLOGICAL INSIGHTS FOR DEVELOPING A SYNTHETIC UNDERWATER ADHESIVE

by

Ching-Shuen Wang

A dissertation submitted to the faculty of
The University of Utah
in partial fulfillment of the requirements for the degree of

Doctor of Philosophy

Department of Bioengineering

The University of Utah

May 2015

The University of Utah Graduate School

STATEMENT OF DISSERTATION APPROVAL

The dissertation of **Ching-Shuen Wang**

has been approved by the following supervisory committee members:

Russell J. Stewart	, Chair	**12/04/2014** Date Approved
Kenneth L. DeVries	, Member	**12/04/2014** Date Approved
Vladimir Hlady	, Member	**12/04/2014** Date Approved
Gregory A. Clark	, Member	**12/04/2014** Date Approved
Grzegorz Bulaj	, Member	Date Approved

and by **Patrick Tresco** , Chair/Dean of

the Department/College/School of **Bioengineering**

and by David B. Kieda, Dean of The Graduate School.

ABSTRACT

Marine Sandcastle worms, *Phragmatopoma californica*, are tube-building sabellariid polychaetes that inhabit the western coast of North American. Sabellariidae have major impacts on the geology and ecology of shorelines. Individual worms build protective tubular shelters by gluing together mineralized materials with a proteinaceous adhesive. The adhesive is the product of at least four distinct secretory cell types, the contents of which are co-secreted from the building organ during tube construction. Prominent hetereogeneous granules contain dense subgranules of Mg and two polyacidic (polyphospho)proteins Pc3A and B, as well as at least two polybasic proteins, Pc1 and Pc4. Equally prominent homogeneous granules comprise at least two polybasic proteins, Pc2 and Pc5, and a sulfated polysaccharide. These distinct sets of oppositely charged components are segregated and packaged into dense secretory granules by electrostatic condensation. Both types of adhesive granules contain latent catechol oxidase, pre-primed with oxygen in the active site. After secretion, activated catechol oxidase ensures rapid and spatially homogeneous oxidative crosslinking of L-DOPA of Pc 1 and 2 proteins with limited mixing of the preassembled adhesive packets. Environmental pH changes also rapidly solidify of multipart polyelectrolytic of sandcastle worm adhesive due to formation of polyphosphoprotein Pc3 and Mg complex. The end result is tough and resilient underwater bonds formed with an energy-dissipating, water-filled adhesive

foam. The natural adhesive has been a valuable model for development of synthetic adhesives for underwater bonding applications, including medical adhesives.

TABLE OF CONTENTS

LIST OF FIGURES

ACKNOWLEDGEMENTS

I would like express my gratitude to my advisor, Dr. Russell Stewart, for giving me a chance to be involved in this project, and always guiding me in the right direction during my academic years. Without his kindly support, I am not confident I would have finished this project in a few years. I am glad that I have learned a lot from Dr. Stewart in many ways, especially his passion and intelligence about scientific research.

Besides my advisor, I would like to thank my committee members, Dr. Vladimir Hlady, Dr. K. Larry DeVries, Dr. Gregory Clark and Dr. Grzegorz Bulaj for helpful suggestions on each meeting and offering insights on this project. I also like to express my thanks to a previous lab colleague, Kelli Svenson for her excellent contribution to this project and helping me with academic writing. I would like to thank undergraduate students, Alicia Watkins and Peter Millson's assistants in this project.

In addition, I would like to thank lab members, Dr. Hui Shao, Dr. Huaizhong Pan, Dr. Mahika Weerasekare, Dr. Sarbjit Kaur, Monika Sima and Nicholas Ashton
for giving feedback about my research during regular lab meetings.

At last, I would like to share my happiness and honor with my wife, Yinshen Wee, who always stands by my side, and gives me courage when I am frustrated with my research.

CHAPTER 1

INTRODUCTION

1.1 The increasing need for developing wet medical adhesive

Adhesives are important to all areas in our daily life including airplane construction, car assembly, books, food packaging and medical applications. It is hard to imagine a world without adhesive. Besides nonmedical use adhesives, there is an increasing trend of research focus on developing medical adhesives that can be applied externally or internally to repair damaged tissues. According to a GIA (Global Industry Analyst, Inc) report on the medical adhesives market in the US, the needs of medical adhesive grow rapidly each year, and counting for the steady growth of aging population worldwide, the expected market size might be underestimated.

Despite the heavy use of adhesive in industrial applications, biomedical applications seem limited to several natural or polymer based adhesives. The use of medical adhesive is difficult to track back into human history due to extensive use of plant polysaccharides as gluing materials found in many cultures thousands of years ago. Natural based adhesives, for example, casein from milk, latex rubber, tree gum, starch and fibrinogen from animal have been developed and some of them were commercialized awhile ago. So far, none of them has been optimized as a "medical" grade adhesive due to low bonding strength, toxicity, immunogenic and most importantly

most of them do not provide good adhesion ability to wet surfaces.[7] It is fair to mention that there are only a few choices in the present market qualified as medical adhesives.

There are few examples of mechanical fasteners in the animal kingdom. Instead, nature has relied on biopolymeric adhesives rather than rivets, nails, staples, screws, or sutures. A couple 1000 million years of tinkering have produced numerous examples of marvelously adapted adhesives. The manufacture of human artifacts it seems is going the way of nature. Since the advent of synthetic polymeric adhesives around the middle of the last century, mechanical fasteners have been increasingly replaced with glue in everything from airplanes fuselages to apartment buildings. In a convergence of sorts, one of the leading edges of adhesives research is the development of new synthetic adhesives by copying natural adhesives. A good example of this approach was the characterization of the biological structures and physical chemical principles that allow some lizards to walk across smooth ceilings and then mimicking those features in a synthetic material—so-called gecko tape. Other examples are the adhesives with which sessile marine invertebrates, like barnacles and mussels, anchor themselves to wet rocks or other substrates.[1-6] Although detailed questions remain, important general features of the bonding mechanisms of these adhesives have been described and copied into "bioinspired" materials.

1.2 Sandcastle worm as a potential study model for developing underwater adhesive

The sandcastle worm *Phragmatopoma Californica* (family *Sabellaridídae),* lived in the intertidal zone of the ocean that suffers strong tides all the time. The

description of a *P. californica* colony from the original classification by Fewkes (Fewkes, 1889) provides a sense of the turbulent habitats preferentially inhabited by sabellariids. The tubular cemented tubes were jointed together with an individual worm, eventually forming a honeycomb like structure along the seashore from a few meters to kilometers. In an early stage, the juvenile is induced by unknown chemicals of existing tube to develop mature adhesive gland for metamorphosis (Fig 1.1 A). In order to provide a safe shelter for living, worms must adapt to the environment with a specialized ability to construct a tubular cemented shelter against strong waves with biological glue. The worm secretes several dabs of proteinaceous glue to join the particles to the anterior end of the existing tube. When an anterior part of the tube was damaged or removed, the worm will gather floating minerals or particles to rebuild the lost portion of the tube (Figure 1.1B-C). In a previous video recording of over 10 worms reconstructing their tubes, gluing a new particle to the existing tube took less than 30s on average.[9]

The cement is an important model for biomimetic adhesives because of its apparent toughness, it adheres strongly to a variety of materials, and it bonds rapidly to these materials in seawater. The idea of using principles or materials derived from natural adhesives produced by sessile marine organisms in medicine is not new.[43] The most studied of these marine adhesives are produced by mussels who meet the challenge of staying put in a high energy ocean environment by gluing themselves to stationary wet substrates. Mussels attach collagenous threads to solid surfaces with a collection of unique proteins assembled into an adhesive plaque through a spatially and temporally orchestrated process.[13] It is difficult to reconstruct some of the critical features of the highly organized mussel adhesive *in vitro*. The *P. californica* adhesive, in contrast, has

been adapted for the comparatively simple task of gluing two similar and external mineral substrates together. Correspondingly, its glue appears to be less structurally organized, likely requires less sophisticated biological processing, and may therefore be an excellent model for clinically practical adhesives based on complex coacervation.

1.3 Gradient foam structure of worm glue reveals mechanical advantages

A closer evaluation of the secreted glue with optical microscopy revealed an interesting structure at microscale. The secreted adhesive is a solid, inhomogeneous porous structure with autofluorescent property over a broad range of wavelength (Figure 1.2A). Autofluorescent analysis of secreted glue with confocal microscopy suggests that the volume of each secreted dab of glue is ~100 pL and average porosity is ~25%. Interestingly, the pores in the adhesive are a steep gradient structure,[9] ranging from 50% in the center of the glue to nearly zero on the outside of the glue that contact with the substrate (Figure 1.2B). The gradient porous glue structure could provide mechanical advantages in the intertidal zone. The pores in the adhesive would perform like foam packing material, absorbing and dissipating the energy of the strong waves. Moreover, studies of the stress distribution on the adhesive joint under tensile or shear stress suggest maximum stresses occur at the edges of the joint. The observation could be used to explain why the sandcastle worm creates a gradient foamy structure where the stress load to the edges of the joint are maximal and the load on the most porous center are minimal. The mechanisms by which *P. californica* produces adhesive bonds with a gradient foam structure is of considerable technological interest. The benefits to the worm may also be

of advantage to human adhesive technologists if the mechanisms can be deciphered and effectively copied.

1.4 The bonding chemistry of worm glue

If examined closely, the tube of the sandcastle worm is composed of varying substrates including sands, seashells and other minerals. This suggests worm adhesive has multiple mechanisms bonding to substrates. Previous findings suggest proteins are the major component of the sandcastle worm bioadhesive.[8,10-11] Three highly repetitive proteins Pc1-3 were identified from the worm glue (Figure 1.3). Pc-1 is a basic (PIs >9) and highly sequence redundant protein that is comprised mostly of three residues, glycine (45 mol%), lysine (14 mol%), and tyrosine (19 mol%). Fifteen repetitive sequences are VGGYGYGGKK. Pc-2 is a basic protein (PIs >9) that has several degenerate copies of the sequence HPAVHKALGGYG. Pc-3 proteins are comprised of a distinct set of serine rich variants that contain a series of 4-13 serine (S) punctuated. Another important feature of glue adhesion chemistry is the posttranslational modification of tyrosine to DOPA (dihydroxy-L-phenylalanine). DOPA is an important player in interfacial adhesion by providing functions either in chelating with metal ions or generating oxidized dopaquinone that can rapidly react with nucleophilic sidechains.[16-18] For example, mussel mfp 4-6 contains 2 to 30 mol% of DOPA, which are shown to bind to the titanium oxide surface with strong dissociation energy (22 kcal/mol).[15] Similar to mussel proteins, ~1/3 of ~10 mol% of tyrosine residues of *P. Californica* glue proteins are modified to DOPA. So far, Pc1 and Pc2 proteins were identified as dopa-containing proteins.[11] Presumably, DOPA in sandcastle worm glue plays a similar role. Additional evidence can be found in

color changes of worm glue over time from milky white color to reddish brown, which is consistent with quinonic crosslinking.

In summary, several key bonding factors were identified in the sandcastle worm glue, for example, highly negative charged polyphosphate Pc3 proteins likely bond to calcareous minerals such as sea shells through electrostatic interactions. This bonding mechanism seems true for phosphoserine-rich proteins. For example, egg protein phosvitin can chelate calcium, forming an aggregation.[42] Almost all calcium binding proteins (osteopontin, sialoprotein, phosphophporyn and etc.) contain high mole% of phosphorylated serine and can regulate the transportation and absorption of divalent cations in animals.[19-21] Like caseins, contain more than 10 mol% of phosphoserine, were used as dry or wet glue for a few decades from glue painting to glassware labeling.[23] In contrast to phosphoserine, proteins with basic sidechains could also contribute bonding to anionic mineralized surfaces. There are at least 16 identified putative glue proteins that have pI value larger than seawater 8.2, suggesting their importance in adhesion. The post-translational modification mechanism of tyrosine residues to DOPA might also provide another bonding mechanism, as an unoxidized DOPA sidechain can displace water, forming a strong bond with metal oxide surfaces.[24-25] It is surprising that DOPA identified in worm adhesive is an unoxidized form, suggesting that strong adsorption is an important mechanism. In addition to identified worm glue composition, the concentration of elements in sandcastle worm adhesive was determined by elemental analysis when compared to background of seawater.[8] Phosphorous, calcium and magnesium were the most abundant elements relative to sea water. Other elements such as S, Fe, Mn, Ni, Cu and Zn, though were relatively low compared to the other elements.

However, they are still several orders of magnitude compared to seawater, implying potential roles maintaining in adhesive protein structure or mediating bonding mechanisms (Figure 1.4).

1.5 Glue setting and curing mechanism

The worm glue setting must be controlled to prevent premature hardening while allowing rapid bonding following secretion. Hardening occurs in two stages. The first stage is a rapid insolubilization reaction that allows the worm to let go of particles in less than 30 s. The second stage, curing, proceeds over several hours through oxidative DOPA crosslinking.

At least part of the trigger mechanism must be the change from pH 5 in secretory vesicles to pH 8.2 in seawater. Calculating the net charge as a function of pH of all the glue components reveals several interesting features (Figure 1.5). The net charge of the glue switches from net positive to strongly net negative between the pH of secretory granules (~5) and seawater (~8.2). The phosphate sidechains go from a single to a double negative charge and would become highly extended without additional charge shielding. The histidine sidechains change from positive to neutral.

The pH jump could drive several chemical events. First, changes in interactions between charged glue components could lead to phase changes responsible for the rapid initial set: from colloidal PECs into a liquid complex coacervate into an insoluble crosslinked solid. The insolubilization reaction could be driven in part by changes in the interactions between Ca^{2+} /Mg^{2+} and the phosphoserines of Pc3. The solubility of Ca^{2+} /Mg^{2+} with $H_xPO_4^{2-}$ is much lower at elevated pH. Second, both the rate of DOPA

oxidation to dopaquinone and the subsequent crosslinking reaction with nucleophilic sidechains increase dramatically at the elevated pH of seawater because deprotonated DOPA (pK_1 9.3) is more prone to oxidation to dopaquinone, and cys (pK 8.0), his (pK 6.0) and lysine (pK 10.3) are strong nucleophiles when deprotonated.

1.6 A comprehensive study of the glue secretion system will be crucial to the success of creating an ideal synthetic underwater adhesive

It will be interesting to note that there are two distinct types of secretory granules ("homogeneous" and "heterogeneous" defined by morphology) that were identified abundantly in the adhesive gland (Figure 1.6) with differential interference contrast (DIC) imaging. Some (heterogenous) contain birefringent material and others (homogeneous) have a uniform appearance. The presence of at least two granule subpopulations raises interesting and critical questions about adhesive disk formation: How are the glue proteins distributed between the granule types? Does mixing of binary components during secretion contribute to the setting and curing reations? How are the divalent cations (Mg^{2+}/Ca^{2+}) that are abundant in the secreted adhesive distribut between the granule types? Identifying the components of individual granules from both types will be a big step toward answering these questions.

To date, our understanding of key bonding factors was sufficient to make synthetic adhesive by copying known features of glue protein chemistry. However, to further optimize the bond strength, the mechanism of adhesive setting, and the crosslinking mechanism of the synthetic adhesive, more efforts will be needed by studying how the animal glue proteins are stored and packed in these two types of

secretory vesicles, how glue proteins are transported for secretion, how glue proteins mix prior to setting, how glue proteins are transformed in different pH environments, and how glue proteins harden.

Answering all these questions will definitely guide us to develop an ideal and optimal synthetic adhesive by copying these important features and mechanism of glue chemistry. The innovation of this project is to investigate the biological processing mechanisms of the bioadhesive. Addressing these questions fully will gain valuable insights for developing long shelf-life, self-initiating, waterborne adhesives for medical applications.

Several important features of natural worm glue process listed below will be innovative to guide us to create an ideal and optimized synthetic adhesive for medical use in the future.

1) A synthetic version of adhesive that is composed of two or more oppositely charged synthetic polyelectrolytes that mimic the key sidechain functionalities of the glue proteins. For example, the acidic and basic proteins, Pc3 and Pc2, for example, can be copied to a degradable polymer backbone containing phosphate and amine sidechains, respectively. The charged monomers can be further copolymerized with dopamine to add DOPA functionality.

2) Multiple bonding mechanisms of worm glue to metal surfaces can be adapted to create a medical adhesive for bone repair. The acid and basic copolymers will both associate with hydroxyapatite (HAP) through ionic and electrostatic bonds. Dopamine, oxidized to the quinone, will covalently couple to nucleophilic sidechains of bone matrix proteins to create robust interfacial bonds. Furthermore,

the cohesive solid (not a brittle hydrogel) that should have dimensional stability, considerable compressive strength, and sufficient shear strength.

3) There is a pH triggering mechanism for glue setting and curing. The controlled pH triggered from acidic vesicle to physiological environment insolubilize the glue components. The same concept can be applied to the synthetic adhesive that allows accurate alignment of bone fragments before hardening. Insolublization of PECs will provide the first stage set, followed by dopaquinone mediated covalent crosslinking. No external energy source is needed to initiate curing.

4) The transient formation of opposite charged proteins will initially allow viscosity and interfacial tension that allow worms to position the glue on the substrates. The same concept can be used for the synthetic adhesive to allow injection with a syringe into fractures. The viscosity of a stable colloidal suspension of polyelectrolyte complexes (PECs) has a lower viscosity than a solution with a comparable concentration of soluble entangled polymers.

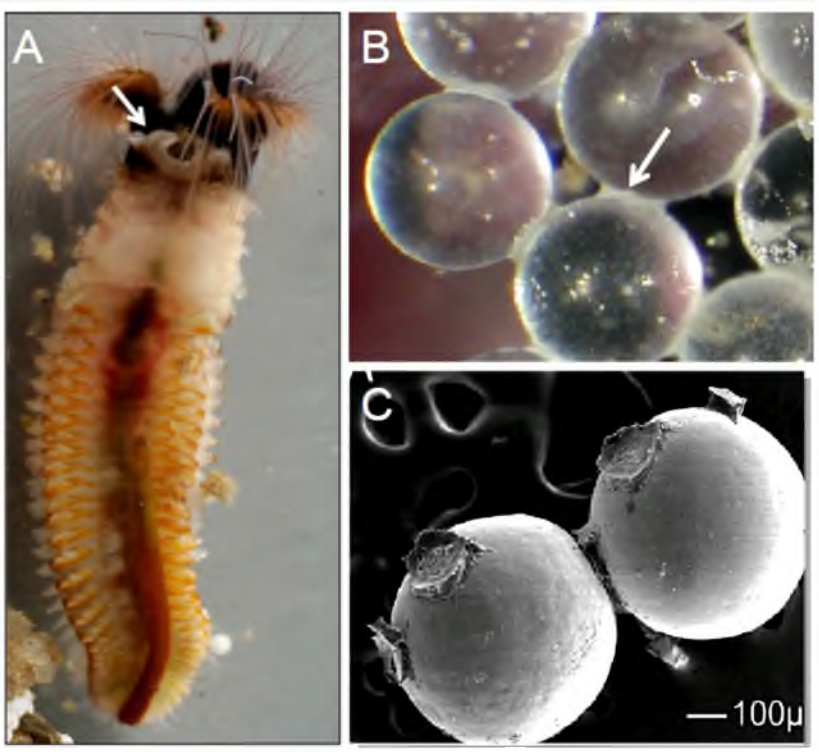

Figure 1.1. Sandcastle worm *Phragmatopoma californica* and its glue. (A) Sandcastle worm morphology. Arrow indicates building organ of sandcastle worm. (B) Glass beads glued by sandcastle worm. Arrow indicates secreted glue. (C) SEM examination of two glued glass beads.[8] Figure was adapted with permission from Stewart, Russell J., et al. "The tube cement of *Phragmatopoma californica*: a solid foam." *Journal of Experimental Biology* 207.26 (2004): 4727-4734. Copyright (2004) American Chemical Society.

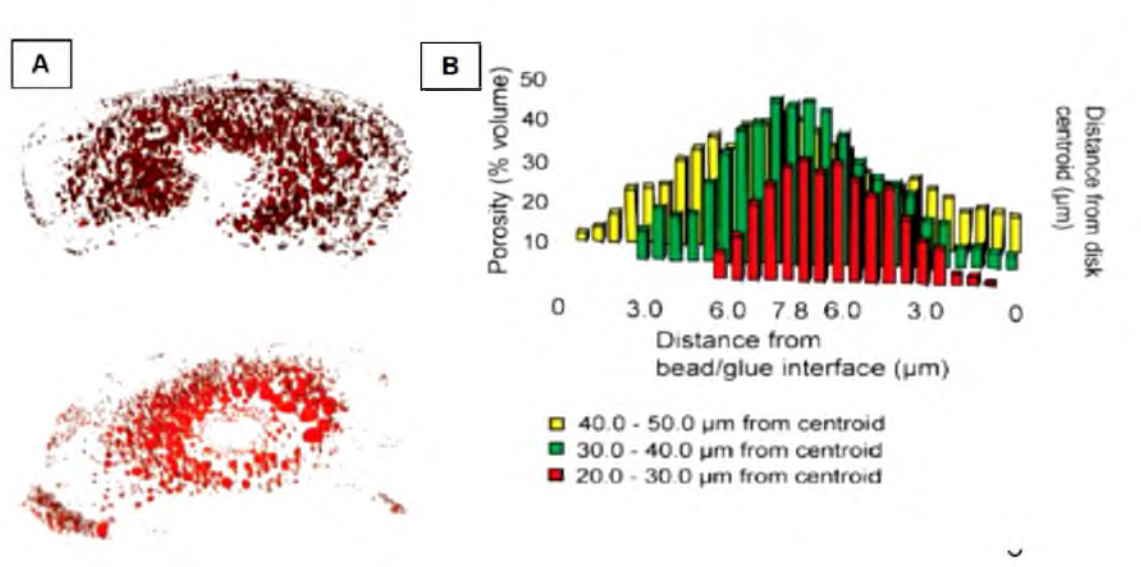

Figure 1.2. The gradient foam structure of worm adhesive. (A) Porous volume of two representative glue disks rendered in three dimensions by reconstructing laser scanning confocal microscopy optical sections. The nearly solid edges and higher porous central regions are evident. (B) Porosity varies as a function of distance from the glue/bead interface and as a function of radial distance (*r*) from the centroid. For clarity error bars were not added to the bar graph; errors in all cases were less than 10%.[9] Figure was adapted with permission from Stevens, Mark J., et al. "Multiscale structure of the underwater adhesive of *Phragmatopoma californica*: a nanostructured latex with a steep microporosity gradient." *Langmuir* 23.9 (2007): 5045-5049. Copyright (2007) American Chemical Society.

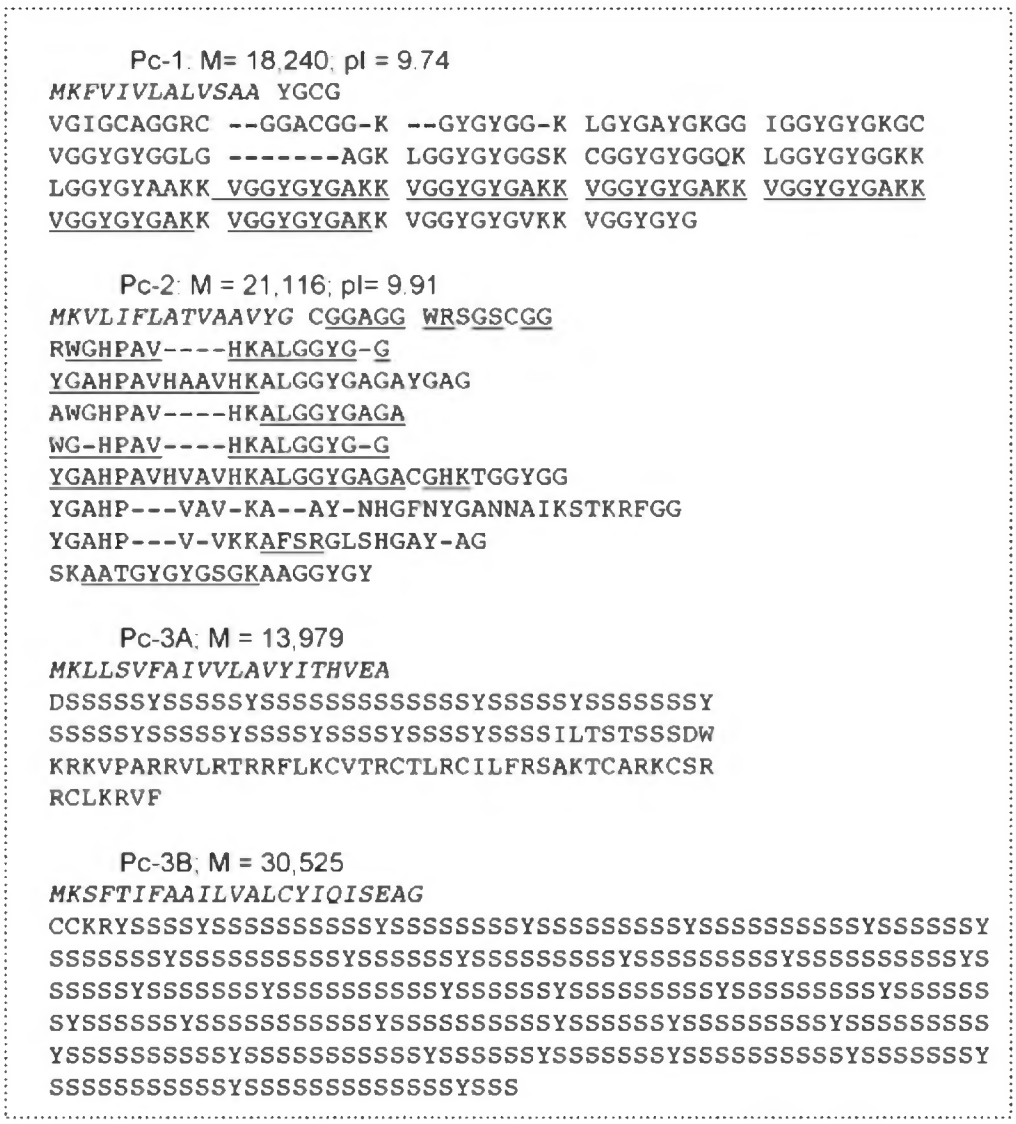

Figure 1.3. The protein sequence of glue proteins Pc1-3. The pI value of Pc3 proteins were much lower than predicted due to high phosphorylated serine content (pI < 2) with single tyrosines. Moreover, it was estimated that ~ 95% of the Ser was in the form of -pSer. Therefore, the overall pI value of Pc3 will be extremely acidic (pI ~2).

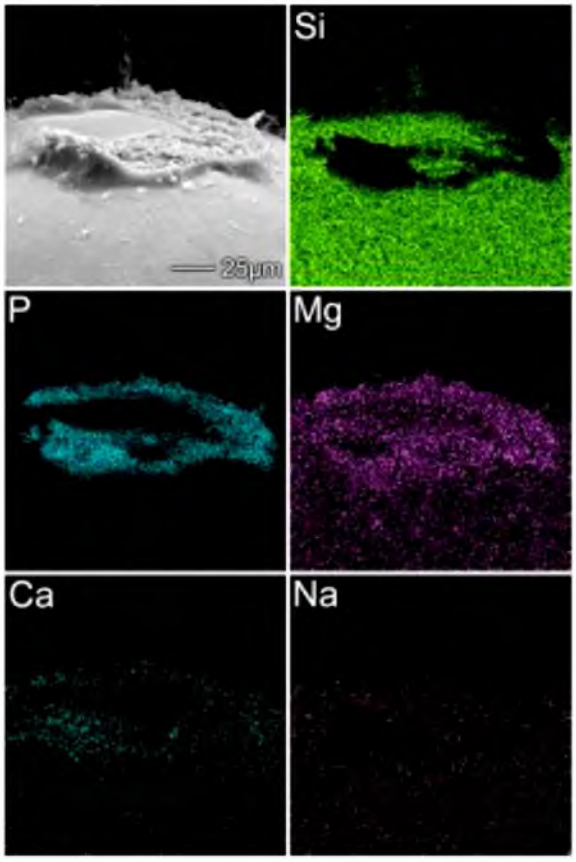

Figure 1.4. SEM and EDS spatial maps of a glue disk washed with deionized water. Scale bar, 25μm.[8] Figure was adapted with permission from Stewart, Russell J., et al. "The tube cement of *Phragmatopoma californica*: a solid foam." *Journal of Experimental Biology* 207.26 (2004): 4727-4734.

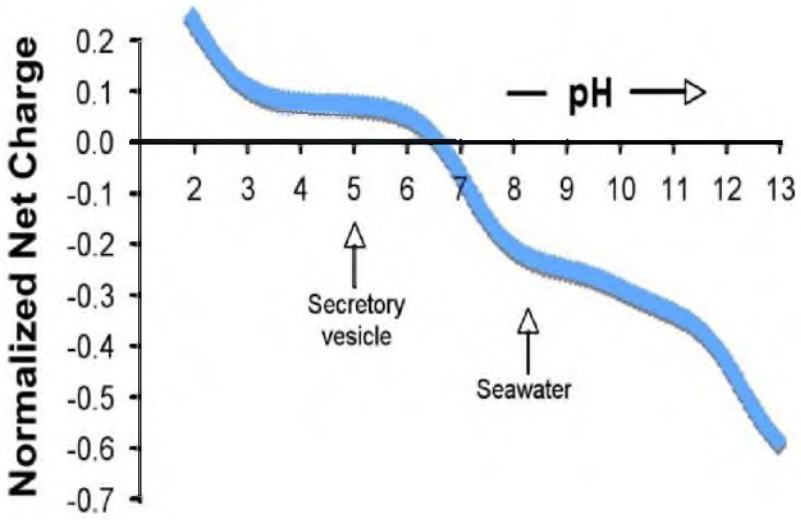

Figure 1.5. Normalized net charge of the glue components as a function of pH. A major transition occurs between the pH of secretory vesicles and seawater due primarily to the poly-L-phosphoserines of Pc3s.

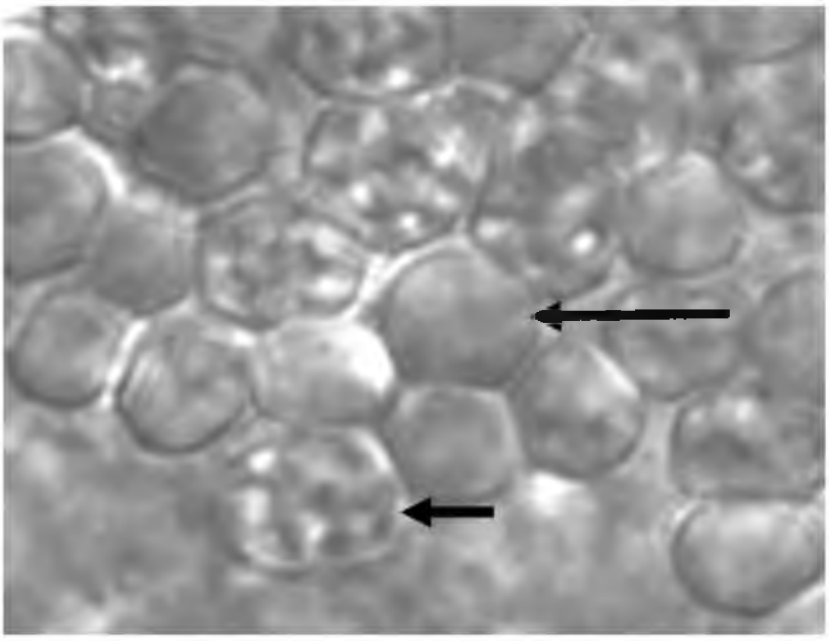

Figure 1.6. *P. californica* secretory granules. DIC imaging. Short arrow: birefringent heterogeneous granule. Long arrow: homogeneous granule.

1.7 References

(1) Aksak, Burak, Michael P. Murphy, and Metin Sitti. "Adhesion of biologically inspired vertical and angled polymer microfiber arrays." *Langmuir* 23, no. 6 (2007): 3322-3332.

(2) Geim, A. K., S. V. Dubonos, I. V. Grigorieva, K. S. Novoselov, A. A. Zhukov, and S. Yu Shapoval. "Microfabricated adhesive mimicking gecko foot-hair." *Nature Materials* 2, no. 7 (2003): 461-463.

(3) Waite, J. Herbert. "Adhesion a la moule." *Integrative and Comparative Biology* 42, no. 6 (2002): 1172-1180.

(4) Lee, Haeshin, Shara M. Dellatore, William M. Miller, and Phillip B. Messersmith. "Mussel-inspired surface chemistry for multifunctional coatings." *Science* 318, no. 5849 (2007): 426-430.

(5) Lee, Haeshin, Bruce P. Lee, and Phillip B. Messersmith. "A reversible wet/dry adhesive inspired by mussels and geckos." *Nature* 448, no. 7151 (2007): 338-341.

(6) Nakano, Masahiro, Jian-Ren Shen, and Kei Kamino. "Self-assembling peptide inspired by a barnacle underwater adhesive protein." *Biomacromolecules* 8, no. 6 (2007): 1830-1835.

(7) Blume, Jessica, and Willi Schwotzer. *Medical products and their application range*. Vienna: Springer, 2010.

(8) Wang, Ching Shuen, Kelli K. Svendsen, and Russell J. Stewart. *Morphology of the adhesive system in the sandcastle worm,* Phragmatopoma californica. Vienna: Springer, 2010.

(9) Stevens, Mark J., Rebekah E. Steren, Vladimir Hlady, and Russell J. Stewart. "Multiscale structure of the underwater adhesive of *Phragmatopoma californica*: a nanostructured latex with a steep microporosity gradient." *Langmuir* 23, no. 9 (2007): 5045-5049.

(10) Jensen, Rebecca A., and Daniel E. Morse. "The bioadhesive of *Phragmatopoma californica* tubes: a silk-like cement containingL-DOPA."*Journal of Comparative Physiology B* 158, no. 3 (1988): 317-324.

(11) Waite, J. Herbert, Rebecca A. Jensen, and Daniel E. Morse. "Cement precursor proteins of the reef-building polychaete *Phragmatopoma californica* (Fewkes)." *Biochemistry* 31, no. 25 (1992): 5733-5738.

(12) Endrizzi, Betsy J., and Russell J. Stewart. "Glueomics: an expression survey of the adhesive gland of the sandcastle worm." *The Journal of Adhesion* 85, no. 8 (2009): 546-559.

(13) Waite, J. Herbert, Niels Holten Andersen, Scott Jewhurst, and Chengjun Sun. "Mussel adhesion: finding the tricks worth mimicking." *The Journal of Adhesion* 81, no. 3-4 (2005): 297-317.

(14) Zhao, Hua, and J. Herbert Waite. "Proteins in load-bearing junctions: the histidine-rich metal-binding protein of mussel byssus." *Biochemistry* 45, no. 47 (2006): 14223-14231.

(15) Lee, Haeshin, Norbert F. Scherer, and Phillip B. Messersmith. "Single-molecule mechanics of mussel adhesion." *Proceedings of the National Academy of Sciences* 103, no. 35 (2006): 12999-13003.

(16) Burzio, Luis A., and J. Herbert Waite. "Reactivity of peptidyl-tyrosine to hydroxylation and cross-linking." *Protein Science* 10, no. 4 (2001): 735-740.

(17) Burzio, Luis A., and J. Herbert Waite. "Cross-linking in adhesive quinoproteins: studies with model decapeptides." *Biochemistry* 39, no. 36 (2000): 11147-11153.

(18) Liu, Bo, Lyle Burdine, and Thomas Kodadek. "Chemistry of periodate-mediated cross-linking of 3, 4-dihydroxylphenylalanine-containing molecules to proteins."*Journal of the American Chemical Society* 128, no. 47 (2006): 15228-15235.

(19) Boskey, A. L., M. Maresca, W. Ullrich, S. B. Doty, W. T. Butler, and C. W. Prince. "Osteopontin-hydroxyapatite interactions in vitro: Inhibition of hydroxyapatite formation and growth in a gelatin-gel." *Bone and Mineral* 22, no. 2 (1993): 147-159.

(20) Somerman, Martha J., Larry W. Fisher, Ruth A. Foster, and John J. Sauk. "Human bone sialoprotein I and II enhance fibroblast attachmentin vitro."*Calcified Tissue International* 43, no. 1 (1988): 50-53.

(21) Ritchie, Helena H., and Lee-Ho Wang. "Sequence determination of an extremely acidic rat dentin phosphoprotein." *Journal of Biological Chemistry* 271, no. 36 (1996): 21695-21698.

(22) Holt, Carl, Peter A. Timmins, Neil Errington, and Jeffrey Leaver. "A core-shell model of calcium phosphate nanoclusters stabilized by β-casein phosphopeptides, derived from sedimentation equilibrium and small-angle X-ray and neutron-scattering measurements." *European Journal of Biochemistry* 252, no. 1 (1998): 73-78.

(23) Geiß, Paul Ludwig, and Jürgen Klingen. *Adhesive bonding: materials, applications and technology*. Darmstadt: Wiley-VCH, 2009.

(24) Dalsin, Jeffrey L., Lijun Lin, Samuele Tosatti, Janos Vörös, Marcus Textor, and Phillip B. Messersmith. "Protein resistance of titanium oxide surfaces modified by biologically inspired mPEG-DOPA." *Langmuir* 21, no. 2 (2005): 640-646.

(25) Fan, Xiaowu, Lijun Lin, Jeffrey L. Dalsin, and Phillip B. Messersmith. "Biomimetic anchor for surface-initiated polymerization from metal substrates."*Journal of the American Chemical Society* 127, no. 45 (2005): 15843-15847.

(26) Vovelle, Jean. *Le tube de Sabellaria alveolata (L.): annélide polychète Hermellidae et son ciment: étude écologique, expérimentale, histologique et histochimique*. Université, Faculté des Sciences, 1965.

(27) Vovelle, Jean. "Les glandes cémentaires de Petta pusilla Malmgren, polychète tubicole Amphictenidae, et leur sécrétion organo-minérale." *Archives de zoologie expérimentale et générale* 120 (1979): 219-246.

(28) Gruet, Yves, Jean Vovelle, and Michèle Grasset. "Composante biominérale du ciment du tube chez Sabellaria alveolata (L.), Annélide Polychète." *Canadian Journal of Zoology* 65, no. 4 (1987): 837-842.

(29) Rzepecki, L. M., and J. H. Waite. "The byssus of the zebra mussel, Dreissena polymorpha. I: Morphology and in situ protein processing during maturation."*Molecular Marine Biology and Biotechnology* 2, no. 5 (1993): 255-266.

(30) Waite, J. Herbert, and Marvin L. Tanzer. "Polyphenolic substance of *Mytilus edulis*: novel adhesive containing L-dopa and hydroxyproline." *Science* 212, no. 4498 (1981): 1038-1040.

(31) Heo, Jinhwa, Taegon Kang, Se Gyu Jang, Dong Soo Hwang, Jason M. Spruell, Kato L. Killops, J. Herbert Waite, and Craig J. Hawker. "Improved performance of protected catecholic polysiloxanes for bioinspired wet adhesion to surface oxides." *Journal of the American Chemical Society* 134, no. 49 (2012): 20139-20145.

(32) Chung, Hoyong, and Robert H. Grubbs. "Rapidly cross-linkable DOPA containing terpolymer adhesives and PEG-based cross-linkers for biomedical applications." *Macromolecules* 45, no. 24 (2012): 9666-9673.

(33) Sparks, Bradley J., Ethan FT Hoff, LaTonya P. Hayes, and Derek L. Patton. "Mussel-inspired thiol–ene polymer networks: influencing network properties and adhesion with catechol functionality." *Chemistry of Materials* 24, no. 18 (2012): 3633-3642.

(34) Holowka, Eric P., and Timothy J. Deming. "Synthesis and crosslinking of

L-DOPA containing polypeptide vesicles." *Macromolecular Bioscience* 10, no. 5 (2010): 496-502.

(35) Nishida, Jin, Motoyasu Kobayashi, and Atsushi Takahara. "Gelation and adhesion behavior of mussel adhesive protein mimetic polymer." *Journal of Polymer Science Part A: Polymer Chemistry* 51, no. 5 (2013): 1058-1065.

(36) Matos-Pérez, Cristina R., James D. White, and Jonathan J. Wilker. "Polymer composition and substrate influences on the adhesive bonding of a biomimetic, cross-linking polymer." *Journal of the American Chemical Society* 134, no. 22 (2012): 9498-9505.

(37) Brubaker, Carrie E., and Phillip B. Messersmith. "The present and future of biologically inspired adhesive interfaces and materials." *Langmuir* 28, no. 4 (2012): 2200-2205.

(38) Solomon, Edward I., Uma M. Sundaram, and Timothy E. Machonkin. "Multicopper oxidases and oxygenases." *Chemical Reviews* 96, no. 7 (1996): 2563-2606.

(39) Olivares, Concepcion, and Francisco Solano. "New insights into the active site structure and catalytic mechanism of tyrosinase and its related proteins."*Pigment Cell & Melanoma Research* 22, no. 6 (2009): 750-760.

(40) Klabunde, Thomas, Christoph Eicken, James C. Sacchettini, and Bernt Krebs. "Crystal structure of a plant catechol oxidase containing a dicopper center."*Nature Structural & Molecular Biology* 5, no. 12 (1998): 1084-1090.

(41) Rozen, Steve, and Helen Skaletsky. "Primer3 on the WWW for general users and for biologist programmers." In *Bioinformatics methods and protocols*, pp. 365-386. Clifton, NJ: Humana Press, 1999.

(42) Belhomme, Corinne, Elisabeth David-Briand, Catherine Guérin-Dubiard, Véronique Vié, and Marc Anton. "Phosvitin–calcium aggregation and organization at the air–water interface." *Colloids and Surfaces B: Biointerfaces* 63, no. 1 (2008): 12-20.

(43) Benedict, Christine V., and Paul T. Picciano. "Adhesives from marine mussels." *Adhesives from Renewable Resources* 385 (1989): 465-483.

CHAPTER 2

MORPHOLOGY OF THE ADHESIVE SYSTEM IN THE SANDCASTLE WORM, *PHRAGMATOPOMA CALIFORNICA*

3 Morphology of the Adhesive System in the Sandcastle Worm, *Phragmatopoma californica*

Ching Shuen Wang, Kelli K. Svendsen and Russell J. Stewart

Contents

3.1 Introduction

The marine Sandcastle worm (*P. californica*) and related species live in composite mineralized tubes for shelter. They gather the mineral phase for free from the environment as sand grains and seashell bits with a crown of ciliated tentacles. The captured mineral particles are conveyed for inspection to the building organ – a pincer-shaped pair of dexterous palps in front of the mouth (Fig. 3.1). A dab of proteinaceous adhesive (Jensen and

Fig. 3.1 ***Phragmatopoma californica*.** At the left side of the photograph the tentacles and operculum of a sandcastle worm protrude from the end of a tube rebuilt with white 0.5 μm zirconium oxide beads. The worm on the right has been removed from its tube. The larger arrow indicates the building organ. The smaller arrow indicates the ventral shield region. Scale bar: 5 mm

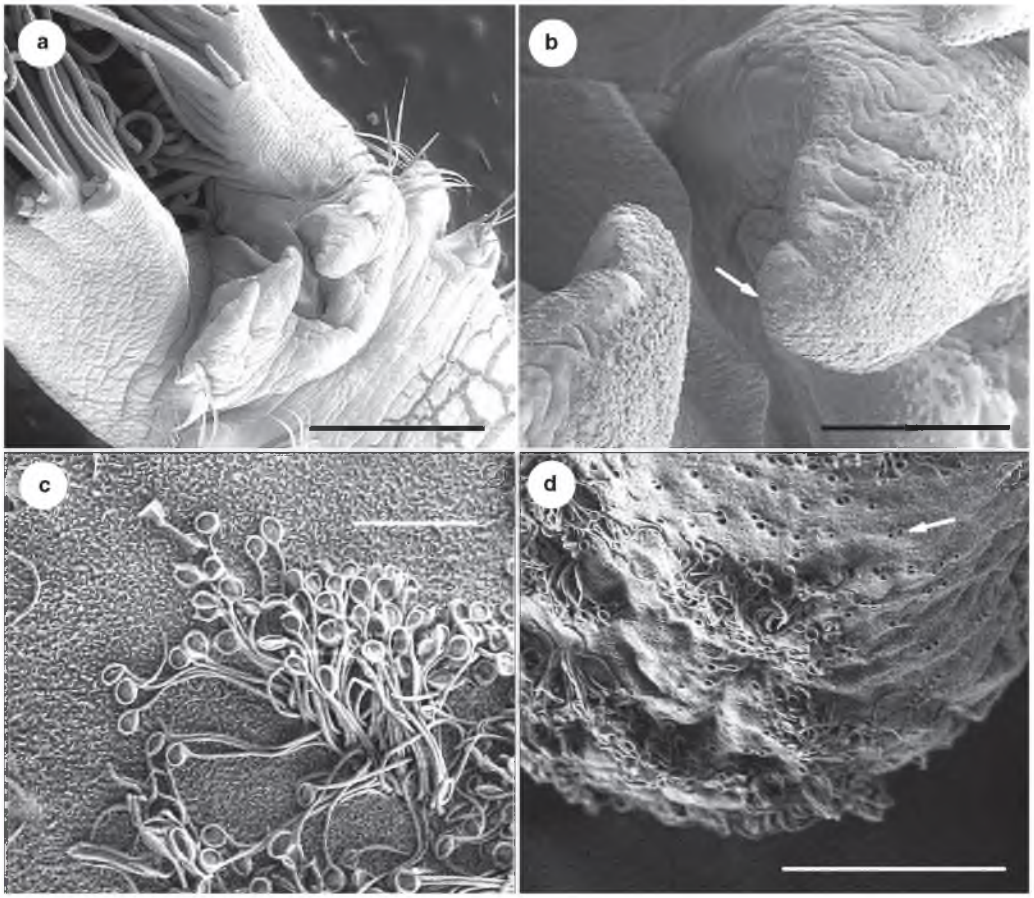

Fig. 3.2 SEM of the Sandcastle building organ. **a** The dexterous and multi-functional building organ; **b** Close up of the heavily ciliated building organ. **c** The area indicated by the arrow in **b**. Paddle-ended cilia occur in dense clusters. **d** The tip of the building organ palps are dotted with small pores that often occur in pairs. Scale bar in **a** 1 mm; **b** 200 μm; **c** 5 μm; and **d** 20 μm

Morse, 1988) is secreted from the building organ onto suitable particles as they are pressed onto the end of the tube. The major protein components of the adhesive are a group of heterogeneous proteins, referred to as Pc3x, characterized by serial runs of 10–14 serine residues punctuated with single tyrosine residues (Zhao et al., 2005). Phosphorylation of more than 90% of the serines (Stewart et al., 2004) makes the Pc3 proteins polyacidic (pI < 3). Other potential protein components identified biochemically (Waite et al., 1992) and by sequencing random cDNAs from an adhesive gland library (Endrizzi and Stewart, 2009) are generally polybasic with predicted pIs greater than 9. Amino acid analysis of secreted glue revealed that, in total, close to 50% of the adhesive protein residues are charged when serine phosphorylation is taken into account. The adhesive also contains Mg^{2+} and Ca^{2+} and a large fraction of the tyrosines are post-translationally hydroxylated to form 3,4-dihydroxyphenylalanine (DOPA), a residue shared with the adhesive plaque proteins of the mussel (Waite and Tanzer, 1981). Phosphates and *o*-dihydroxyphenols are well-known adhesion promoters.

The secreted glue is initially fluid as evident from its crack filling capability and the contact angles of the

adhesive on glass substrates (Fig. 3.2d). Within 30 s after secretion the fluid adhesive sets into a force-bearing solid foam (Stevens et al., 2007) (Fig. 3.2) and covalently cures over the next several hours into material with the consistency of shoe leather. The foam is a mix of open and closed cells, covered by a non-porous skin, and often associated with silky fibers (Fig. 3.2e). The skin and perhaps lining of the pores appear to be denser than the matrix of the adhesive (Fig. 3.2f). The set and cure of the adhesive was proposed to be triggered by the pH differential between secretory granules (pH ~5) and seawater (pH 8.2); the set by insolubilization of the divalent cations and polyphosphate, the cure by accelerated oxidation and subsequent crosslinking of some of the DOPA residues (Stewart et al., 2004).

The high charge content and segregation of opposite charges into separate proteins suggested a model in which complex coacervation of polyacidic and polybasic adhesive proteins drove formation of the initial cohesive fluid phase of the secreted adhesive (Stewart et al., 2004). Complex coacervates phase separate from aqueous solutions of oppositely charged polyelectrolytes when the conditions (pH, charge ratios, and ionic strength) are such that the solution is near electrical neutrality (Bungenberg de Jong, 1949). Complex coacervates are dense, cohesive, water-immiscible fluids with low interfacial tension and as such are ideal vehicles for water-borne underwater bioadhesives. Indeed, copying the charge characteristics and ratios of the adhesive proteins with synthetic polyelectrolytes resulted in adhesive complex coacervates that qualitatively replicated several features of the natural underwater adhesive, namely interfacial adhesion to wet substrates, underwater deliverability, and controlled setting reactions (Shao et al., 2009; Shao and Stewart, 2010).

Although the Sandcastle worm has already provided significant insights it has much more to teach us about making underwater adhesives. The sandcastle glue is comprised of separated active components that when mixed just before application react to form bonds – superficially analogous to two-part epoxy adhesives found in hardware stores. Little is known about which components of the multi-part adhesive are segregated into which compartments, when or how the separated components are mixed prior to bonding, the chemical details of the mechanisms that initiate hardening of the adhesive, and when or how water is removed or segregated from the fluid adhesive to produce a solid foam underwater. To address these and other questions morphological analyses of the adhesive gland and secretion process were initiated and preliminary findings are described here. These studies provide a map to investigate the detailed organization of the adhesive system with specific protein and nucleic acid probes. They are also the first step in studying the physiology of glue secretion. The knowledge, of course, will guide development of more sophisticated synthetic analogs of the Sandcastle worm adhesive.

3.2 Sandcastle Worm Morphology

Early morphological studies of the adhesive secretion process were conducted by Jean Vovelle in three related worm species that build composite tubes: *Sabellaria alveolata* (Vovelle, 1965) in the sub-order Sabellida that builds reef-like colonies of conjoined tubes; and *Lagis koreni* (Vovelle and Grasset, 1976) and *Petta pusilla* (Vovelle, 1979) in the sub-order Terebellida, family Pectinariidae, that build solitary conical tubes. They are commonly known as Honeycomb worms and Ice Cream Cone worms, respectively, for their tube-building habits. To summarize Vovelle's observations, all three species had clustered glandular tissue situated around the coelomic cavity of the first three parathoracic metameres. The glands contained two major secretory cell types distinguished by the appearance of their densely packed secretory granules; "homogeneous" granules appeared to have a uniform composition, "heterogeneous" granules contained dense inclusions. Both types of granules exited intact from their respective secretory cells through narrow cellular extensions that extended in bundles to the building organ. The granules remained intact and in separate channels until evacuating from the building organ through clustered pores, which in *P. pusilla* was described as a "strainer". Vovelle also reported the presence of Mg, Ca, and P in the heterogeneous granules of *S. alveolata* (Gruet et al., 1987) and *L. koreni* (Truchet and Vovelle, 1977).

3.2.1 The Building Organ

As the name implies, the building organ is the principle appendage used to carry out the detailed work of tube building. The Sandcastle worm, as mason, feels around the end of the tube with the fingers of the building organ evaluating where next to place a particle and the required size and shape. Particles delivered by the tentacles are turned and rotated between the fingers to check the size and it seems surface chemistry or texture. Tubes rebuilt with chicken egg shell fragments, for example, always

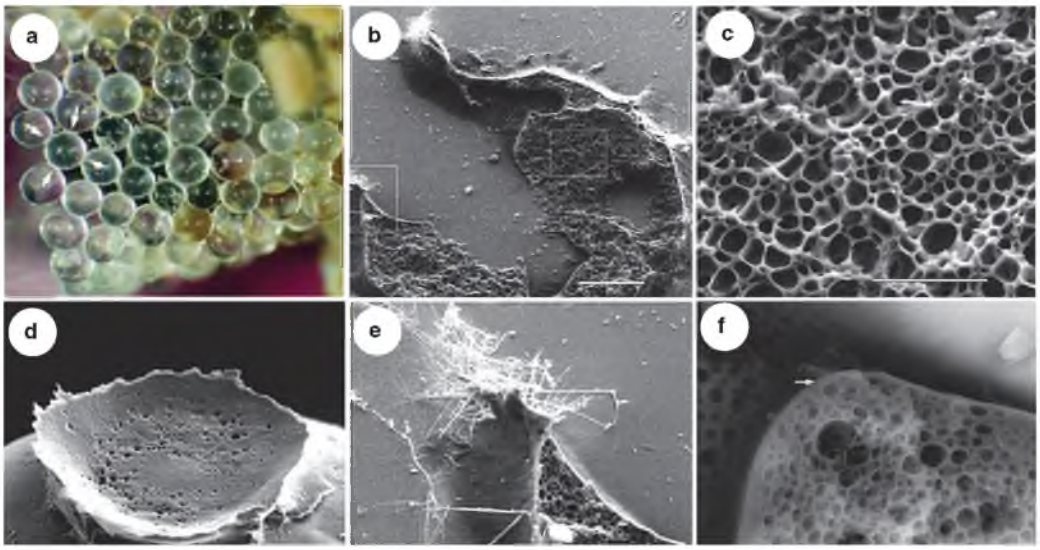

Fig. 3.3 SEM of sandcastle adhesive. **a** A tube partially rebuilt with glass beads. The glue was applied only at the four contact points (arrows); **b** Sandcastle worms placed on coverslips glue glass beads to the surface. The glue fractured when the bead was pried away; **c** The foamy interior in the right box in **b**; **d** A spot of glue left on a glass bead; **e** Threads and non-porous skin layer on glue; **f** Foamy interior imaged with backscattered electron detector. Distinct layers on the surface (arrow) and lining the pores are visible. Scale bar in **b** and **d** 50 μm; **c** and **e** 15 μm; **f** 5 μm

have the outside of the eggshell oriented toward the inside of the tube. When the appropriate particle is in position the worm calculates where to apply the adhesive most effectively. With uniform round particles, like glass beads, the glue is applied precisely at the points where stacked spheres make contact – only at contact points and generally at all contact points (Fig. 3.2a). After observing the placement of numerous particles it appears the worm feels the contact point between particles from the side with the building organ and injects adhesive at that point. In addition to providing the muscle, protractor and compass, the building organ also provides sensory information required for precise and efficient sandcastle construction.

Scanning electron microscopy (SEM) revealed dense clusters of paddle-shaped cilia, which may play a role in sensory functions, sporadically carpeting the surface of the building organ (Fig. 3.3b–d). Clustered pores were observed in the building organ surface that may be the exit points for adhesive components (Fig. 3.3f). At ~0.5 μm in diameter the pores are much smaller than the major 2–4 μm adhesive granules.

3.2.2 The Adhesive Gland

The gross structure of the adhesive gland was revealed with Arnow stain on cryosectioned worms (Fig. 3.4). Arnow's reagent becomes bright red after reacting with DOPA (Arnow, 1937). The main glandular region is apparent in the body cavity, the building organ is uniformly stained, and the so-called ventral shield [the layer of milky white tissue on the ventral surface of the first three segments (Fig. 3.1)] is stained lighter red and in a more punctate pattern. The red striations below the building organ in Fig. 3.4c are channels leading from the adhesive gland to the building organ. A more detailed overview of the adhesive gland is provided by observing the autofluoresence of the adhesive precursors (Fig. 3.5). Secretory cells densely packed with fluorescent secretory granules are distributed around the body cavity of the three parathoracic segments. Individual granules exit from the packed secretory cells and move in single-file clusters through channels toward the building organ (Fig. 3.5c). The granules are still intact when they arrive at the building organ, which appears to be laced around

Fig. 3.4 Distribution of DOPA-containing proteins in the Sandcastle worm. a Cryosection through the second parathoracic segment stained with Arnow's reagent. The adhesive gland stains dark red. The ventral shield and building organ stain lighter red; **b** Coronal cryosection unstained; **c** Same section as **b** stained with Arnow's reagent

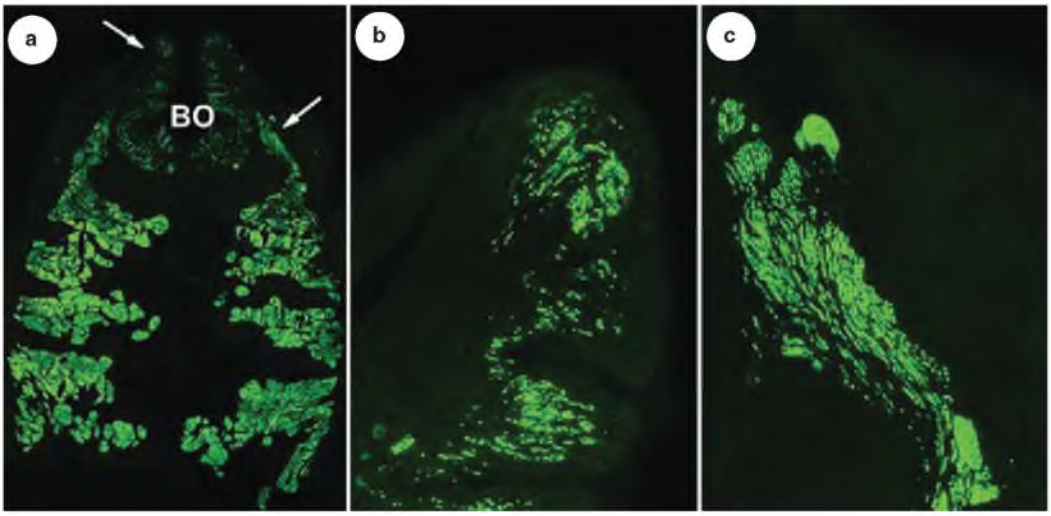

Fig. 3.5 Auto-fluorescence of the sandcastle worm secretory system. a Secretory cells in the tri-partite adhesive gland are intensely fluorescent due to the densely packed secretory granules. The channels leading from the secretory cells are apparent as well as radially distributed channels around the building organ (*BO*). **b** The building organ region identified by left arrow in **a**. Granules are lined up in channels and positioned a few microns from the surface. **c** Area of channel identified by left arrow in **a**. Granules are in single file lanes in a broad channel leading to the building organ

its entire circumference with radial channels (Fig. 3.5b). The granules move toward the surface between the clefts of the puckered building organ. Most of the intact granules seem to be parked several microns from the surface of the building organ in the unstimulated condition. Although granules are positioned around the entire building organ, the shape of the glue spots on glass beads and slides (Fig. 3.2) suggests the adhesive is released from localized areas of the building organ.

Like the adhesive precursors, the final set and cured sandcastle glue is autofluorescent over the entire visible spectrum (Stevens et al., 2007). The origin of this autofluorescence has not been studied in detail but a reasonable assumption has been that extensive conjugation resulting from oxidative crosslinking between DOPA residues would create fluorescent structures. If this were the mechanism it suggests the adhesive is at least partially DOPA-crosslinked before secre-

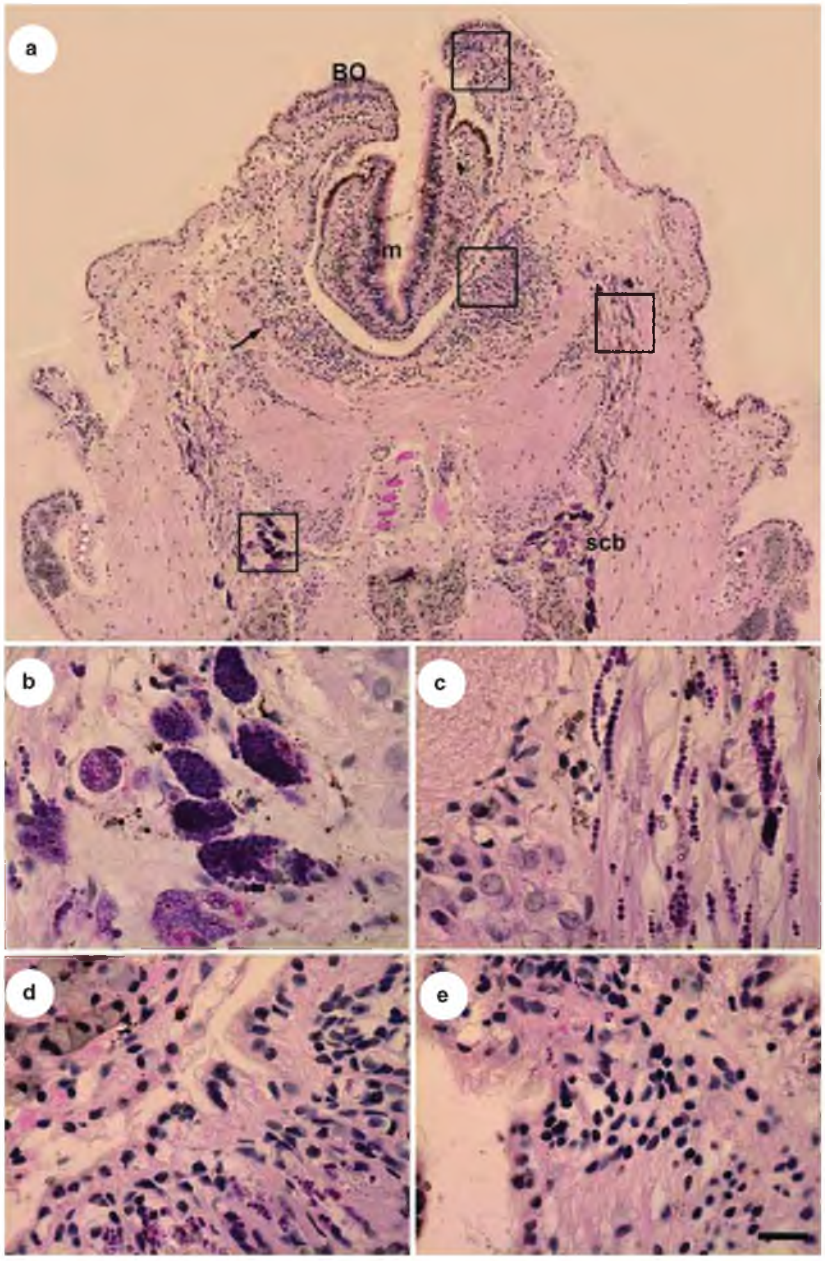

Fig. 3.6 Coronal sections stained with hematoxylin and eosin showing various regions of the secretory system. **a** and **b** Densely packed secretory cells containing homogeneous (*dark*) or heterogeneous granules (*light*) in the lower left boxed region; **c** Boxed channel region. Granules are segregated in single file channels; **d** and **e** Two regions containing granules from the periphery of the building organ. Scale bar in **a** 100 μm; **b–e** 10 μm

tion. A second possibility is that the worms were fixed with paraformaldehyde which has been shown to create fluorescence in dopamine containing brain tissue (Lofstrom et al., 1976). While the fluorescence may have been enhanced by paraformaldehyde fixation this was not the sole mechanism because isolated unfixed granules are strongly fluorescent with the same broad spectrum (not shown). Other potential structures responsible for the autofluorescence, though speculative, may be DOPA-metal complexes in the adhesive precursors, or the cofactors of redox enzymes, such as tyrosinase, involved in modifying the glue proteins. The autofluorescence merits further investigation because it could reveal details of the adhesive structure and the curing mechanism.

Coronal sections stained with H&E (Fig. 3.6) reveal two prominent secretory cell types in the adhesive gland loaded with either heterogeneous that stain light reddish purple or homogeneous granules that stain dark purple. The granules appear to leave the secretory cells in single file ranks and enter a broad secretory highway with separate lanes for each secretory cell (Fig. 3.6c). The homogeneous and heterogeneous granules remain segregated within their ranks as they move along their lanes to the building organ where they are positioned for rapid deployment (Fig. 3.6d). More dorsal sections reveal similar secretion channels connected to the most posterior regions of the adhesive gland. The structure of the channels is not well understood. Vovelle described them as cellular extensions (Vovelle, 1979). Likewise, the mechanisms

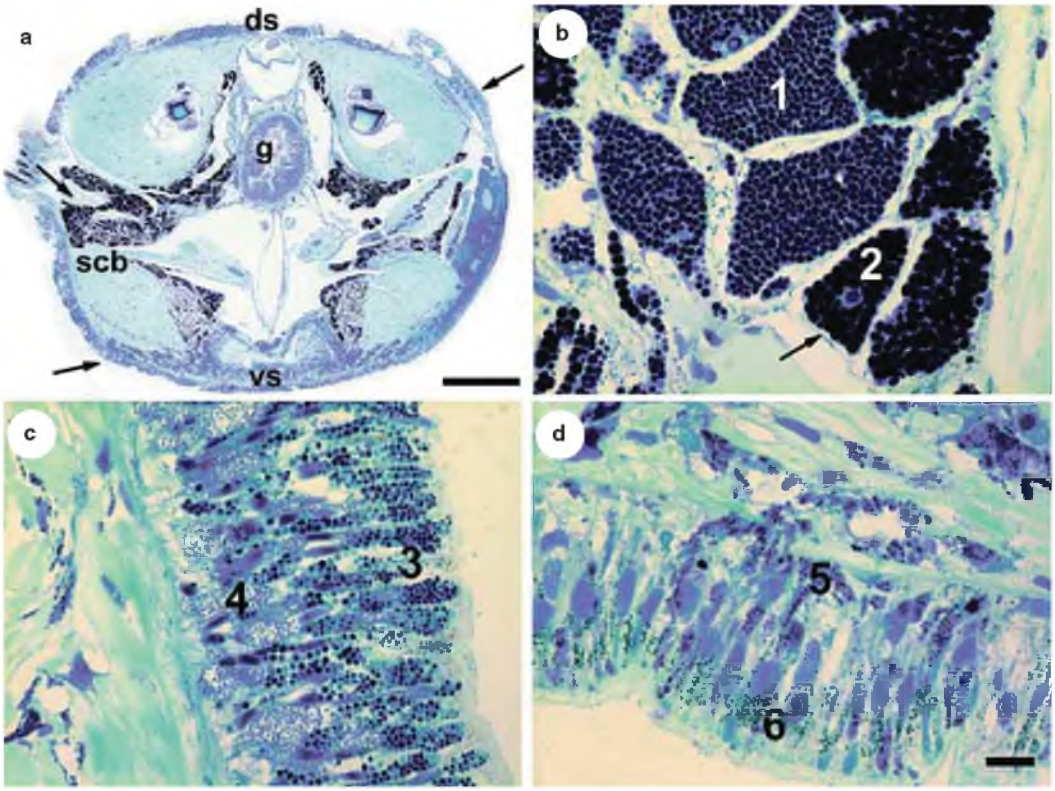

Fig. 3.7 Cross section through the center of the adhesive gland stained with toluidine blue. At least six distinct granule types are apparent (*1–6*); **a** Abbreviations are *ds* dorsal region; *vs* ventral shield; *g* gut; and *scb* secretory cell body; **b** Region of adhesive gland indicated by top-left arrow. Homogeneous granules (*1*), heterogeneous (*2*); **c** Region indicated by top right arrow; **d** Region of the ventral shield. Scale bar in **a** 500 μm; **d** 10 μm

that power granule transport through the channels are unknown. The bundled channels are interspersed with what appears to be loose connective tissue and are surrounded by bands of smooth muscle tissue.

The most prominent secretory cells in the adhesive gland produce the homogeneous and heterogeneous granules, but several other types of secretory granules are also present. Small cells with small bright red granules (<1 μm) line the outer edges of the building organ (Fig. 3.6a, arrow). In addition to the size differences, the contents of these granules are not autofluorescent. The small granules were often observed in the proximity of the heterogeneous and homogeneous granules in the building organ. We cannot rule out that the contents of the small granules are components of the adhesive.

In a cross section through the second thoracic segment stained with Toluidine Blue (TB) the adhesive gland clings to the outside wall of the body cavity (Fig. 3.7). The heterogeneous and homogeneous granules stained distinctly, the heterogeneous granules are dark blue, homogeneous lighter blue (Fig. 3.7b). Several types of columnar epithelial cells with distinct granules are apparent around the entire circumference of the worm (Fig. 3.7c, d). The products of these cells are not known but at least some are likely to produce mucus secretions as described by Vovelle (1965) in *Sabellaria alveolata*. Other products could include proteins identified by sequencing random clones from a cDNA library made with RNA isolated from tissues that included the epithelial secretory cells (Endrizzi and Stewart, 2009). Over 20 cDNAs encoding proteins with secretion signal peptides, most with characteristics of structural proteins, were identified during the expression survey. Some of these secreted proteins are likely components of the sandcastle glue but others could be components of the thin, reddish-brown, fabric-like sheath that lines the inside of the tubes. Neither the composition nor origin of the lining has been carefully studied but it could be secreted from the ventral shield. The punctate Arnow staining (Fig. 3.4a) suggests secretions originating from the ventral shield contain DOPA, which could account for the reddish-brown color of the lining. Other candidate products of the epithelial secretory cells identified in the expression survey include a small collagen with a secretion signal peptide that could be a component of the lining and a secreted laccase enzyme that may be the phenoloxidase activity reported by Vovelle (1965) in the ventral shield. The laccase may be responsible for quinonic tanning of the lining.

3.2.2.1 Granule Composition

A thin section of an epon embedded Sandcastle worm was examined by SEM and energy dispersive X-ray spectroscopy to investigate the composition of the homogeneous and heterogeneous granules (Fig. 3.8). Heterogeneous granules contain high-contrast sub-structures of variable size while no sub-structure is apparent in the homogeneous granules. Spectra acquired in a line scan through both granule types revealed abundant phosphorus and magnesium colocalized with the bright sub-granules in the heterogeneous granules. The relative height of the peaks in Fig. 3.8b does not represent the molar ratios of

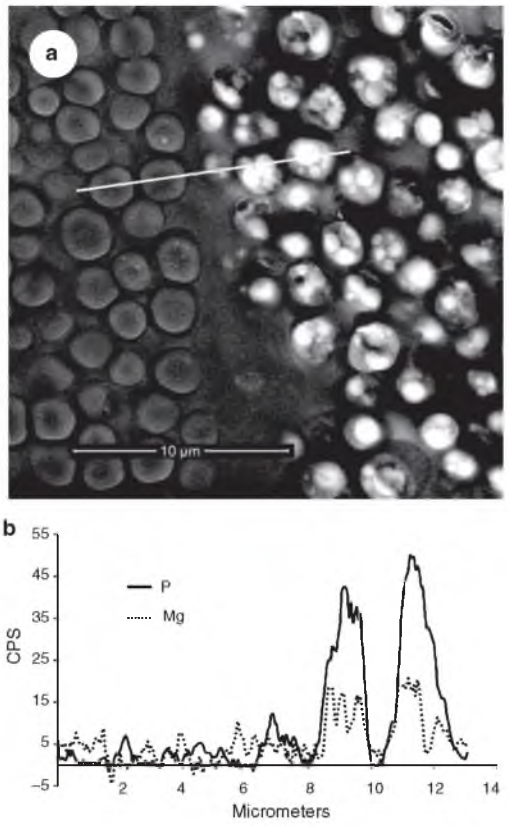

Fig. 3.8 Energy dispersive X-ray spectroscopy of granules within secretory cells. **a** Heterogeneous granules contain bright irregularly sized inclusions; **b** Phosphorus and magnesium along the line crossing through homogeneous and heterogeneous granules in panel a. Phosphorus and magnesium were colocalized in the heterogeneous sub-granules

P and Mg. The homogeneous granules contained only background levels of phosphorus and magnesium. The results demonstrate the highly phosphorylated Pc3 proteins (Zhao et al., 2005) are located exclusively in the heterogeneous granules. The colocalized Mg may play a role in condensing the highly charged Pc3 proteins into the heterogeneous substructures. Efforts to identify other protein components of each granule type are in progress using antibodies raised against synthetic peptides from Pc1 and 2, which were identified biochemically (Waite et al., 1992), and Pc4 and 5, which were identified in the adhesive gland cDNA library (Endrizzi and Stewart, 2009). In another approach, isolated granules of both types are being analyzed by tandem mass spectrometry to identify peptides for comparison to predicted peptides in the expressed sequence database.

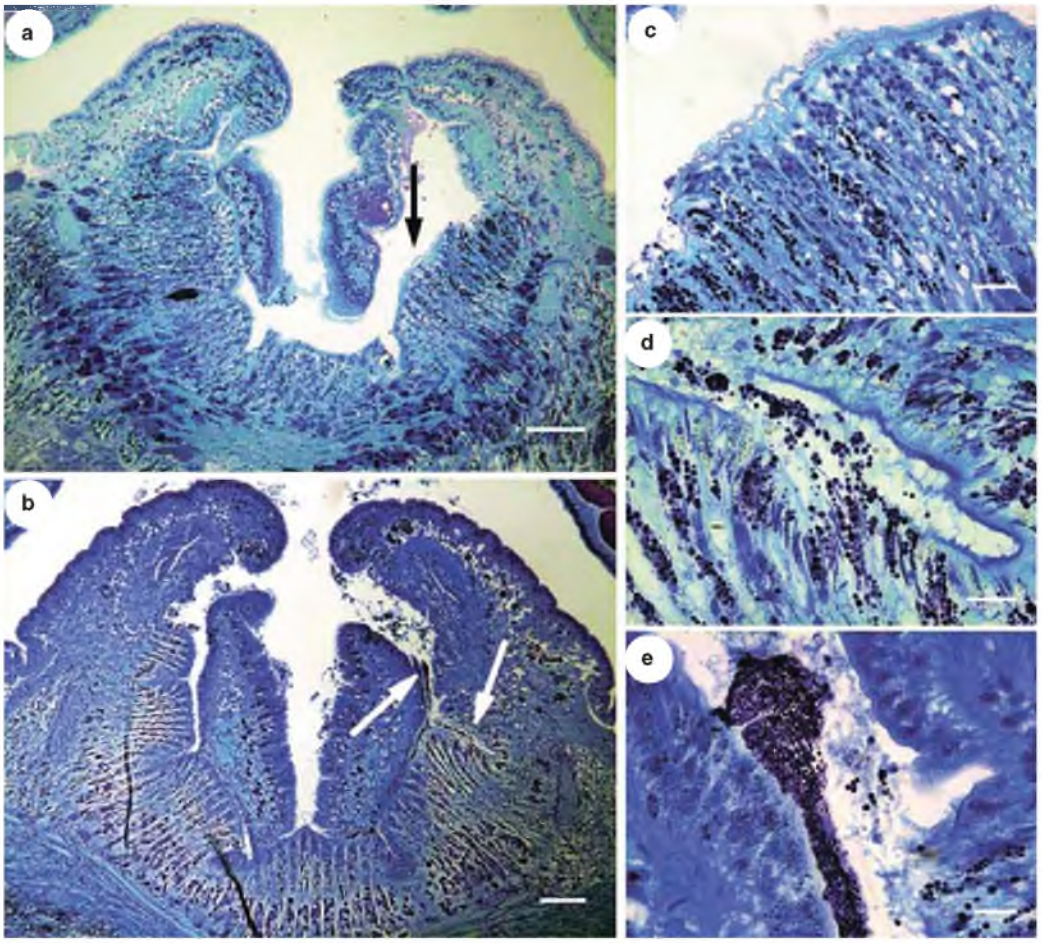

Fig. 3.9 Stimulated secretion. **a** Coronal section through the center of the building organ of an unstimulated worm; **b** Building organ after exposure to dopamine and electric shock. Glue appeared at several points around the building organ; **c** Region of building organ indicated by black arrow in panel **a**; **d** Secretory granules liberated from channels in the building organ flood into an exterior wrinkle. Granules begin to agglomerate; **e** Adhesive composed of mostly intact secretory granules along the outer portion of the mouth. Scale bar in **a** and **b** 100 μm; **c** 20 μm; **d** and **e** 10 μm

3.2.2.2 Stimulated Secretion

The Sandcastle worm glue is a multi-part adhesive that appears to be mixed just after secretion and before application to its gathered building materials. To uncover the biochemical and physiological details of the process it will be helpful to be able to stimulate secretion during observation. We found that one method to artificially trigger secretion is to externally expose the worms to 20 mM dopamine for 20 min followed by electric shocks in the vicinity of the building organ. Secretion did not occur when either stimulus was applied separately. Viscous white glue oozed from several areas around the building organ. As mentioned above, during naturally triggered secretion glue issues only from regions of the building organ in the vicinity of contact points between particles. Worms were immediately fixed during secretion events for histological analysis.

Coronal sections of secreting worms stained with TB revealed a dramatic widening of channels within the building organ compared to unstimulated worms (Fig. 3.9). The channels mostly terminated at the surface of the building organ but some terminate in the folded clefts. The widened channels may be due to muscular contractions resulting from electric shocks, are not the exit pathways for adhesive granules, and their role if any in the natural secretion process is unknown. At the site of secretion in the example shown in Fig. 3.9d, three distinct granule types, dark blue homogeneous, purplish heterogeneous, and unstained, were secreted intact into a cleft before exiting the building organ. Shortly after secretion the granules agglomerate into a viscous mass and the color of the TB stain changed from blue to a purple-violet. The color change, known as metachromasy, is a characteristic of some dyes, such as TB, when bound to particular substances (Bergeron and Singer, 1958). Polyphosphates are known to cause a metachromatic shift with basic dyes (Harold, 1966). The TB color change immediately after secretion is evidence of an unknown chemical change in the adhesive. Perhaps the phosphate sidechains of the Pc3x proteins may become more exposed as a result of heterogeneous granules rupturing.

3.3 Adhesive Models

Our first depictions of the complex coacervate model (Stewart et al., 2004; Stevens et al., 2007) to describe the assembly, secretion, and underwater bonding mechanisms of the Sandcastle worm glue did not take detailed anatomy of the adhesive gland and secretory pathways into full consideration. From the observations reported here and Vovelle's earlier studies it is clear that the adhesive components are packaged into granules in separate cell types. The distinct granules, as they move from the secretory cells to the point of exit at the building organ, remain segregated from one another as they travel by an unknown mechanism in channels of unknown structure. The granules exit intact from points distributed evenly around the entire building organ surface and only then do the contents of the distinct granules mix and become a viscous, presumably adhesive mass. If complex coacervation through electrostatic association of the oppositely charged proteins is part of the process of adhesive formation it must occur immediately after secretion rather than in a compartment of the secretory system. If so, this implies coacervation would have to occur in the high ionic strength of seawater.

In the original sandcastle glue model the foam structure of the set adhesive was attributed to phase separation of the complex coacervate from water with the water phase coalescing into vacuoles to become the cells of the foam. Vovelle described the heterogeneous granules as dilating during secretion with the dense inclusions becoming the pores of the foamy glue, and the contents of the homogeneous granules forming a matrix around the porous heterogenous granules. The observations reported here are consistent with Vovelle's obervations; the dense inclusions of the heterogeneous granules seem to become the pores of the foamy adhesive. Whether complex coacervation as commonly defined is part of the mechanism or not the Sandcastle Worm-inspired concept has nevertheless proven to be a useful paradigm for creating synthetic water-borne underwater adhesives (Shao et al., 2009; Shao and Stewart, 2010).

3.4 Materials and Methods

3.4.1 Animal Preparation

Phragmatoma Californica colony were collected near Santa Barbara, California and maintained in a laboratory aquarium with circulating artificial salt water at 14°C. Worms were carefully removed from their tubes and rinsed with filtrated seawater 3 times before fixation. Fixation was done with 4% paraformaldehyde in PBS at 4°C overnight. After fixation, the worms were dehydrated in a series of ethanol solutions (50, 70, 95, and 100%) at room temperature. The worms were then embedded

with ImmunoBed (PolyScience, CA, USA) according to manufacturer's instruction.

3.4.2 Scanning Electron Microscopy

Worms were fixed with 4% paraformaldehyde and 2% glutaraldehyde in 0.1 M sodium cacodylate buffer at 4°C overnight, post-fixed with 2% osmimium tetroxide, dehydrated with serial ethanol at room temperature for several hours, and then mounted on carbon tape. The specimens were examined with a FEI Quanta 600 SEM in low vacuum at the University of Utah Surface and Nanoimaging Facility. An EDAX X-ray detector was used for elemental analysis. The fixed worms were embedded in epon plastic medium according to the manufacturer's instructions. Semi-thin (0.5 µm) sections were cut with an ultramicrotome and immediately mounted on a superfrost slide (VWR).

3.4.3 Fluorescent Microscopy

ImmunoBed embedded worm blocks were cut with a microtome to 2 µm and mounted on a superfrost slide (VWR) and covered with a No. 1 coverslip using antifade embedding medium. Longitudinal sections were imaged with either 20× or 100× objectives using a green filter set. ImageJ was used for image processing and montages were created with Photoshop.

3.4.4 Histological Staining

Two or four micrometer ImmunoBed embedded sections were rehydrated with serial ethanol solutions (95%, 70%, and 50%, 5 min each), rinsed with DI water at RT for 5 min, and then stained with Toluidine Blue according to routine histological protocols.

References

Arnow LE (1937) Colorimetric determination of the components of 3,4-dihydroxyphenylalanine-tyrosine mixtures. Journal of Biological Chemistry 118: 531–537.

Bergeron JA and Singer M (1958) Metachromasy: an experimental and theoretical reevaluation. Journal of Biophysical and Biochemical Cytology 4(4): 433–457.

Bungenberg de Jong HG (1949) Crystallization – coacervation – flocculation. In: Kruyt HR (ed) Colloid Science, vol. II. Elsevier Publishing Company, New York: pp 232–255.

Endrizzi BJ and Stewart RJ (2009) Glueomics: an expression survey of the adhesive gland of the sandcastle worm. The Journal of Adhesion 85: 546–559.

Gruet Y, Vovelle J, and Grasset M (1987) Composante biominerale du ciment du tube ches *Sabellaria alveolata* (L.) Annelide Polychete. Canadian Journal of Zoology 65: 837–842.

Harold FM (1966) Inorganic polyphosphates in biology: structure, metabolism, and function. Bacteriological Reviews 30(4): 772–794.

Jensen RA and Morse DE (1988) The bioadhesive of *Phragmatopoma californica* tubes: a silk-like cement containing L-DOPA. Journal of Comparative Physiology B 158: 317–324.

Lofstrom A, Jonsson G, Wiesel FA, and Fuxe K (1976) Microfluorimetric quantitation of catecholamine fluorescence in rat median eminence. II. Turnover changes in hormonal states. Journal of Histochemistry and Cytochemistry 24(2): 430–442.

Shao H and Stewart RJ (2010) Biomimetic underwater adhesives with environmentally triggered setting mechanisms. Advanced Materials 22(6): 729–733.

Shao H, Bachus KN, and Stewart RJ (2009) A water-borne adhesive modeled after the sandcastle glue of *P. californica*. Macromolecular Bioscience 9(5): 464–471.

Stevens MJ, Steren RE, Hlady V, and Stewart RJ (2007) Multiscale structure of the underwater adhesive of *Phragmatopoma californica*: a nanostructured latex with a steep microporosity gradient. Langmuir 23(9): 5045–5049.

Stewart RJ, Weaver JC, Morse DE, and Waite JH (2004) The tube cement of *Phragmatopoma californica*: a solid foam. Journal of Experimental Biology 207(Pt 26): 4727–4734.

Truchet M and Vovelle J (1977) Study of the element secretory glands of a tubicolous polychaete (Pectinaria (= Lagis) koreni) with the help of electron microprobe and ion microanalyzer. Calcified Tissue Research 24(3): 231–238.

Vovelle J (1965) Le tube de *Sabellaria alveolata* (L.) Annelide Polychete Hermellidae et son ciment. Etude ecologique, experimentale, histologique et histochimique. Archives de Zoologie Experimentale & Generale 106: 1–187.

Vovelle J (1979) Les Glandes Cementaires de Petta Pusilla Malmgren, Polychete Tubicole Amphictenidae, et leur Secretion Organo-minerale. Archives de Zoologie Experimentale & Generale 120: 219–246.

Vovelle J and Grasset M (1976) Les Pectinaires et leur ciment. Bulletin de la Societe Zoologique de France 101(5): 1022–1023.

Waite JH, Jensen RA, and Morse DE (1992) Cement precursor proteins of the reef-building polychaete *Phragmatopoma californica* (Fewkes). Biochemistry 31(25): 5733–5738.

Waite JH and Tanzer ML (1981) Polyphenolic Substance of *Mytilus edulis*: Novel Adhesive Containing L-Dopa and Hydroxyproline. Science 212(4498): 1038–1040.

Zhao H, Sun C, Stewart RJ, and Waite JH (2005) Cement proteins of the tube-building polychaete *Phragmatopoma californica*. Journal of Biological Chemistry 280(52): 42938–42944.

CHAPTER 3

LOCALIZATION OF THE BIOADHESIVE PRECURSORS OF THE SANDCASTLE WORM, *PHRAGMATOPOMA CALIFORNICA* (FEWKES)

The Journal of Experimental Biology 215, 351-361

doi:10.1242/jeb.065011

RESEARCH ARTICLE

Localization of the bioadhesive precursors of the sandcastle worm, *Phragmatopoma californica* (Fewkes)

Ching Shuen Wang and Russell J. Stewart*

Department of Bioengineering, University of Utah, Salt Lake City, UT 84112, USA

*Author for correspondence (rstewart@eng.utah.edu)

Accepted 27 October 2011

SUMMARY

The marine sandcastle worm bonds mineral particles together into underwater composite dwellings with a proteinaceous glue. The products of at least four distinct secretory cell types are co-secreted from the building organ to form the glue. Prominent hetereogeneous granules contain dense sub-granules of Mg and the (polyphospho)proteins Pc3A and B, as well as at least two polybasic proteins, Pc1 and Pc4, as revealed by immunolabeling with specific antibodies against synthetic peptides. Equally prominent homogeneous granules comprise at least two polybasic proteins, Pc2 and Pc5, localized by immunolabeling with anti-synthetic peptide antibodies. The components of the sub-micrometer granule types are unknown, though positive staining with a redox-sensitive dye suggests the contents include *o*-dihydroxy-phenylalanine (dopa). Quantitative PCR and *in situ* hybridization demonstrated that a tyrosinase-like enzyme with a signal peptide was highly expressed in both the heterogeneous and homogeneous granules. The contents of the granules are poorly mixed in the secreted mixture that forms the glue. Subsequent covalent cross-linking of the glue may be catalyzed by the co-secreted tyrosinase. The first three parapodia of the sandcastle worm also contain at least two distinct secretory tissues. The Pc4 protein was immunolocalized to the anterior secretory cells and the tryosinase-like gene was expressed in the posterior secretory cells, which suggests these proteins may have multiple roles.

Supplementary material available online at http://jeb.biologists.org/cgi/content/full/215/2/351/DC1

Key words: bioadhesive, polyelectrolytes, sandcastle worm, *Phragmatopoma californica*, polychaeta, sabellariidae, tyrosinase, dopa, quinonic cross-linking.

INTRODUCTION

Marine polychaetes in the family Sabellariidae live in tubular shells cobbled together with sandgrains, the broken skeletons of marine invertebrates and a protein-based underwater glue. Juvenile worms build new tubes adjoining existing tubes of the same species to create reef-like intertidal and subtidal colonies. *Phragmatopoma californica* (Fewkes), known commonly as the sandcastle worm, is found along the west coast of the USA. The description of a *P. californica* colony from the original classification by Fewkes (Fewkes, 1889) provides a sense of the turbulent habitats preferentially inhabited by sabellariids. To paraphrase, the 'aggregation' was a continuous mass, several feet across and 1–2 feet thick, encrusted onto the roof of a cavern carved by the sea into soft rock cliffs near Santa Barbara, CA, USA. The colony was exposed for several hours between tides. Colonization of high-energy shoreside environments, such as that described by Fewkes, requires robust construction of the honeycomb-like colonies, which reflects the durability of the waterproof adhesive bonds holding the composite tubes together. These qualities have sparked interest in the sandcastle worm glue (Shao et al., 2009), as well as in other marine bioadhesives, notably the byssal adhesive plaques of mytilid mussels (Waite et al., 2005), as sources of natural materials and design principles for underwater adhesives. The potential applications of these bioinspired synthetic adhesives include the repair of wet living tissues (Winslow et al., 2010; Lee et al., 2011).

During tube construction, the sandcastle worm applies miniscule spots of glue to millimeter-sized mineral particles as they are pressed onto the end of the tube. The initially fluid glue sets into a solid foam within 30 s of secretion into seawater (Stevens et al., 2007). Jensen and Morse (Jensen and Morse, 1988) discovered that the protein glue contains *o*-dihydroxy-L-phenylalanine (dopa) – post-translationally hydroxylated tyrosine – previously identified in the adhesive plaque proteins of mytilid mussels. The authors also noted the similarities in amino acid composition to the underwater adhesive silk of caddisfly larvae (Trichoptera), in particular the presence of high molar ratios of glycine, serine and basic residues. The chemical similarities have since been shown to go further; the serines in both adhesives are extensively phosphorylated. In total, the sandcastle worm glue and caddisfly silk contain more than 26 mol% and nearly 10 mol% phosphoserine, respectively (Stewart et al., 2004; Stewart and Wang, 2010). Extensive serine phosphorylation and high proportions of basic residues, especially arginine, are common in aquatic adhesives (Flammang et al., 2009; Stewart et al., 2011). As another example, the giant salivary secretory proteins of midge fly larvae (Diptera), which are drawn as insoluble fibers that are used in the construction of underwater filter feeding webs and pupal cases, contain 25 mol% basic residues and 8 mol% phosphoserines (Galler et al., 1984; Case et al., 1994). Intermolecular charge neutralization through electrostatic association of oppositely charged regions of polyelectrolytic proteins, with consequent expulsion of water and small counter-ions, may be part of a common mechanism that drives the initial insolubilization of these highly phosphorylated underwater bioadhesives (Case et al., 1994; Stewart et al., 2004; Stewart and Wang, 2010).

Taking into account serine phosphorylation, nearly 50% of the amino acids in the sandcastle worm glue are charged. The first putative glue proteins, Pc1 and Pc2, were isolated from homogenates of the adhesive gland-containing parathorax and sequenced by automated Edman degradation (Waite et al., 1992). Both are highly repetitive, glycine rich, and contain 27 and 34 mol% amine side-chains, respectively. Genes encoding a set of serine-rich proteins, Pc3A and Pc3B, were cloned with oligo serine-encoding PCR primers from a parathorax cDNA library (Zhao et al., 2005). Pc3B is a polyacid consisting entirely of runs of 6–12 phosphoserines punctuated with single tyrosine residues. In contrast, Pc3A is a polyampholytic diblock protein: the N-terminal block contains runs of 4–6 phosphoserines interrupted with single tyrosine residues; the C-terminal block, of roughly equal length, is strongly basic (predicted pI 11.8) comprising 26 and 12 mol% arginine and lysine residues, respectively. The C-terminal domain also contains 10 mol% cysteine residues. The primary structure of Pc3A highlights another striking similarity between the sandcastle worm glue and caddisfly silk proteins – phosphoserine-rich motifs alternate with arginine-rich motifs in both cases. The caddisfly silk heavy chain fibroin protein has short phosphoserine $(pSX)_4$ blocks flanked by short arginine-rich blocks, creating a larger motif that repeats hundreds of times (Yonemura et al., 2006; Stewart and Wang, 2010). In addition to Pc1, Pc2 and Pc3AB, an additional 14 genes encoding proteins with characteristics of structural glue proteins – secretion signal peptides, low complexity sequences and highly repetitive primary structures – were identified by sequencing random clones from a parathorax cDNA library. Most are basic, though some may be ampholytic (Endrizzi and Stewart, 2009).

The sandcastle worm glue originates in a prominent adhesive gland situated around the coelomic cavity of the first three parathoracic segments. The gland consists of multiple cell types, each producing distinct types of secretory granules. The largest and most abundant secretory cell types, present in roughly equal proportions, are densely packed with either 'homogeneous' or 'heterogeneous' granules, both 2–3 μm in diameter (Vovelle, 1965). The contents of the homogeneous granules appear to be of uniform ultrastructure, while the heterogeneous granules contain multiple sub-granules of widely varying diameter. Elemental analysis by energy dispersive x-ray spectroscopy revealed P and Mg concentrated exclusively in the sub-granules of the heterogeneous granules, undoubtedly in the form of Mg^{2+} complexed with phosphorylated Pc3 (Wang et al., 2010). The homogeneous and heterogeneous granules travel, intact, through narrow extensions leading from their respective secretory cell bodies to the periphery of the building organ, some from as far away as the posterior boundary of the third segment. At least two other types of much smaller, sub-micrometer secretory granules originate in cells situated around the base of the building organ. Only after the granules have exited intact through the building organ surface do their contents mix and become a viscous adhesive foam (Wang et al., 2010).

Clearly, the sandcastle worm builds composite mineral structures with a multi-part adhesive, the reactive components of which are separately packaged in condensed granules, though much remains unknown about the natural bioadhesive. Conclusive evidence that Pc1 and Pc2 are components of the primary glue used to bond mineral particles into tubes has not been reported. Because the proteins were isolated from parathorax homogenates it remains possible that they are constituents of the several other secretory cell types that surround the parathorax (Wang et al., 2010). Likewise, the cDNA library in which putative glue protein genes were identified was constructed with parathorax mRNA (Zhao et al., 2005). Transcripts of proteins actively secreted from other regions of the parathorax would be well represented in the library in addition to the adhesive gland. Better understanding of which components are packaged into which adhesive granules, when and how the separated components are mixed prior to bonding, and the chemical details of the setting and hardening reactions will guide development of more sophisticated next-generation mimetic adhesives (Shao et al., 2009). Toward this goal, the catalog of genes expressed in the adhesive gland (Zhao et al., 2005; Endrizzi and Stewart, 2009) was used to create specific nucleic acid and antibody probes to better understand the molecular organization of the sandcastle worm adhesive system.

MATERIALS AND METHODS

Animal preparation

Phragmatopoma californica colonies were collected near Santa Barbara, CA, USA, and shipped overnight to Salt Lake City, UT, USA. The colonies were maintained in a laboratory aquarium with circulating artificial salt water (Instant Ocean, Spectrum Brands Inc., Madison, WI, USA) chilled to 14°C.

Histochemistry

Worms were carefully removed from their tubes and rinsed with filtered saltwater three times before fixation. Worms were fixed with 4% paraformaldehyde (Polyscience Inc., Warrington, PA, USA) in phosphate-buffered saline (PBS) at 4°C overnight. After fixation, the worms were dehydrated in a series of ethanol solutions (50%, 70%, 95% and 100%), then stored in the freezer or processed immediately. Fixed worms were infiltrated with Immunobed (EM Science, Gibbstown, NJ, USA) according to the manufacturer's instructions. Fully polymerized blocks were serially sectioned (2 μm) on a microtome and mounted on superfrost slides (Fisher Scientific, Pittsburgh, PA, USA). Sections were rehydrated with deionized (DI) water at room temperature (RT) for 5 min, then stained with Toluidine Blue (TB) using standard protocols. Dopa-containing compounds were detected by staining with nitroblue tetrazolium chloride (NBT; 1 mg ml^{-1} NBT in 2 mol l^{-1} potassium glycinate, pH 9.5) at RT for at least 2 h for color development. Sections were de-stained in 0.16 mol l^{-1} sodium borate buffer at RT for 2 h and mounted with a coverslip for light microscopy.

Scanning electron microscopy

Whole worms were fixed in 2% glutaraldehyde with 1% paraformaldehyde in 0.1 mol l^{-1} sodium cacodylate buffer at 4°C overnight. Fixed whole worms were dehydrated with serial ethanol and dried with hexamethyldisilazane (HMDS) before scanning electron microscopy (SEM) imaging. To prepare tissue sections, worms were fixed and dehydrated as described above and embedded in Immuno-Bed Resin (Electron Microscopy Science, Hatfield, PA, USA). Worms were sectioned (5 μm) longitudinally, dehydrated with ethanol, and dried with HMDS before SEM imaging.

Sequencing

Random clones from a parathoracic cDNA library were sequenced as described in detail previously (Endrizzi and Stewart, 2009).

Quantitative real-time PCR

RNA was isolated only from worms that rebuilt substantial portions of their tubes with 0.5 mm glass beads within 12 h after the anterior portion of their tubes was removed. Eighteen worms were removed from their tubes and rinsed with filtered seawater three times, then randomly divided into three sets. After the parathorax had been

dissected, total RNA was purified with an RNAeasy kit (Qiagen, Valencia, CA, USA). The amount of RNA from each set was normalized using the ratio of absorbance at 260 and 280 nm. Total RNA was reverse transcribed into cDNA with a SuperScript III first-strand synthesis kit (Invitrogen, Carlsbad, CA, USA). PCR primer sets were designed (supplementary material Table S1) using the Primer3 software analysis tool (Rozen and Skaletsky, 2000). The three separate pools of total cDNA were amplified with gene-specific primers and SYBR mix (Rox, Roche, Indianapolis, IN, USA). Samples were analyzed on a 7900 HT fast real-time PCR system (Applied Biosystems, Concord, MA, USA).

In situ hybridization

Double-stranded DNA templates were amplified by PCR with specific primer sets (supplementary material Table S2). A T7 promoter binding site was added to all reverse strand PCR primers. After PCR amplification, dsDNA templates were isolated with a QIAquick PCR purification kit (Qiagen) and used for RNA probe synthesis. Digoxigenin (DIG)-labeled RNA probes were prepared with T7 RNA polymerase and DIG–dUTP at 37°C for 2 h, then isolated on an RNAeasy mini column (Qiagen). Purified RNA probes were stored in Rnase-free DI water at –80°C until use.

Worms were fixed in 4% paraformaldehyde in DEPC-treated PBS at 4°C overnight. Fixed worms were cryoprotected in freezing medium (Tissue Freezing Medium, EM Science) and cut into 70 µm serial sections on a cryotome. Sections were post-fixed with 4% paraformaldehyde at RT for 15 min. Samples were dehydrated with serial ethanol, followed by rehydration with the reverse serial ethanol solutions. Sections were bleached with 3% H_2O_2 in 0.5% KOH in DEPC-treated de-ionized PBS at RT for 2 h to remove pigmentation for better visualization. Tissue sections were permeabilized with 0.25% Triton X-100/PBS at RT for 20 min, then incubated in pre-hybridization buffer (50% de-ionized formamide, 5× SSC, 1 mg ml^{-1} salmon sperm DNA, 1% Tween-20 and 1% ascorbic acid) at 50°C for 2 h. Before hybridization, RNA probes were denatured at 70°C for 5 min and chilled on ice. Tissue sections with RNA probes were incubated in hybridization buffer (50% de-ionized formamide, 10% dextran sulfate, 5× SSC, 0.5 mg ml^{-1} salmon sperm DNA and 1% Tween-20) at 50°C for 16 h. Post-washing steps were done at 50°C as follows: (1) 2×30 min in 1:1 ratio of pre-hybridization buffer and 2× SSC + 0.1% Triton X-100, (2) 2×30 min 2× SSC + 0.1% Triton X-100, and (3) 2×30 min 0.2× SSC + 0.1% Triton X-100. Sections were returned to RT in PBST (PBS plus 0.05% Triton X-100) for 2×30 min, then blocked with 1% blocking buffer (Blocking reagent, cat. no. 11096176001, Roche) at RT for at least 4 h. Alkaline phosphatase-labeled anti-DIG (1:5000 dilution, cat. no. 11093274910, Roche) was added at 4°C overnight. After washing at least five times with PBST at RT for 30 min each, blue color was developed at RT with NBT/BCIP substrate (Fisher Scientific) in the dark. The signal to background ratio was improved by adding 100% ethanol to the sections for 30 min at RT. Sections were then rehydrated with serial ethanol and mounted on glass slides for imaging. Controls for non-specific antibody binding used anti-DIG as the primary antibody and anti-mouse alkaline phosphatase-conjugated secondary antibody.

Antibodies

Synthetic peptides predicted to be immunogenic (Pc2, residues 133–148, GFNYGANNAIKSTKRF; Pc4, residues 46–60, KKTYRGPYGAGAAK; Pc5, residues 114–128, ALGALGGN-GGFWKRR) were used to generate antibodies in rabbits (Pacific Immunology, Ramona, CA, USA; supplementary material Fig. S1). Anti-Pc2, anti-Pc4 and anti-Pc5 serum were purified from serum by affinity chromatography with the synthetic peptides coupled to a column (SulfoLink Immobilization Kit, Pierce, Rockford, IL, USA) and stored in PBS with 10% glycerol and 0.05% sodium azide at –20°C until use. Commercial anti-phosphoserine (mouse, ab6639, Abcam, Cambridge, MA, USA) was used to detect highly phosphorylated Pc3 proteins.

Immunostaining

Paraformaldehyde-fixed worms were rehydrated with serial ethanol, frozen in cryoprotectant (Tissue-Tek, Sakura, Torrance, CA, USA) and cryosectioned into 40 µm coronal sections. Sections were bleached with 3% H_2O_2/0.5% KOH in PBS at RT until pigmentation disappeared. Sections were permeabilized with 0.25% Triton X-100 in PBS at RT for 20 min and washed 3×5 min with PBS. Sections were transferred to blocking solution (1% BSA in PBS, 0.1% Triton X-100) at RT for at least 2 h. Blocking solution was replaced with 1:1000 dilution of anti-phosphoserine (Abcam) or the custom-made anti-Pc2, anti-Pc4 and anti-Pc5 antibodies and incubated at 4°C for 12 h. Sections were washed at least 5×15 min in PBST at RT. The sections were then incubated with 1:5000 dilution of either anti-mouse (ab6729, Abcam) or anti-rabbit secondary antibody (ab6722, Abcam) at 4°C for 12 h. Sections were washed at least 5×15 min in PBST at RT. Color was developed with NBT/BCIP substrate (Fisher Scientific) at RT in the dark and monitored carefully under the dissecting microscope. The sections were incubated in 100% ethanol for 30 min at RT to improve the signal to background ratio. Sections were rehydrated with serial ethanol and mounted on glass slides for imaging. Controls for non-specific binding of the mouse anti-phosphoserine antibody used anti-DIG as the primary antibody and alkaline phosphatase (AP)-conjugated, or Alexa 647-conjugated, anti-mouse secondary antibody. Controls for non-specific binding of the rabbit anti-Pc2, anti-4 and anti-5 used pre-immune rabbit serum and AP-conjugated, or Alexa 594-conjugated, anti-rabbit secondary antibody.

Western blots

Secretory granules were isolated by passing parathorax homogenates through a cell strainer (40 µm pore size, BD Biosciences, Sparks, MD, USA). Material passing through the strainer, including homogeneous and heterogeneous secretory granules, was collected in an Eppendorf tube and centrifuged immediately (3000*g* for 1 min). Centrifuged pellets were denatured in modified SDS sample buffer (1× SDS sample buffer, 6 mol l^{-1} urea, 0.5 mol l^{-1} DTT), separated by 12% SDS-PAGE, and transferred to PVDF membranes (Fisher Scientific). The membranes were blocked with 1% BSA in PBST solution at RT for 2 h, then incubated with 1:1000 dilution of anti-Pc2, anti-phosphoserine, anti-Pc4 or anti-Pc5 antibody at 4°C overnight. After washing, blots were incubated with anti-mouse (1:5000 dilution, ab6728, Abcam) or anti-rabbit (1:5000 dilution, ab6721, Abcam) secondary antibody at 4°C for 12 h. Incubated film was washed with PBST three times at RT for 5 min then developed with enhanced chemiluminescence substrate (Pierce).

Secreted glue immunostaining

Glass beads bonded by worms to the ends of their tubes were collected with forceps. Glue spots were washed off the glass beads with 30% acetic acid. The glue was collected by centrifugation and mounted in Immuno-Bed resin (Electron Microscopy Science), cut into 5 µm sections and adhered to Superfrost slides (Fisher Scientific). Sectioned glue was dehydrated and rehydrated with serial ethanol solutions at RT for 5 min each then digested with proteinase

K in digestion buffer (2 μg ml^{-1} proteinase K in PBS, 0.05% Triton X-100 and 0.1% SDS) at 37°C for 30 min. Samples were blocked with 1% BSA in PBST at RT for 2 h and double-labeled with anti-phosphoserine and anti-Pc2, anti-Pc4 or anti-Pc5 antibody (1:1000 dilution) at 4°C for 12 h. After washing, the sections were incubated with peroxidase-conjugated anti-mouse (1:1000, Alexa647, Invitrogen) or anti-rabbit (1:1000, Alexa594, Invitrogen) secondary antibody at 4°C for 12 h in the dark. Slides were washed with PBST three times at RT for 15 min each and mounted under a coverslip with Prolong anti-fade mounting media (Invitrogen) before imaging. Negative control samples were incubated with anti-DIG (1:1000, mouse, ab420, Abcam) and pre-immune rabbit serum (1:1000, Pacific Immunology) followed by anti-mouse or anti-rabbit secondary antibody. Samples were imaged on a Fluoview FV1000 fluorescent microscope (Olympus) with filter sets (594 and 647 nm) in default settings. Non-specific binding controls were as described earlier. The sandcastle worm glue is weakly autofluorescent. To avoid interference from this autofluorescence, the laser intensity and detector settings were adjusted to levels where the autofluorescence was not visible in unlabeled glue sections. The same laser and detector settings were then used to image the immunolabeled glue sections.

RESULTS

Adhesive gland morphology and secretion pathway

A TB-stained coronal section provides an overview of the adhesive gland system (Fig. 1A). The building organ is the distinct U-shaped structure, within which is the V-shaped mouth. Below the building organ a bowtie-shaped structure is outlined by a layer of distinct cell type. In the main adhesive gland, contained within large secretory cells clustered around the cavity of the first three parathoracic segments, heterogeneous granules were stained dark blue by the cationic dye and homogeneous granules were stained lighter blue. Cellular extensions containing single file heterogeneous or homogeneous granules lead from the major secretory cells to the building organ (Fig. 1D). The granules arrived intact and remained in separate channels around the entire circumference of the building organ (Fig. 1B). At least two additional secretory cell types, differentially stained by TB, were apparent between the base of the building organ and the bowtie (Fig. 1B). The first three, and only the first three, parapodia also stained strongly with TB (Fig. 1A). At higher magnification, multiple types of secretory cells, distinguished by the intensity of staining, were apparent in the anterior and posterior regions of each parapodia (Fig. 1C). The red metachromatic shift at the periphery of the anterior region is characteristic of TB-stained acidic carbohydrates and other acidic biomacromolecules (Bergeron and Singer, 1958). Parapodia posterior to the parathorax did not stain strongly with TB, which suggests the first three parapodia have specialized secretory functions. Nuclei throughout the entire section stain dark blue.

Dopa proteins and other quinonoids, at high pH in the presence of excess glycine, reduce NBT creating a deep blue formazan compound (Paz et al., 1991). Coronal sections of resin-embedded worms were stained with NBT/glycinate to reveal the distribution of dopa proteins in the parathorax. Both homogeneous and heterogeneous granules stained deep blue, outlining the three adhesive gland segments, the bundled channels and the building organ (Fig. 2). The small granules that originate from around the base of the building organ also stained darkly and appeared to be in channels moving toward the surface of the building organ (Fig. 2B). The posterior region of the three parathorax parapodia also stained with NBT (Fig. 2C).

Cells containing sub-micrometer secretory granules were observed by scanning electron microscopy of thin sections through the base of the building organ (Fig. 3A). The small granules were gathered at the edge of the building organ with the much larger heterogeneous and homogeneous granules, all of which emerged from separate channels still intact (Fig. 3B). Addition of dopamine

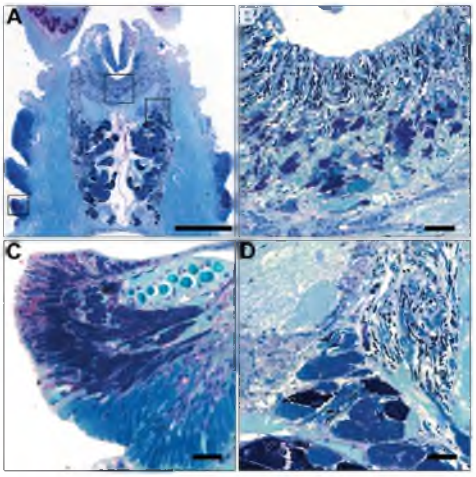

Fig. 1. Coronal section of parathorax stained with TB. (A) Low magnification image of the parathorax. (B) Higher magnification of the region in the top-center box in A. (C) Higher magnification of the parapodia secretory tissues in the region indicated by the bottom-left box in A. (D) Higher magnification of the cellular extensions in the region indicated by top-right box in A. Scale bars: A, 500 μm; B–D, 20 μm.

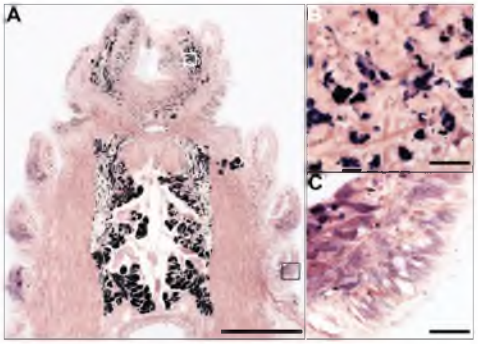

Fig. 2. Nitroblue tetrazolium chloride (NBT) labeling of dopa-containing cells in the parathorax. (A) Coronal cryosection stained with NBT. Redox active groups stain blue. (B) Higher magnification of small secretory granules in the region indicated by the upper box in A. (C) Higher magnification of the parapodia area indicated by the lower box in A. Scale bars: A, 500 μm; B and C, 20 μm.

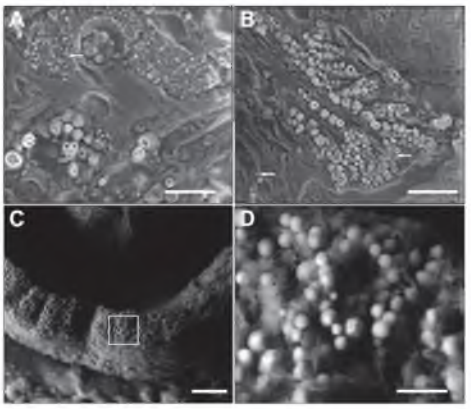

Fig. 3. Scanning electron microscope (SEM) imaging of adhesive precursor granules. (A) SEM image of a thin section through the base of the building organ. The arrow indicates a small granule-producing cell. (B) SEM image of a thin section through the adhesive precursor exit site of the building organ. The arrow indicates small granules in a secretory channel. (C) SEM image of the exterior of the building organ after stimulation of secretion. (D) Higher magnification of the region indicated by the white box in C. Scale bars: A, 10 μm; B, 15 μm; C, 50 μm; D, 5 μm.

to the external seawater caused intact homogeneous and heterogeneous granules to emerge from around the external periphery of the building organ (Fig. 3C,D). The small granules were not apparent and the large granules appeared to be partially embedded in fibrous material.

Expression analysis

Previously, 14 genes encoding proteins with characteristics of secreted structural proteins, a gene encoding a secreted laccase 2, and a gene encoding a cytoplasmic tyrosinase were identified by sequencing clones picked at random from a parathoracic cDNA library (Endrizzi and Stewart, 2009). Additional sequencing of random cDNA clones identified four additional complete open reading frames encoding proteins with characteristics of secreted structural proteins, as well as a second tyrosinase gene (Fig. 4). The new tyrosinase contained a signal peptide, in contrast to the cytoplasmic tyrosinase found earlier, which suggests it is secreted and functions externally.

As a first step in determining their role in the sandcastle worm glue, if any, the expression levels relative to actin of 16 of the putative glue protein genes were estimated by quantitative real-time PCR (Fig. 5). In the laboratory, healthy worms will rebuild damaged portions of their tubes if sand or glass beads are provided as building materials (Jensen and Morse, 1988). For quantitative expression analysis, mRNA was isolated from the parathoracic region only of worms actively rebuilding tubes in the lab to ensure active expression of glue protein genes. The Pc3A and Pc3B PCR primers were designed to amplify all variants of the transcripts (supplementary material Fig. S2). Pc1–5 and tyrosinase 1 had the highest expression levels, with Pc1 expressed at nearly the same level as actin (Fig. 5). Combined, expression of all variants of the polyphosphoserine proteins Pc3A and Pc3B was approximately 40% that of Pc1. Notably, tyrosinase 1 was the fourth most abundant transcript. Expression of all other genes, including the cytoplasmic tyrosinase 2 and laccase 2, was 1% or less than that of Pc1 and therefore they may not play major structural or enzymatic roles in glue formation (supplementary material Tables S3, S4). Further analysis of the low expression genes was not pursued.

In situ hybridization

Tissue and cellular expression sites were located by *in situ* hybridization with DIG-labelled RNA probes from unique regions

Pc19 MW 20,466 pI 6.98
MKLSIALVLFAVLVSSING
GGYGDNQGGYGGSIYIGQFTGKCGSDGLYS
MTENSYVSCTHGRAYVLPCAPGTLDRSGAL
CGVNLVDRGYAAVKSVTSVIK
GYGQSSGGHSGGG
GYGSSSGGYSSGGGYGYGSGGHSGGS
GYGSSSGGPSGGGGYGYSSGGHSGGS
GYGSSSGGYSGGSGGYEYSSGGHIGGS
GYGSSSGGYSGGSSGYGKSGGHEDSG

Pc21 MW 22,347 pI 7.62
MKFFILAACLALVYASGPVKDDDEYKETREYT
KEYTVDRNKGYNRK
GYGDDVSAKETFLRTTEYNDKD
GYGSKNDGKQVKESYTREYEIDKD
GYGKDDDVTGKETYRREVTVDDD
GYSPRGRYGRTDAY
GLNDGYVRKDAY
GLRRGP
GLGVYPGP
GLGRKDVYPATGLGRKDVYPVT
GLGRKDVYPATGLGRKDVYPAT

Pc22 MW 18,631 pI 5.32
MLVSLLLIGLVMIVRSDIHGLV
MEDAPGPSPSTSRVRESRDIHGLV
MEDAPGPSPSTSRVRESRDIHGLV
MEDAPGPSPSTSRVRESRDIHGLV
MEDAPGPSPSTSRVRESRDIHGLV
MEDAPGPSPSTSRVRESRDIHGLV
MEDAPGPSPSTSRVRESRDIHGLV
MEDAPGPS

Pc26 MW 30,252 pI 9.57
MKTLAIVTLAVAFCYANAILTNYGTGYGKI
GGVGGLG
HGGYGG
HGGYGG
HGGYGGHGVLAGHGGYGAHGVLAG
HGGYGGHGVLAGHGGYGGHGVLAG
HGGYGGHGILAGHGYGYG
KKGSSSSISSSDLYKHHHGYGT
SSSLSSSDLRRG
LGYGHHGHGYGYG
KSSSSSSSSSSSSSSSSSSSSSSSSSS
HYGRGYGHHGHHHGHSSSSISSSDLH
HGLHGYGYKSPTSSISSSDIHYHAKKLLLVTQCIC
GLGRKDVYPATGLGRKDVYPVP
GLGRKDVYPGPGLGRKGVYPGR
GFGVPGPFW

Tyrosinase like protein-1 MW 22,654 pI 8.37
MLFKIALLVLVCVFIIVTGFEDDETDLDKMKIMEEMIKEWKSDNDEIKFTPTQISYLNHLDNRGRGSGRGRGRGNVRGR
GNGQGRGKGNNRSKRQYEYLPVRKAYRHLSDSERKDFHDAIYQLKHTFSDPTSDLSNYDLFVNLHRSNSAPYAHGG
HAFAGWHRHCLYRFEKALQEINEDVTLCYLDTTMEYNVGR

Fig. 4. Putative secretory gland protein sequences. Underlined sequences indicate signal peptides. Accession numbers: Pc19, JN607210; Pc21, JN607211; Pc22, JN607212; Pc26, JF806320; and tyrosinase-like protein-1, JN607213. Red residues in tyrosinase-like protein-1 indicate conserved sequences in the copper binding sites of tyrosinases.

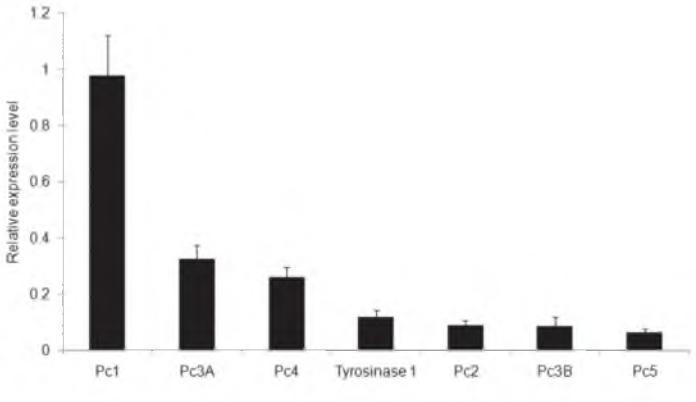

Fig. 5. Quantitative real-time PCR. Expression is normalized to that of actin (supplementary material Tables S3, S4).

of the Pc1–5 and tyrosinase 1 genes. Control DIG-labeled Pc3A sense RNA showed negligible background staining (Fig. 6A,B). The Pc1 probe strongly labeled the adhesive gland (Fig. 7A) and at higher magnification labeling occurred only in cells producing heterogeneous granules (Fig. 7B). The Pc2 probe hybridized only in cells producing homogeneous granules (Fig. 7C,D). Of the two major Pc3 variants, *in situ* hybridization was carried out only with the RNA of the most abundantly expressed variant, Pc3A, which labeled only those cells producing heterogeneous granules (Fig. 7E,F), consistent with elemental analysis (Wang et al., 2010). The Pc4 probe labeled heterogeneous granule cells. (Fig. 7G,H). The Pc5 probe labeled the adhesive gland unevenly and localized to homogeneous granule-producing cells (Fig. 7I,J). The tyrosinase 1 probe strongly labeled both heterogeneous and homogeneous granule-producing cells throughout the entire adhesive gland. Additionally, tyrosinase 1 labeling in the posterior region of the parathorax parapodia was unambiguous (Fig. 7K,L).

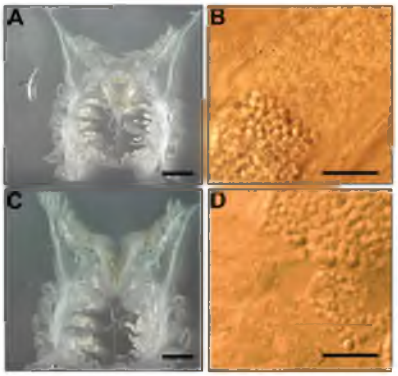

Fig. 6. *In situ* hybridization and immunostaining of negative controls. (A,B) *In situ* hybridization with sense strand Pc3A. (C,D) Immunostaining with anti-digoxigenin. Scale bars: A and C, 100 μm; B and D, 10 μm.

Immunohistochemistry

Antibodies against synthetic peptides predicted to be immunogenic were used to immunolocalize Pc2, Pc4 and Pc5. Highly repetitive, glycine-rich Pc1 did not have a sequence with a predicted high probability of generating an immune response; therefore, raising a peptide antibody to recognize Pc1 was not attempted. The synthetic Pc2, Pc4 and Pc5 peptides generated high-titer antibodies in rabbits. Specificity of the antibodies was verified on western blots with secretory granules isolated from the parathorax (Fig. 8). Anti-Pc2 recognized a pair of bands at ~21 kDa on western blots, consistent with its predicted molecular mass of 21.1 kDa. The anti-phosphoserine antibody recognized a band at ~15 kDa, perhaps corresponding to Pc3A. Anti-Pc4 and anti-Pc5 recognized single bands at ~25 and ~15 kDa bands, consistent with their predicted molecular masses of 24.3 and 14.9 kDa.

The Pc2 antibody produced punctate staining in the adhesive gland (Fig. 9A), which at closer examination localized only in the homogeneous granules (Fig. 9B), consistent with the *in situ* hybridization staining. Phosphorylation of serine is a common modification; therefore, weak staining occurred in much of the tissue with the generic anti-phosphoserine antibody that recognizes Pc3 (Fig. 9C). Nevertheless, close examination of the adhesive gland tissue revealed strong anti-phosphoserine staining of the heterogeneous granules and comparatively little staining of the homogeneous granules (Fig. 9D), consistent with *in situ* hybridization results and elemental mapping. Although it recognized a protein of the expected size on western blots of isolated granules (Fig. 8), anti-Pc4 labeled neither type of granule in tissue cryosections (Fig. 9F). Instead, it labeled the anterior region of the parathorax parapodia and the cells lining the bowtie of tissue below the building organ (Fig. 9E, Fig. 1A). Anti-Pc5 labeled only homogeneous granules (Fig. 9H). Tissue staining controls with anti-DIG as the primary antibody gave negligible background immunostaining (Fig. 6C,D).

A transverse section through the parathorax of a resin-embedded worm was treated with proteinase K, then probed with anti-Pc4. In contrast to cryosections of the adhesive gland (Fig. 9F), heterogeneous granules in the proteolyzed adhesive gland were immunolabeled with anti-Pc4 (Fig. 10A,B). The Pc4 epitope was apparently not accessible in cryosections, but became accessible after protease treatment of resin-embedded tissue. Tyrosinase 1 and Pc4 are both expressed in the first three parapodia. To sub-localize their expression in the

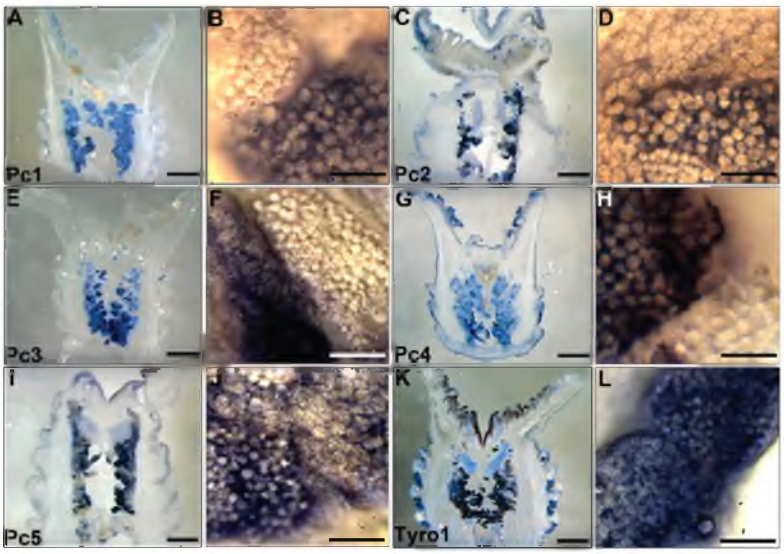

Fig. 7. *In situ* hybridization with highly expressed genes. (A,C,E,G,I,K) Low magnification of coronal cryosections. (B,D,F,H,J,L) Higher magnification of homongeneous and heterogeneous secretory granules. Probes are identified in the lower left of each panel. Scale bars: low magnification panels, 100 μm; high magnification panels, 10 μm.

parapodia, a cryosection was double-labeled with tyrosinase 1–DIG RNA and anti-Pc4 (Fig. 10C). Tyrosinase 1, visualized with an alkaline phosphatase secondary antibody and a blue chromogenic substrate, was expressed in the posterior base of the parathorax parapodia. Pc4, visualized with a far-red fluorescently labeled secondary antibody then false colored green for better contrast, was present in the anterior tips and did not overlap with tyrosinase 1.

Set and cured glue from glass beads that had been bonded by worms during tube reconstruction was recovered for immunolabeling by washing the beads. The glue spots were easily dislodged from the glass beads with 30% acetic acid. The glue was double–labeled with anti-phosphoserine (Pc3), secondarily labeled red, and anti-Pc2, anti-Pc4 or anti-Pc5, secondarily labeled green. The foam structure of the glue was readily apparent in the confocal images (Fig. 11). In several instances, distinct red rings around the pores were apparent inside a more evenly distributed green matrix. The presence of only small areas of yellow demonstrated that the phosphoserine staining (red) and Pc2, Pc4 and Pc5 (green) staining were mostly non-overlapping, and, by inference, the polyanionic and polycationic proteins were poorly mixed.

DISCUSSION

Protein localization

A total of 18 full-length transcripts from a parathorax cDNA library that encode proteins with general characteristics of secreted structural proteins have now been reported, as well as a tyrosinase 1 with a secretion signal peptide. A serine kinase that phosphorylates the polyserines of the Pc3 proteins remains conspicuously absent from the cDNA catalog. Not surprisingly, the most highly expressed structural proteins in healthy adult worms, actively rebuilding tubes, were the first six proteins discovered, either biochemically or through sequencing cDNAs (Fig. 5). The other structural proteins with low relative expression levels may be components of the chitinous cuticle, or chetae, and may be more highly expressed during rapid growth and/or development. Some time after gluing together the mineral tube the worm lines the interior of the tube with a fabric-like sheath. Little is known about the origin or composition of the sheath; some of the secreted structural proteins may be sheath components.

The localization of the highly expressed proteins is summarized schematically in Fig. 12. On the basis of *in situ* hybridization, polybasic Pc1 and Pc4 were unambiguously co-expressed with

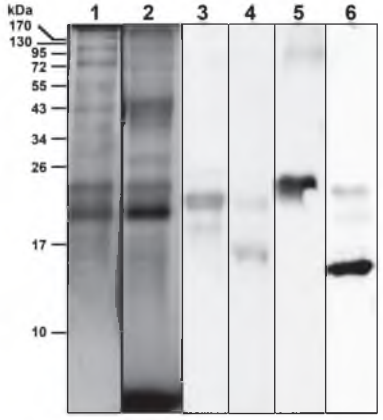

Fig. 8. Gel electrophoresis and western blot analysis of secretory granule proteins. Proteins in granules isolated from the parathorax region were separated by SDS-PAGE. Lanes: 1, Coomassie Blue; 2, NBT stain; 3, anti-Pc2; 4, anti-phosphoserine; 5, anti-Pc4; 6, anti-Pc5.

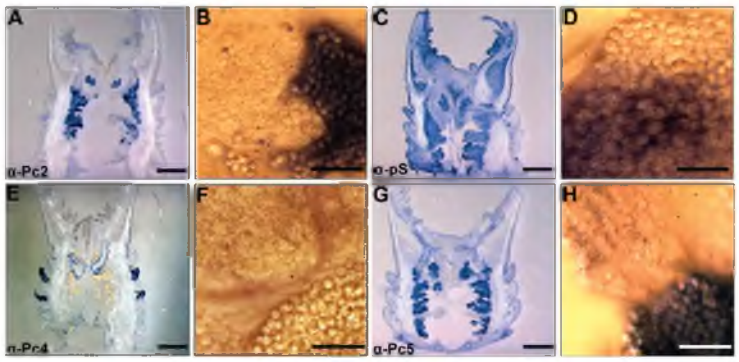

Fig. 9. Immunolabeling of parathorax cryosections. (A,C,E,G) Low magnification of coronal cryosections. (B,D,F,H) Higher magnification of heterogeneous and homogeneous secretory granules in the gland. Scale bars: low magnification panels, 100 μm; higher magnification panels, 10 μm.

polyacidic Pc3A in the cells producing heterogeneous granules. The Pc4 antibody, however, did not recognize either heterogeneous or homogeneous granules in tissue cryosections, although it did label a single band of the expected size on western blots of isolated granules and a region of the first three parapodia in tissue sections, and it convincingly labeled the secreted glue. The epitope was inaccessible in intact tissue secretory granules, but became accessible after denaturation for gel electrophoresis and after protease treatment of the adhesive gland, which localized Pc4 to the heterogeneous granules, consistent with *in situ* hybridization. Exposure of the epitope in the secreted glue may have resulted from the processing of the secreted glue for immunolabeling. The more interesting possibility is that the cryptic epitope was exposed as a result of a structural reorganization concomitant with secretion of the glue. If so, the Pc4 antibody may be a useful probe for glue maturation in future experiments. Its presence in the parapodia suggests Pc4, the fourth most abundantly expressed protein, may be a component of multiple materials secreted by the sandcastle worm. Interestingly, the epitope was not hidden in non-proteolyzed parapodia tissue. Of significance, perhaps, the absence of co-localized NBT staining in the anterior of the thorax parapodia suggests Pc4 does not contain a significant number of dopa residues, at least in the parapodia. Polybasic, histidine-rich Pc2 and Pc5 proteins are both components of the homogeneous granules, as well as the final secreted glue. In short, immunolocalizaton provided definitive evidence for a direct role of Pc2, Pc4 and Pc5 in the formation and structure of the final glue.

The relatively high expression of tyrosinase 1 in heterogeneous and homogeneous granule-producing cells of adults actively synthesizing glue suggests it may have a direct role in the curing, and perhaps even the structure, of the secreted glue. Secreted as a viscous, milky white fluid, the glue turns progressively more reddish brown over several hours, presumably as a result of covalent curing of the glue through quinonic cross-linking. Tyrosinases can catalyze two reactions, the hydroxylation of tyrosines to form dopa, and the further oxidation of dopa to form reactive dopaquinones that undergo Michael addition with nucleophilic sidechains, and other reactions (Sanchez-Ferrer et al., 1995). Covalent cross-linking of the structural dopa proteins may be catalyzed by the tyrosinase, which may be activated during co-secretion. The mussel provides a precedent for such a mechanism. The mussel byssus contains an extractable catechol oxidase activity (Waite, 1985). The mussel enzyme was described as a catechol oxidase because it lacks tyrosine hydroxylase activity. It remains to be determined whether the sandcastle tyrosinase has both oxidase activities. The mussel catechol oxidase is co-packaged in secretory granules with dopa proteins and co-secreted, whereupon it is activated to catalyze dopa-mediated cross-linking (Waite, 1992). The activation trigger for the granular oxidase enzymes, in mussels and sandcastle worms, may be the pH jump that occurs during secretion – from the low pH of secretory granules to the higher external pH – as suggested for other granular enzymes (Johnson et al., 1980; Kelly, 1987). Expression in the parapodia suggests tyrosinase 1, like Pc4, may have multiple functions, perhaps in quinonic tanning of the tube lining. The secreted tyrosinase may be the phenoloxidase activity reported by Vovelle in the sabellarid *Sabellaria aveolata* (Vovelle, 1965).

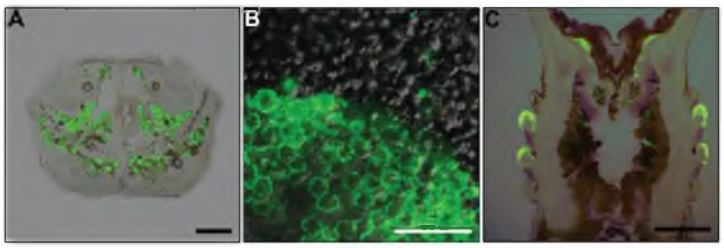

Fig. 10. Localization of Pc4 in proteolyzed tissue. (A) Anti-Pc4 labeling (green) of a resin-embedded transverse section treated with proteinase K. (B) Higher magnification of A. Anti-Pc4 labeled only heterogeneous granules (green). (C) Anti-Pc4 immunolabel (green) overlaid on tyrosinase 1 *in situ* hybridization (purple–dark blue). Scale bars: A and C, 250 μm; B, 10 μm.

Formation of the sandcastle worm glue

The precursors of the sandcastle worm glue are products of the regulated secretory system, which is the secretion pathway for proteins that are released in bursts at rates much faster than protein synthesis. The proteins destined for regulated secretion are concentrated as much as 200-fold during transit from the Golgi apparatus to mature secretory vesicles (Kelly, 1985). The cytoplasm becomes packed with dense secretory vesicles because of their relatively long half-life. It is well known that condensation of proteins into dense secretory granules is, in general, driven by low pH and electrostatic charge neutralization between oppositely charged polyions (Gorr et al., 2005). Mucin, as an example, is an acidic polyanionic glycoprotein condensed into granules through charge shielding by H^+ and divalent Ca^{2+}. Sulfated proteoglycans are polyanionic components of numerous secretory cell types that condense polycationic secreted proteins (Reggio and Dagorn, 1978). In addition to the contribution of low secretory vesicle pH, the requisite condensation of the sandcastle worm glue proteins into the heterogeneous granules could proceed through several electrostatic interactions: polybasic Pc1 and Pc4 may be components of a matrix that neutralize and condense the polyphosphates; or, polyphosphorylated Pc3 may be neutralized and condensed by divalent Mg^{2+} as suggested by colocalization of Mg^{2+} with phosphate exclusively in subgranules; or, as a polyampholyte with acidic and basic domains, Pc3A could self-condense into granules. Of course, more than one of these condensing mechanisms could be operative. What is the counter polyanion that condenses polycationic Pc2 and Pc5 in the homogeneous granules? One possibility is that the secreted glue may contain a significant amount of sulfur (Stewart et al., 2011), the source of which could be an unidentified sulfated proteoglycan that condenses the polybasic proteins.

The final set glue is a solid foam with a mix of open and closed pores, with diameters ranging from less then 1 to greater than 6 μm (Stevens et al., 2007). The average pore diameter, ~2 μm, is roughly the same diameter as the homogeneous and heterogeneous granules, but much larger than the polyphosphate/Mg-containing sub-granules. Vovelle reported that the sub-granules swelled after secretion and became the pores of the foamy adhesive mass, while the contents of the homogeneous granules formed a matrix around the pores (Vovelle, 1965). Vovelle's observations are supported by the apparent concentration of polyphosphoserine around the walls of the pores and the non-overlapping distribution of the polybasic proteins observed by immunolocalization (Fig. 11). If the glue was well mixed, as arising from a fluid complex coacervate precursor, the fluorescence would have appeared mostly yellow from the blending of the red and green labels. Instead, for the most part, red and green are distinct with all three antibodies against polybasic proteins. Similarly, the granular components of fresh glue, derived by electrical stimulation of secretion, stained differentially with cationic TB, and also appeared to be poorly mixed (Wang et al., 2010). A caveat is that the polybasic Pc1 protein, highly expressed in heterogeneous granule cells, has not been immunolocalized; therefore, intimate complexation with Pc3A,B in the secreted glue cannot be ruled out.

The detailed mechanisms that cause the granules to swell and aggregate after secretion, turn into a load-bearing glue within 30 s (Stevens et al., 2007), then covalently cure over several hours into a solid foam, are unknown and likely complex. Comparatively well-studied mucin secretion serves as a starting point for discussion. Mucin granules are secreted intact and under normal physiological conditions swell several hundredfold within tens of milliseconds as a result of an influx of water driven by a Donnan potential (Tam and Verdugo, 1981). The sudden swelling has been described as a critical phenomenon; a 'jack-in-the-box' discontinuous transition from the condensed state to an expanding state – a phase transition unlatched by small changes in environmental conditions (Verdugo, 1991). Accordingly, during mucin exocytosis, exposure to extracellular Na^+ displaces Ca^{2+} in the condensed granules, triggering the transition into small hydrated gels that subsequently anneal into a continuous mass. Similar ion-triggered critical swelling phenomena have been studied in synthetic hydrogels (Tanaka and Fillmore, 1979). For completeness, specific interactions between mucin chains, in addition to Ca^{2+}/H^+ charge shielding, contribute to condensation and expansion (Kesimer et al., 2010).

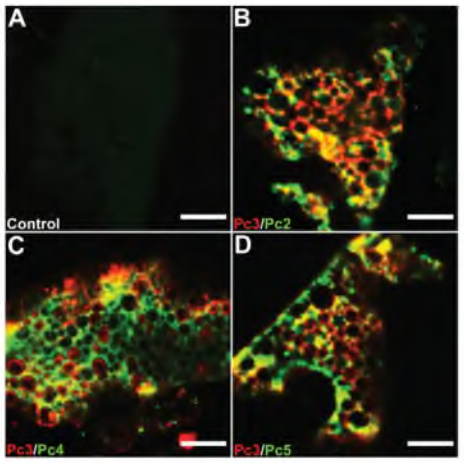

Fig. 11. Glue immunolabeling. (A) Negative controls. (B–D) Double immunolabel with (B) anti-Pc2 (green) and anti-phosphoserine (red), (C) anti-Pc4 (green) and anti-phosphoserine (red), (D) anti-Pc5 (green) and anti-phosphoserine (red). Scale bars: A–D, 20 μm.

In broad outline, similar mechanisms may be operative in the swelling and aggregation of the sandcastle worm glue granules. Upon secretion into seawater, the granules are exposed to approximately 0.5 mol l^{-1} monovalent Na^+ and Cl^- ions and pH>8, which would have pronounced effects on ionic and electrostatic interactions within the glue. The spike in external ionic strength may disrupt some electrostatic interactions; perhaps between phosphate sidechains and Mg^{2+}, causing the heterogeneous sub-granules to swell as Mg^{2+} is exchanged for Na^+ with an accompanying osmotic influx of water. The nominal pK_a of Pc4 histidines and the nominal second pK_a of Pc3A,B phosphoserines lie between the internal pH of secretory granules (assumed to be low as in other secretory granules) and the elevated pH of seawater, which may effect an increase in the net negative charge of the glue upon secretion that contributes to an influx of Na^+ and water. But none of this explains why heterogeneous sub-granules swell like balloons into polyphosphoserine-lined pores. Further, an influx of water seems counter-productive to formation of a strong glue. Segregation of water, somehow, into the pores of the foam structure may minimize the effects of dilution on cohesive integrity. A solid foam structure may be mechanically and metabolically advantageous (Stewart et al., 2004; Stevens et al., 2007).

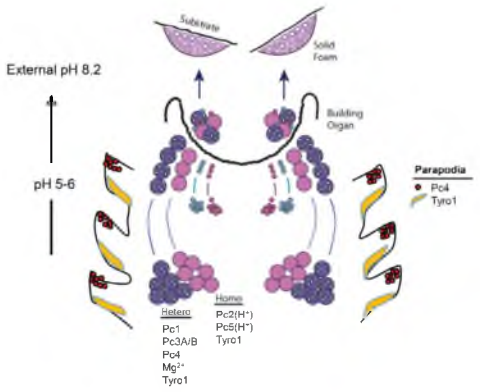

Fig. 12. Summary of adhesive precursor localization.

The rapid setting and slower cure of the secreted glue can proceed through one or more of several speculative pathways. First, associative gelling of the adhesive could occur through electrostatic interactions between the polyphosphates (Pc3A,B) in the heterogeneous granules and the polyamines (Pc2,5) in the homogeneous granules. The worm wiggles newly placed particles as if checking the set before letting go (Stevens et al., 2007). This process could physically facilitate partial mixing of the granule contents and initial gellation. Second, Mg^{2} and polyphosphate are soluble at low pH but insoluble at pH 8.2 in 450 mmol l^{-1} NaCl (Stewart et al., 2010). Transition of Pc3A,B from a gel-like state to an insoluble complex would harden the initially fluid glue, though this mechanism seems contradictory to swelling induced by Mg^{2} /Na exchange. Third, the secreted glue contains significant quantities of transition metals, including Fe, Mn, Zn and Cu (Stewart et al., 2011). Fe is concentrated 10^{5}-fold in the glue relative to seawater; the others are concentrated 10^{3}- to 10^{4}-fold. Formation of intermolecular histidine–transition metal coordination complexes, as the imidazolyl sidechains are deprotonated by the pH increase upon secretion, would provide rapid pH-triggered cohesive integrity. There is also potential for the formation of tris-dopa–Fe(III) coordination complexes, as demonstrated in the mussel adhesive plaque proteins (Harrington et al., 2010; Wilker, 2010; Zeng et al., 2010). The Fe to dopa molar ratio in the sandcastle worm glue was estimated to be between 1:5 and 1:10 (Stewart et al., 2011). Fourth, as discussed earlier, the co-secreted tyrosinase could catalyze quinonic cross-linking during secretion. Both heterogeneous and homogeneous granules are fluorescent while still in the secretory cells of the adhesive gland. One source of this fluorescence could be quinone cross-links, which suggests the adhesive proteins may be partially cross-linked before secretion.

CONCLUSIONS

The glue with which sandcastle worms build composite mineralized tubes consists of oppositely charged polyelectrolytes, distinguished by extremely phosphorylated proteins and a set of polyamino proteins. The components are separately packaged into at least four co-secreted parts, though the complete significance of the pre-secretion separation remains obscure. The involvement of polyelectrolytes and electrostatic interactions may be a general theme in natural underwater bioadhesives. In addition to the sandcastle worm glue, several other natural bioadhesive examples suggest phosphatidyl side-chains may contribute specific and advantageous functionalities to underwater adhesives; functionalities that include ionic strength-independent interfacial adhesion, formation of electrostatic complexes with polyamines, formation of coordination complexes with metal ions, and pH-dependent solubility with divalent Ca^{2} /Mg^{2} (Stewart et al., 2011). The greatest advantage, compared with other acidic functional groups, may be a nominal pK_{a2} close to neutral pH, which allows the chemical functionality of peptidyl phosphates to be modulated by small, near-physiological pH changes. Covalent curing of the sandcastle worm glue subsequent to secretion may be catalyzed by a co-secreted tyrosinase. As a final point, the regulated secretory system, in numerous cases based on electrostatic condensation of polyions, may have been a pre-adaptation upon which bioadhesives based on oppositely charged polyelectrolytes evolved. Correlatively, the requirement for intracellular condensation of secreted proteins may have restricted the composition of underwater bioadhesives secreted *via* the regulated pathway to paired oppositely charged polyelectrolytes, a general observation that may inform characterization of other natural underwater adhesives. The identification and localization of the sandcastle worm glue components mark a path for detailed experiments to sort through the potential mechanisms of sandcastle worm glue formation and curing in the first few 10s of seconds after secretion.

ACKNOWLEDGEMENTS

We thank Dr Chris Rodesch for help with confocal microscopy (Cell Imaging Core Facility, University of Utah), Eric Gibbons for help with SEM imaging (Surface and Nanoimaging Facilty, University of Utah) and Nancy Chandler for help with specimen preparation (Electron Microscopy Facility, University of Utah).

FUNDING

Funding from the National Science Foundation [DMR-0906014] is gratefully acknowledged.

REFERENCES

Bergeron, J. A. and Singer, M. (1958). Metachromasy: an experimental and theoretical reevaluation. *J. Biophys. Biochem. Cytol.* **4**, 433-457.
Case, S. T., Powers, J., Hamilton, R., Burton, M. J. (1994). Silk and silk proteins from two aquatic insects. In *ACS Symposium Series*, Vol. 544. Washington, DC: American Chemical Society.
Endrizzi, B. J. and Stewart, R. J. (2009). Glueomics: an expression survey of the adhesive gland of the sandcastle worm. *J. Adhes.* **85**, 546-559.
Fewkes, J. W. (1889). New Invertebrata from the coast of California. *Bull. Essex Inst.* **21**, 99-147.
Flammang, P., Lambert, A., Bailly, P. and Hennebert, E. (2009). Polyphosphoprotein-containing marine adhesives. *J. Adhes.* **85**, 447-464.
Galler, R., Rydlander, L., Riedel, N., Kluding, H. and Edstrom, J. E. (1984). Balbiani ring induction in phosphate metabolism. *Proc. Natl. Acad. Sci. USA* **81**, 1448-1452.
Gorr, S. U., Venkatesh, S. G. and Darling, D. S. (2005). Parotid secretory granules: crossroads of secretory pathways and protein storage. *J. Dent. Res.* **84**, 500-509.
Harrington, M. J., Masic, A., Holten-Andersen, N., Waite, J. H. and Fratzl, P. (2010). Iron-clad fibers: a metal-based biological strategy for hard flexible coatings. *Science* **328**, 216-220.
Jensen, R. A. and Morse, D. E. (1988). The bioadhesive of *Phragmatopoma californica* tubes: a silk-like cement containing L-DOPA. *J. Comp. Physiol. B* **158**, 317-324.
Johnson, R. G., Carty, S. E., Fingerhood, B. J. and Scarpa, A. (1980). The internal pH of mast cell granules. *FEBS Lett.* **120**, 75-79.
Kelly, R. B. (1985). Pathways of protein secretion in eukaryotes. *Science* **230**, 25-32.
Kelly, R. B. (1987). Protein transport. From organelle to organelle. *Nature* **326**, 14-15.
Kesimer, M., Makhov, A. M., Griffith, J. D., Verdugo, P. and Sheehan, J. K. (2010). Unpacking a gel-forming mucin: a view of MUC5B organization after granular release. *Am. J. Physiol. Lung Cell Mol. Physiol.* **298**, L15-L22.
Lee, B. P., Messersmith, P. B., Israelachvili, J. N. and Waite, J. H. (2011). Mussel-inspired adhesives and coatings. *Annu. Rev. Mater. Res.* **41**, 99-132.
Paz, M. A., Fluckinger, R., Boak, A., Kagan, H. M. and Gallop, P. M. (1991). Specific detection of quinoproteins by redox-cycling staining. *J. Biol. Chem.* **266**, 689-692.
Reggio, H. and Dagorn, J. C. (1978). Ionic interactions between bovine chymotrypsinogen A and chondroitin sulfate: a possible model for molecular aggregation in zymogen granules. *J. Cell Biol.* **78**, 951-957.

Rozen, S. and Skaletsky, H. J. (2000). Primer3 on the WWW for general users and for biologist programmers. In *Bioinformatics Methods and Protocols: Methods in Molecular Biology* (ed. S. Krawetz and S. Misener), pp. 365-386. Totowa, NJ: Humana Press.
Sanchez-Ferrer, A., Rodriguez-Lopez, J. N., Garcia-Canovas, F. and Garcia-Carmona, F. (1995). Tyrosinase: a comprehensive review of its mechanism. *Biochim. Biophys. Acta* **1247**, 1-11.
Shao, H., Bachus, K. N. and Stewart, R. J. (2009). A water-borne adhesive modeled after the sandcastle glue of *P. californica*. *Macromol. Biosci.* **9**, 464-471.
Stevens, M. J., Steren, R. E., Hlady, V. and Stewart, R. J. (2007). Multiscale structure of the underwater adhesive of *Phragmatopoma californica*: a nanostructured latex with a steep microporosity gradient. *Langmuir* **23**, 5045-5049.
Stewart, R. J. and Wang, C. S. (2010). Adaptation of caddisfly larval silks to aquatic habitats by phosphorylation of h-fibroin serines. *Biomacromolecules* **11**, 969-974.
Stewart, R. J., Weaver, J. C., Morse, D. E. and Waite, J. H. (2004). The tube cement of *Phragmatopoma californica*: a solid foam. *J. Exp. Biol.* **207**, 4727-4734.
Stewart, R. J., Wang, C. S. and Shao, H. (2010). Complex coacervates as a foundation for synthetic underwater adhesives. *Adv. Colloid. Interface. Sci.* **167**, 85-93.
Stewart, R. J., Ransom, T. C. and Hlady, V. (2011). Natural underwater adhesives. *J. Polym. Sci. Pol. Phys.* **49**, 757-771.
Tam, P. Y. and Verdugo, P. (1981). Control of mucus hydration as a Donnan equilibrium process. *Nature* **292**, 340-342.
Tanaka, T. and Fillmore, D. J. (1979). Kinetics of swelling of gels. *J. Chem. Phys.* **70**, 1214-1218.
Verdugo, P. (1991). Mucin exocytosis. *Am. Rev. Respir. Dis.* **144**, S33-S37.
Vovelle, J. (1965). Le tube de *Sabellaria alveolata* (L.) Annelide Polychete Hermellidae et son ciment. Etude ecologique, experimentale, histologique et histochimique. *Arch. Zool. Exp. Gen.* **106**, 1-187.
Waite, J. H. (1985). Catechol oxidase in the byssus of the common mussel, *Mytilus edulis* L. *J. Mar. Biol. Assoc. UK* **65**, 359-371.
Waite, J. H. (1992). The formation of mussel byssus: anatomy of a natural manufacturing process. *Results Probl. Cell Differ.* **19**, 27-54.
Waite, J. H., Jensen, R. A. and Morse, D. E. (1992). Cement precursor proteins of the reef-building polychaete *Phragmatopoma californica* (Fewkes). *Biochemistry* **31**, 5733-5738.
Waite, J. H., Andersen, N. H., Jewhurst, S. and Sun, C. (2005). Mussel adhesion: finding the tricks worth mimicking. *J. Adhes.* **81**, 297-317.
Wang, C. S., Svendsen, K. K. and Stewart, R. J. (2010). Morphology of the adhesive system in the sandcastle worm, *Phragmatopoma californica*. In *Biological Adhesive Systems: From Nature to Technical and Medical Applications* (ed. J. von Byern and I. Grunwald). New York: Springer.
Wilker, J. J. (2010). Marine bioinorganic materials: mussels pumping iron. *Curr. Opin. Chem. Biol.* **14**, 276-283.
Winslow, B. D., Shao, H., Stewart, R. J. and Tresco, P. A. (2010). Biocompatibility of adhesive complex coacervates modeled after the sandcastle glue of *Phragmatopoma californica* for craniofacial reconstruction. *Biomaterials* **31**, 9373-9381.
Yonemura, N., Sehnal, F., Mita, K. and Tamura, T. (2006). Protein composition of silk filaments spun under water by caddisfly larvae. *Biomacromolecules* **7**, 3370-3378.
Zeng, H., Hwang, D. S., Israelachvili, J. N. and Waite, J. H. (2010). Strong reversible Fe^{3+}-mediated bridging between dopa-containing protein films in water. *Proc. Natl. Acad. Sci. USA* **107**, 12850-12853.
Zhao, H., Sun, C., Stewart, R. J. and Waite, J. H. (2005). Cement proteins of the tube-building polychaete *Phragmatopoma californica*. *J. Biol. Chem.* **280**, 42938-42944.

CHAPTER 4

MULTIPART COPOLYELECTROLYTE ADHESIVE OF THE SANDCASTLE WORM, *PHRAGMATOPOMA CALIFORNICA* (FEWKES): CATECHOL OXIDASE CATALYZED CURING THROUGH PEPTIDYL-DOPA

BioMACROMOLECULES

Article

pubs.acs.org/Biomac

Multipart Copolyelectrolyte Adhesive of the Sandcastle Worm, *Phragmatopoma californica* (Fewkes): Catechol Oxidase Catalyzed Curing through Peptidyl-DOPA

Ching Shuen Wang and Russell J. Stewart*

Department of Bioengineering, University of Utah, 20 South 2030 East, Room 506C, Salt Lake City, Utah 84112, United States

Supporting Information

ABSTRACT: Tube-building sabellariid polychaetes have major impacts on the geology and ecology of shorelines worldwide. Sandcastle worms, *Phragmatopoma californica* (Fewkes), live along the western coast of North America. Individual sabellariid worms build tubular shells by gluing together mineral particles with a multipart polyelectrolytic adhesive. Distinct sets of oppositely charged components are packaged and stored in concentrated granules in separate cell types. Homogeneous granules contain sulfated macromolecules as counter-polyanion to polycationic Pc2 and Pc5 proteins, which become major components of the fully cured glue. Heterogeneous granules contain polyphosphoproteins, Pc3A/B, paired with divalent cations and polycationic Pc1 and Pc4 proteins. Both types of granules contain catechol oxidase that catalyzes oxidative cross-linking of L-DOPA. Co-secretion of catechol oxidase guarantees rapid and spatially homogeneous curing with limited mixing of the preassembled adhesive packets. Catechol oxidase remains active long after the glue is fully cured, perhaps providing an active cue for conspecific larval settlement.

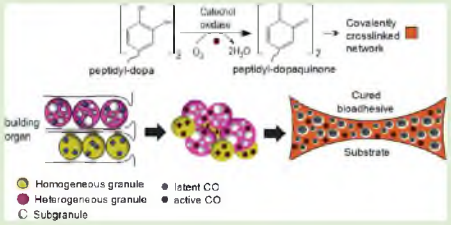

INTRODUCTION

Sabellariidae polychaetes are gregarious, reef-building tubeworms. Individual worms live in composite tubular shells constructed with sandgrains, comminuted shells, and a secreted underwater bioadhesive. The particles used in construction are captured from the turbulent water column with ciliated tentacles and transported to the building organ near the mouth.[1] The building organ is a dexterous pair of opposed appendages used to evaluate the size, shape, and surface of the particles (Figure 1C). Satisfactory particles are precisely pressed onto the end of the existing tube in the best position and orientation to minimize gaps in the construction. Minute aliquots of the bioadhesive[2] are then applied at points of direct contact between the new particle and the edge of the existing tube and only at points of contact (Figure 1C). The bioadhesive of existing tubes contain settlement cues that induce planktonic sabellariid larva of the same species to settle, undergo metamorphosis, and initiate construction of new tubes.[3] Preferential settlement on the periphery of the colony results in lateral expansion of initially mound-like colonies into table-like structures that can cover an entire beach (Figure 1A). Sabellariid sandtube reefs can extend continuously for hundreds of kilometers, parallel to the shore, and occur along coastlines worldwide, with the exception of the artic.[4,5] The wave-resistant intertidal structures,[6] which can be more than 2 m high, have a major impact on stabilization and evolution of the beach environment. The sandtube reefs dissipate wave energy, modify local hydrodynamics, filter and trap sediments, and provide habitat for a rich fauna within the interstices of the sandtube reef and in their immediate proximity.[7] Lithification of dead sabellariid reefs can extend the beach foundation seaward and provides a hard substrate for new colony formation.[4] Through their collective, one-sandgrain-at-a-time masonry, the sabellariidae tubeworms are major geoengineers of the world's coastlines.

The bioadhesive produced by *Phragmatopoma californica* (Fewkes), a sabellariid that lives off the coast of western North America, consists of at least six highly repetitive and oppositely charged polyelectrolytic proteins: Pc1, 2, 4, and 5 are lysine- and histidine-rich polycations, Pc3B is a polyanion consisting entirely of 6−12 residue phosphoserine blocks separated by single tyrosine residues, and Pc3A is a diblock polyampholyte with a polyphosphoserine-rich N-terminus and a lysine- and arginine-rich C-terminus of roughly equal size.[8−10] The components of the multipart sabellariid bioadhesive transit through the regulated secretory pathway, wherein they are packaged into micrometer-sized granules and stored in two distinct secretory cell types within the parathorax. The cells are distinguished by the morphology and contents of their granules.[11−13] "Homogeneous" granules have a uniform appearance and contain the polycationic Pc2 and Pc5 proteins. "Heterogeneous" granules, which have a mottled appearance

Received: February 18, 2013
Revised: March 20, 2013
Published: March 26, 2013

dx.doi.org/10.1021/bm400251k | *Biomacromolecules* 2013, 14, 1607−1617

(A) Photo courtesy of Dr. Jérôme Fournier.

Figure 1. Reef-building sabellariid tubeworms. (A) Lateral growth of isolated dome-shaped colonies of *S. alveolota* (foreground) leads to fusion of colonies into a continuous tabular surface covering the beach. (B) Closer view of a colony of *P. californica*. Each tube contains an individual worm. (C) Left: *P. californica* removed from tubular shell. White bracket indicates parathorax region that contains the adhesive gland. Right: Zirconium oxide beads have been glued onto the anterior end of the natural tube. Arrow indicates the operculum.

due to polydisperse subgranules, contain the polycationic Pc1 and Pc4 proteins and the polyphosphorylated Pc3A/B proteins. The Pc3 phosphoproteins are concentrated with Mg^{2+} in the subgranules of the heterogeneous granules.[14]

Each secretory cell stores hundreds of the dense membrane-bound packets, prepared for "burst" delivery of the bioadhesive components. When signaled, the adhesive packets are delivered, apparently intact, through the surface of the building organ directly from each secretory cell body after traveling through long, narrow cellular extensions structurally analogous to the axons of a nerve cell. The cellular extensions, and adhesive exit points, are distributed around the entire circumference of the building organ, interspersed with columnar epithelial cells that have clusters of paddle-ended cilia.[14] There is no common duct, or storage gland, in the secretion pathway where mixing of the separate components can occur before secretion. Similar cellular organization, morphologies, and secretion of intact granules have been observed in several examples of invertebrate bioadhesives secreted directly through epithelial surfaces.[15−17] The distinct contents of the homogeneous and heterogeneous granules do not mix until after they exit the building organ, whereupon they fuse together, partially mix (perhaps facilitated by the paddle-ended cilia), and set up into a liquid-filled solid foam in less than 30 s.[2,11]

Sabellariidae bioadhesives contain 3,4-dihydroxy-L-phenylalanine (L-DOPA) residues,[18] a feature they share with the bioadhesive byssal plaques of dreissenid[19] and mytilid mussels.[20] The role of L-DOPA in interfacial adhesion of the mussel bioadhesive has spawned widespread interest in synthetic "mussel-inspired" materials with pendant catechol side chains.[21−28] Of the *P. californica* bioadhesive proteins, only Pc1 and Pc2 have been directly demonstrated to contain L-DOPA residues, at a little less than 10 mol % each.[29] The reddish darkening of the bioadhesive after secretion implies a role for DOPA in oxidative curing through dopaquinone intermediates. It has also been suggested that DOPA-derived aromatic compounds may be the specific settlement cue recognized by larva in conspecific tubes.[3]

Consistent with a role for the peptidyl-DOPA in covalent cross-linking of the bioadhesive, a gene encoding a tyrosinase homologue with a secretion signal peptide, was highly expressed in both the homogeneous and heterogeneous secretory cells.[11] Tyrosinases (also called phenoloxidases) are ubiquitous multicopper oxidases, distributed throughout all kingdoms of life. They are members of the type 3 copper protein family, related by a structurally homologous active site that contains a pair of coupled copper ions coordinated by conserved histidine residues in a 4 α-helix bundle motif. The oxy form of the active site, with an activated O_2 molecule bound side-on between the two Cu(II) ions, is capable of binding either phenol or catechol substrates to initiate two distinct reactions: the ortho-hydroxylation of tyrosine to DOPA (monophenoloxidase activity) and the oxidation of DOPA to dopaquinone (catechol oxidase activity).[30−32] Although the bicopper active sites are virtually identical, some type 3 copper oxidases (tyrosinases) bind phenols and sequentially catalyze both phenol hydroxylation and catechol oxidation reactions, while other type 3 copper oxidases (catechol oxidases) only bind catechol substrates and catalyze only catechol oxidation.

The goals of the research described here were to identify additional components of the *P. californica* bioadhesive, to characterize the organization and interactions between the components, before secretion, as packaged in their natural context, and to determine if tyrosinase plays a direct role in adhesive curing. The results are crucial for understanding the dynamic biochemical events that occur within the first few tens of seconds after secretion, as the bioadhesive parts interact, set, and cure into a liquid-filled solid foam. Studies of the *P. californica* bioadhesive are motivated, in part, by its potential as a source of chemical insight and design principles for developing synthetic underwater adhesives.[33−35] In this context, holistic understanding of the biological assembly of the micrometer-sized adhesive packets may provide insight into new strategies for packaging, storage, and controlled curing systems for long self-life, self-initiating, water-borne adhesives.

■ EXPERIMENTAL SECTION

Materials. Basketball-sized fragments of live *Phragmatoma californica* colonies were collected near Santa Barbara, California, and shipped overnight on ice to Salt Lake City, UT. The colonies were maintained in a laboratory aquarium with circulating artificial salt water (Instant Ocean, Blacksburg, VA) at 14 °C. Hyaluronic acid (HA), heparan sulfate (HS), Alcian Blue (AB), L-tyrosine, L-3,4-dihydroxyphenylalanine (L-DOPA), 2,2′-azino-bis-3-ethylbenzothiazoline-6-sulfonic acid (ABTS), phenylthiourea (PTU), salicylhydroxamic acid (SHAM), cetyltrimethylammonium bromide (CTAB), arbutin, paraformaldehyde, proteinase K, mushroom tyrosinase, and laccase were purchased from Sigma Aldrich, Inc. (St. Louis, MO). Molecular biology grade agarose was purchased from ISC Bioexpress (Kaysville, UT).

Elemental Analysis of *P. californica* Glue. Individual tubes with their resident worms were carefully removed from the colony and placed on a layer of 0.5 mm Yttrium Stabilized Zirconia beads (YSZ; Inframat Advanced Materials, Farmington, CT) in a glass dish submerged in a saltwater aquarium. The beads were washed with ethanol, soap, and deionized water prior to placement in the dish. The worms separated from the colony compulsively rebuild their tube by gluing beads to the anterior end of the natural tube segment (Figure

dx.doi.org/10.1021/bm400251k | *Biomacromolecules* 2013, 14, 1607−1617

1C). The freshly bonded beads were retrieved after 12−24 h, washed at least three times in excess 10 mM Tris (pH 8.2) to remove seawater, and lyophilized. Beads from multiple animals were pooled. The beads from the same dish, untouched by the worms, were collected at the same time for background measurements. The collected beads were visually inspected under a dissecting microscope (20×) to ensure there was no nonbead material incorporated into the tube by the worms. Equal quantities by weight of the glued beads and nonglued background beads (~1000 beads per sample) were boiled in 250 μL of concentrated nitric acid for 60 min to digest the glue, then mixed with 650 μL of deionized water. The samples were analyzed by inductively coupled plasma optical emission spectroscopy (ICP-OES, Perkin-Elmer Optima 3100 XL) calibrated with standards for Ca, Co, Cd, Cu, Fe, Mg, Mn, Ni, Zn, S, P, Ag, and Se. Four independent samples of glued and unglued background beads were analyzed. Concentrations of the elements are reported in ppm per dry weight of the glue. Dry weight was determined by subtracting the weight of 1000 unglued beads from 1000 glued beads.

Alcian Blue Staining. To ensure polysulfate could be distinguished from polyphosphate by alcian blue, staining controls were done with known polyelectrolytes. Hyaluronic acid, heparan sulfate, and polyphosphoacrylamide[36] were dissolved (50 μg/mL each) with agarose (0.8 w/v%) by heating. After complete dissolution, the agarose solutions were transferred to a mold for solidification at room temperature. The agarose gel blocks were stained with Alcian Blue (0.05 wt %) in either 0.1 N HCl (pH ~1) or 10% acetic acid (pH ~4) overnight at room temperature. The agarose gel blocks were destained with either 0.1 N HCl or 10% acetic acid overnight at room temperature.

Worms were carefully removed from their tubes and rinsed with filtered artificial seawater three times before fixation in 4% paraformaldehyde overnight at 4 °C. After fixation, the worms were dehydrated in a series of ethanol solutions (50, 70, 95, and 100%) at room temperature. The dehydrated worms were embedded in Immuno-Bed (PolyScience, Inc. Warrington, PA) according to the manufacturer's instructions. Coronal sections (1 μm) through the parathoracic region were dehydrated with serial ethanol solutions at room temperature for 2 min each to remove unpolymerized resin. The sections were then rehydrated with PBS (pH 7.2) and treated with proteinase K solution (10 μg/mL in 0.1% SDS and 0.05% Triton X-100 in PBS) at 37 °C for 2 h. Sections were then rinsed with ultrapure water and stained with Alcian Blue in 0.1 N HCl (pH ~1) or 10% acetic acid (pH ~4). The tissue sections were destained with 0.1 N HCl or 10% acetic acid until there was no more change in color.

Scanning Electron Microscopy. Removing a portion of their natural tubes induced worms to rebuild their tube if provided with suitable building materials, like glass or ceramic beads. This provides a convenient method to collect cured glue in its final form.[8] Glass beads bonded by worms to the ends of their tubes were collected with forceps. Segments of set and cured glue samples were harvested in artificial seawater by vigorously vortexing the beads for 10 min to fracture and dislodge the glue spots. After allowing the glass beads to settle, the supernatants containing glue fragments were transferred to a clean Eppendorf tube and centrifuged at 13,000 g for 5 min. The segments of glue were washed several times by resuspension and recentrifuged in ultra pure water. Without further treatment, the collected glue fragments were embedded in Immuno-Bed and sectioned for staining the interior of the glue samples. Surface staining could be misinterpreted if sulfated mucopolysaccharides originating from mucocytes on the tentacles[1] was deposited on the adhesive after secretion. Thick sections (5 μm) were adhered to carbon tape (PolyScience, Inc.) and examined with a FEI Quanta 600 SEM (Hillsboro, Oregon) in the Surface and Nanoimaging Facility at the University of Utah. Images were acquired in low vacuum mode with a backscattered electron (BSE) detector.

Catechol Oxidase Cloning. Worm adhesive gland tissue was excised from the parathorax with a razor blade and dounce homogenized. Total lysate was collected and purified with RNAeasy Kit according to manufacturer's instruction (QIAGEN, Gaithersburg, MD). The purity and yield of total RNAs were measured by UV/vis spectrometry (Biomad 20, Perkin-Elmer, Waltham, MA). Total RNA (200 ng) was reverse transcribed following the manufacturer's instruction (3′-RACE, Invitrogen, Grand Island, NY). Reverse transcripted cDNAs was amplified with the CO gene specific primer (CO-forward, 5′-TTGGATGATGGGTCTGAACA-3′) and Abridged universal amplification primer (AUAP-reverse, 5′-GGCCACGC-GTCGACTAGTAC-3′). PCR products were separated by agarose gel electrophoresis. The highest MW band was excised from the gel and purified with DNA gel elution Kit (QIAGEN). The purified PCR product was sequenced with the following primers (CO-forward 5′-TTGGATGATGGGTCTGAACA-3′, CO-forward-2,5′-CTACTGAA-GAATACACATATCAACAGG-3′ and AUAP-reverse 5′-GGCCA-CGCGTCGACTAGTAC-3′). The signal peptides and propeptide cleavage sites were predicted with Signal P and ProP 1.0, respectively.

Catechol Oxidase Activity. Freshly collected worms, isolated granules, or glued glass beads were fixed in 4% paraformaldehyde in PBS (pH 7.4) overnight at 4 °C. For tissue staining, worms were transferred to 30% sucrose in PBS (pH 7.4) until sinking to the bottom of the container. Worms were then embedded in freezing medium (Sakura Finetek, Torrance, CA) and cryo-sectioned to 20 μm. Tissue sections were incubated in MES buffer (50 mM MES, 150 mM NaCl, pH 6.4) at room temperature for 30 min before addition of enzyme substrates. To collect isolated granules, the parathorax region was excised with a razor blade and homogenized with a cell strainer (40 μm, ISC Bioexpress) in degassed MES buffer. The homogenate was layered on top of a 1 mL 0.6 M sucrose cushion prepared in MES buffer (pH 6.4). To concentrate the granules, samples were centrifuged at 2500 rpm for 5 min. The sucrose cushion was carefully removed and the granule pellets were gently resuspended and fixed with 4% paraformaldehyde in MES buffer (pH 6.4) at 4 °C for at least 2 h. The fixed granules were washed three times with MES buffer (pH 6.4) before adding substrates. Glued glass beads were prepared as previously described; rebuilt glass beads were harvested by forceps and fixed in 4% paraformaldehyde at 4 °C overnight. Before adding substrates, glued beads were rinsed with MES buffer (pH 6.4) at least three times. To assay for enzyme activity, the fixed tissues, isolated granules, or glue on glass beads were incubated with 1 mM solutions of L-tyrosine, L-dopa, or ABTS, in MES buffer (pH 6.4) for 12 h at room temperature. To stop the reaction, the samples were washed three times with MES buffer (pH 6.4). Enzyme inhibition studies were done by adding 10 mM of either the inhibitors PTU, SHAM, CTAB, or Arbutin to the sectioned tissue, isolated granules, or glued beads, before incubating in 1 mM L-DOPA for 12 h.

Protein Sample Preparation for Denaturing Gel Electrophoresis. Isolated granules were prepared as described earlier. Granules were resuspended in proteinase K digestion buffer (0.1% SDS, 0.1% Trixton X-100, pH 7.5 in PBS) and aliquoted into two vials. One aliquot was digested at 37 °C for 4 h with 10 μg/mL of proteinase K. Both aliquots were then denatured in SDS sample buffer and boiled at 95 °C for 5 min (50 mM Tris-Cl pH 6.8, 2% SDS, 10% glycerol, 0.5 M 2-mercaptoethanol, 0.02% bromophenol blue, 12.5 mM EDTA) before protein electrophoresis.

RESULTS

Sulfated Macromolecular Bioadhesive Component. The detailed workings of regulated secretion are diverse, but one frequent feature is the pairing within secretory granules of oppositely charged, multivalent components. Mutual charge neutralization contributes to condensation of the multivalent components into concentrated packets, which, in turn, is critical for regulating the osmotic pressure in secretory cells stuffed with polyelectrolytes. Based on these precedents, it is reasonable to expect a counter-polyanion in the homogeneous granules. Elemental analysis of cured *P. californica* glue revealed relatively large quantities of P, Ca, and Mg (Figure 2). The P occurs in the form of phosphoserines on the Pc3 proteins.[8] The Ca and Mg are complexed with the peptidyl-phosphates in the heterogeneous subgranules. Sulfur was the fourth most

dx.doi.org/10.1021/bm400251k | *Biomacromolecules* 2013, 14, 1607−1617

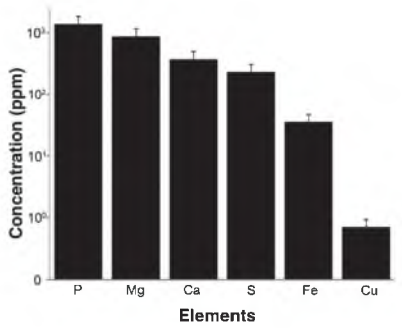

Figure 2. Elemental composition of sandcastle glue.

abundant element in the glue (231 ± 77 ppm) and occurred at nearly 1/10th the concentration of P. The cysteine content of the known *P. californica* bioadhesive proteins is much too low to account for the S in the cured glue.[9,10] The high unexplained concentration of S, the absence of a counter polyanion to the polycationic proteins in the homogeneous granules, and biological precedent suggested the bioadhesive may contain a sulfated macromolecular component.

Alcian Blue is a common polycationic, copper-containing dye used in histochemistry to stain acidic polysaccharides and is considered specific for sulfated macromolecules at low pH.[37] To experimentally verify that Alcian Blue could distinguish polysulfates from the known polyphosphate components of the bioadhesive, staining controls with known polyanions were conducted. At pH 1, agarose blocks prepared with 50 μg/mL heparan sulfate stained dark blue, while blocks prepared with an equivalent concentration of a synthetic polyphosphate, or a polycarboxylate, did not stain (Figure 3A). Only sulfates are still negatively charged at pH 1.

To locate potential sulfated macromolecules in the *P. californica* adhesive gland and other tissues, coronal cryosections through the parathorax were stained with Alcian Blue at pH 1 and 4 (Figure 3B,C). The distinctive adhesive granule producing tissues in the body cavity were stained at pH 1, as were the parapodia and mucus producing tissues around the mouth and tentacles. Acid mucopolysaccharides secreted by mucocytes previously identified on the tentacles are important for particle retention and transport.[1] At higher magnification, it was apparent the sulfated components were present in the homogeneous granules, and only in the homogeneous granules (Figure 3C). At pH 4, both granules types stained strongly as expected (Figure 3D). As a preliminary investigation of the identity of the sulfated component, whether polysaccharide or proteoglycan, adhesive granules were isolated from the adhesive gland for gel electrophoresis. Samples were prepared with and without proteinase K digestion. Alcian blue staining of the gel revealed a low MW (<10 kDa) band representing the major sulfated component in the adhesive granules (Supporting Information, Figure 1). The apparent MW of the sulfated component was not affected by proteolysis, evidence it was a polysaccharide. In addition, there was a minor Alcian Blue stained band at ~45 kDa, which disappeared after proteinase treatment. The comparatively low abundance of the proteoglycan band precluded it as a major component of the bioadhesive.

The localization of a sulfated polysaccharide in the homogeneous granules within secretory cells was not definitive proof that the final secreted bioadhesive contained the sulfated

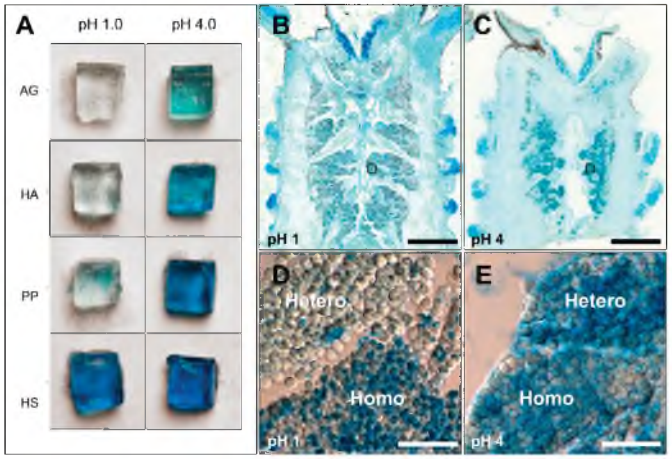

Figure 3. Alcian Blue staining. (A) Agarose gels containing equal concentrations of known polyelectrolytes stained with AB at pH 1 and 4: agarose only (AG), hyaluronic acid (HA), polyphosphate (PP), heparan sulfate (HS). (B) Coronal cryosection stained with AB at pH 1. (C) Coronal cryosection stained with AB at pH 4. (D) Closer view of secretory granules stained with AB at pH 1 from boxed region in panel B . (E) Closer view of secretory granules stained with AB at pH 4 from boxed region in (C). Scale bars in (A–C) = 250 μm; (D, E) = 10 μm.; Homo = homogeneous granules; Hetero = heterogeneous granules.

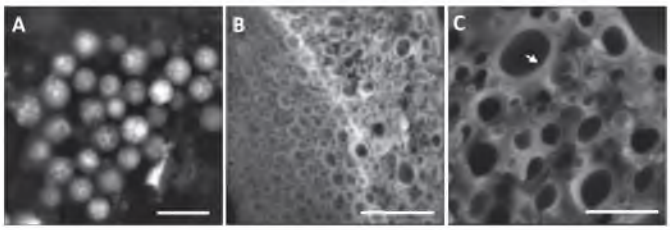

Figure 4. SEM BSE images. (A) Secretory granules isolated from the adhesive gland: scale bar = 5 μm. (B) Thin section of cured glue isolated from glass beads: scale bar = 5 μm. (C) Higher magnification of sectioned cured glue. Arrow indicates the distinct wall; scale bar = 4 μm.

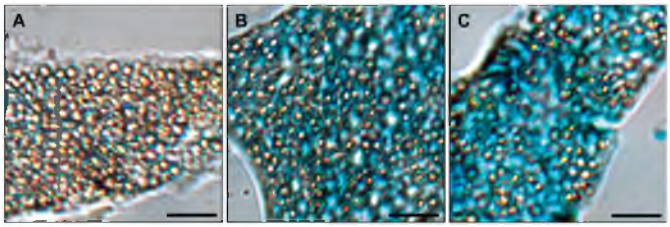

Figure 5. Sulfated polysaccharides in the final secreted glue. (A) Unstained sectioned glue. (B, C) Sectioned glue stained with Alcian Blue at pH 1 and 4, respectively. Scale bars in (A–C) = 5 μm.

polysaccharide. Therefore, fragments of the final cured glue were recovered from tubes rebuilt in the lab with glass or YSZ bead tubes (Figure 1C), resin embedded, and thin sectioned to provide a clean interior surface for Alcian Blue staining. As prelude, the glue sections were examined by SEM using backscattered electrons (BSE). Larger atomic nuclei (higher Z number) backscatter more electrons, creating atomic number contrast or, in other words, compositional contrast in the SEM BSE images.[38] The subgranules appear as bright, polydisperse, solid spherical inclusions in BSE images of heterogeneous granules isolated intact from the adhesive gland (Figure 4A). The final cured glue has the appearance of a solid foam (Figure 4B) with bright bubbles dispersed in a darker matrix in BSE images (Figure 4C). The polyphosphorylated Pc3 proteins and Mg were shown previously to be segregated into the heterogeneous subgranules.[14] The Z numbers of P and Mg are higher than the much more abundant C, N, and O atoms; therefore, the bright shells surrounding the bubbly pores of the cured adhesive likely comprised concentrated P and Mg/Ca originating from heterogeneous subgranules (Figure 4C, arrow). Similarly prepared sections of cured glue, observed by light microscopy, stained strongly with Alcian Blue at pH 1 (Figure 5B) and more strongly at pH 4 (Figure 5C). We conclude the set and cured bioadhesive contained a sulfated polysaccharide originating from the homogeneous granules.

Catechol Oxidase. The full-length gene of the *P. californica* tyrosinase-like protein, obtained by 3′ RACE, encoded a 442 residue protein (Figure 6). The first 19 residues are a predicted secretion signal peptide that is followed by an unstructured, highly charged propeptide (19–94), predicted based on a high probability propeptide cleavage site at R94. The protein contains highly conserved copper A and copper B binding domains, each with three copper coordinating histidine

```
MLFKIALLVLVCVFIIVTGFEDDETDLDKM   30
KIMEEMIKEWKSDNDEIKFTPTQISYLNHL   60
DNRGRGSGRGRGRGNVRGRGNGQGRGKGNN   90
RSKRQYEYLPVRKAYRHLSDSERKDFEDAI  120
YQLKHTFSDPTSDLSNYDLFVNLHRSNSAP  150
YAHGGHAFAGWHRHCLYRFEKALQEINEDV  180
TLCYLDTTMEYNVGDRLEDSAIFGPDTLGN  210
ADGKVVTGPFAIIFKVLWETCLKNNRTSLSR 240
NIQNDGRFFYSPADLRIFDTWNTFEEMNTL  270
RPNFFAEHDGVHIGIGGHMLEIACAPFDPI  300
FWLHHTFVDYLWWEIRQHQTTDPETEYPNG  330
TRPGHGRDDPMSPFMLELDDGSEQPLTNIA  360
GLSNSYTTEEYTYQQAPGRIVCSTYSDCRS  390
KFLYCSGRRCRAKVREGGQLEGRSTVSCYC  420
PPGFIPGRRRRGRQYYCRCRPR*         442
```

Figure 6. Full-length sequence of *P. californica* catechol oxidase. The secretion signal peptide (1–19) is underlined in black. The predicted propeptide (20–94) is highlighted in blue. The conserved copper A and copper B binding domains are underlined in blue and red, respectively. The six histidine residues in red bold are the conserved copper coordination residues. * = stop codon.

residues, that are common to type 3 copper oxidases. The C-terminal region contains eight cysteine residues.

The expression and location of the enzyme was experimentally verified by adding the substrate L-DOPA to fixed parathorax tissue sections at pH 6.5, where nonenzymatic autooxidation of endogenous peptidyl-DOPA is slow. Oxidation of the exogeneous L-DOPA to dopaquinone led to polymerization of dark melanin-like compounds in the adhesive gland tissue (Figure 7B). At higher magnification, the dark coloration was apparent in both homogeneous and heterogeneous secretory cell types (Figure 7F). The color of control tissue sections, without added L-DOPA, was unchanged after 12 h at pH 6.5 (Figure 7A). As stated earlier, tyrosinases can have both

dx.doi.org/10.1021/bm400251k | *Biomacromolecules* 2013, 14, 1607–1617

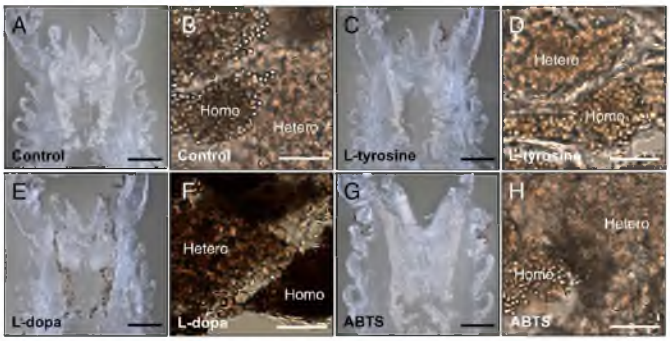

Figure 7. Enzyme activity in cryosectioned adhesive glands. (A, C, E, G) Low magnification of coronal cryosections through the parathorax region, which were incubated with phenoloxidase substrates to localize potential enzyme activies. (B, D, F, H) Higher magnification images of the stained cryosection showing both types secretory cells. Scale bars in (A, C, E, and G) = 250 μm; (B, D, F, and H) = 10 μm; Homo = homogeneous granules; Hetero = heterogeneous granules.

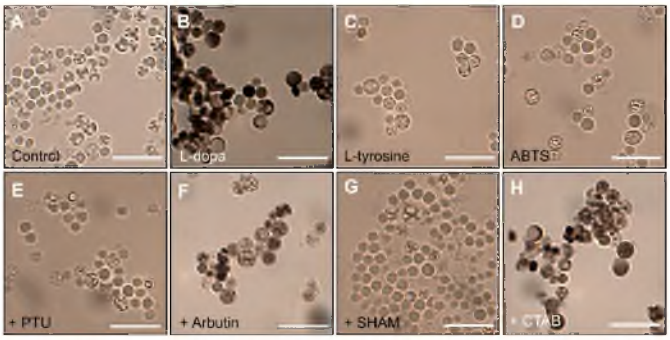

Figure 8. Enzyme activity in isolated secretory granules. (A) No substrate control. (B–D.) Granules incubated with L-DOPA, L-tyrosine, and ABTS. (E–H) Granules incubated with L-DOPA plus the enzyme inhibitors PTU, arbutin, SHAM, and CTAB. Scale bars = 10 μm.

monophenoloxidase activity and catechol oxidase activity, or just catechol oxidase activity. Tissue sections incubated for 12 h at pH 6.5 with 1 mM tyrosine showed no change in coloration, evidence that the *P. californica* adhesive gland enzyme was in the latter category.

A gene encoding a laccase homologue with a signal peptide was also identified in the parathorax EST library,[9] but its expression was undetectable in the parathorax of adult worms by in situ hybridization and was very low by qRT-PCR.[11] Laccases are also copper-containing phenoloxidases but are structurally unrelated to type 3 copper proteins, have a different reaction pathway, and have broader substrate specificity.[30] Laccase activity in fixed parathorax tissue sections was assayed with 2,2′-azino-bis-3-ethylbenzothiazoline-6-sulfonic acid (ABTS), a laccase substrate not recognized by catechol oxidases.[39] After 12 h, at pH 6.5, the color of the tissue sections (Figure 7G) and granules at high magnification (Figure 7H) was unchanged. Laccase was either not expressed (consistent with in situ hybridization results) or remained latent in the adult parathorax.

Intact secretory granules can be isolated from the adhesive gland by gentle homogenization, followed by centrifugation through a sucrose cushion to remove most cellular debris. The color and morphology of isolated granules fixed in 4% paraformaldehyde remains unchanged for 12 h in Ringer's Buffer at pH 6.5 (Figure 8A). Addition of 1 mM L-DOPA causes the granules to turn dark brown, at pH 6.5, after 12 h (Figure 8B). Neither L-tyrosine, nor the laccase substrate ABTS caused a color change in the granules, consistent with the tissue section results. To verify that L-DOPA oxidation was enzyme-catalyzed, several enzyme inhibitors were added to the granules along with L-DOPA. Arbutin, a tyrosine analog and inhibitor of the phenoloxidase activity of tyrosinases but not catechol oxidase activity,[40] had little affect on the color change. Phenylthiourea (PTU), a copper chelator that binds at the active site of all phenoloxidases and laccases,[41,42] completely inhibited L-DOPA melanization, as did salicylhydroxamic acid (SHAM), a copper chelator that inhibits catechol oxidases but not laccases.[43] The absence of color development in the presence of these inhibitors also served to demonstrate that melanization was not due to spontaneous oxidation of L-

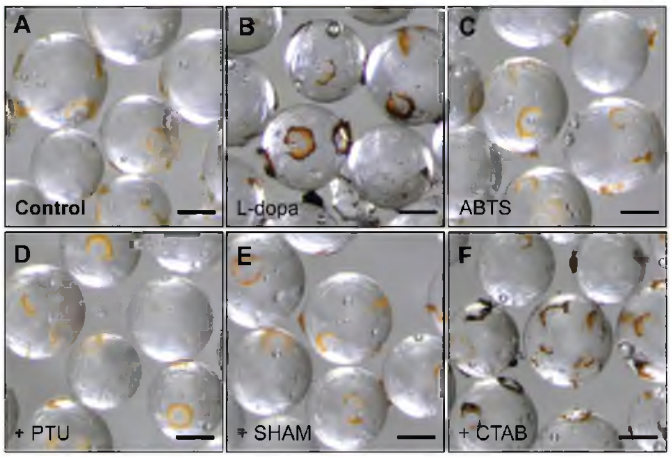

Figure 9. Enzyme activity in fully cured glue. (A) No substrate control. (B, C) Granules incubated with L-DOPA, and ABTS. (D−F) Granules incubated with L-DOPA plus the enzyme inhibitors PTU, SHAM, and CTAB. Scale bars = 250 μm.

Table 1. Granule Components

Hetero	M_w (kDa)	pI	DOPA (mol %)	Homo	M_w (kDa)	pI	DOPA (mol %)
Pc3B (−)	52.1[a]	<2		pSulfate (−)	<10	<0	
Pc3A (−)	26.2[a]	<2		Pc2 (+)	20.1	9.9	7.3[b]
Pc1 (+)	20.0	9.8	9.8[b]	Pc5 (+)	15.0	10.3	
Pc4 (+)	26.7	9.6		cat. ox.	51.0	6.8	
Mg^{2+} (+)							
Cat. Ox.	51.0	6.8					

[a]Includes phosphates. [b]From ref 30; cat. ox. = catechol oxidase.

DOPA. Cetyltrimethylammonium bromide (CTAB), a cationic detergent that displaces Cu^{2+} from the active site of laccases,[44] did not inhibit the L-DOPA color change. In short, the substrate and inhibitor pattern is consistent with the *P. californica* bioadhesive containing a type 3 phenoloxidase that catalyzes only catechol oxidation. The substrate and inhibitor profile in the final glue was identical to the profile in isolated granules (Figure 9). Therefore, the catechol oxidase remained active long after the bioadhesive had cured. Laccase appears to play no role in adhesive curing.

Returning to the elemental analysis (Figure 2), at 0.7 ppm, the concentration of Cu in the set and cured glue was several orders of magnitude higher than the Cu concentration in natural seawater.[45] More significantly, Cu was undetectable by ICP-OES in the artificial seawater of the lab aquarium. Therefore, the Cu in the glue was cosecreted in the bioadhesive, most likely in the active site of the catechol oxidase. The functional significance of Fe, the concentration of which is also substantially higher in the adhesive than in seawater,[46] has not been investigated.

■ DISCUSSION

The overall effectiveness of natural bioadhesives is as much a product of the biological assembly and packaging pathways as it is of its final composition. At the same time, the biological machinery imposes severe constraints on the composition and organization of the packaged adhesives. The separated parts of sabellariid bioadhesives were adapted for transit through the regulated secretory pathway, an ancient cellular machinery for concentrating and storing components destined for extracellular function. This is by no means a profound observation; the cellular biogenesis of several bioadhesives has been previously described.[16,47−49] Nonetheless, holistic consideration of the general features of the presecretion cellular packaging and storage can provide insight into the postsecretion macromolecular composition, organization, and trigger mechanisms for the set and cure reactions, that may not be apparent from studying individual adhesive components in isolation.

Condensation of oppositely charged polyelectrolytes and multivalent cations has long been recognized as an important process in packaging and storing proteins in the regulated secretory system.[50] Fitting this pattern, the *P. californica* bioadhesive is packaged in separate secretory cells, in dense granules, as sets of oppositely charged sulfated polysaccharides, polybasic and polyphosphorylated proteins, and divalent cations (Table 1). Natural electrostatic condensation of secreted polyelectrolytes is similar to the phenomenon known in the field of colloid chemistry as complex coacervation.[51] Electrostatic association of oppositely charged, water-soluble polyelectrolytes leads to partial dehydration and self-concentration of the polymers into dense, phase-separated aqueous fluids: complex coacervates (see Sprujit[52] for a

dx.doi.org/10.1021/bm400251k | *Biomacromolecules* 2013, 14, 1607−1617

comprehensive description). The major thermodynamic driving force that concentrates the oppositely charged polyelectrolytes into the complex coacervate phase is the gain in entropy of small counterions that are released as the macroions associate.[53−57] Complex coacervation, in vitro, occurs within a narrow range of conditions determined by a complex interplay between the structure of the polyelectrolytes (e.g., molecular mass, shape, flexibility, ionizable species, and mol % of ionizable groups) and solution parameters (e.g., pH, ionic strength, and dielectric constant) that affect the charge density of the polyelectrolytes and strength of charge−charge interactions.[58−63] Hence, for a given set of polyelectrolytes, upper and lower critical values of pH and ionic strength define boundaries of the complex coacervation conditions; outside of these conditions the polyelectrolytes can be soluble, form stable colloidal complexes, ionic hydrogels, or insoluble aggregates.[34] In other words, a small change in solution conditions can cause the fluid coacervate phase to solidify. The foregoing properties make complex coacervates an ideal intermediate state for storage and delivery of both natural and synthetic water-borne, underwater adhesives.[8,33]

The early model of complex coacervation of the *P. californica* bioadhesive[8] can be refined based on the present and other recent findings.[11] Condensation, partial dehydration, and phase separation of the adhesive polyelectrolytes, that is, complex coacervation, occurs in a membrane delimited space during transit from the golgi apparatus to mature secretory storage granules. The underlying thermodynamics may be the same as in vitro complex coacervation, but in the cell, conditions conducive to polyelectrolyte condensation are dynamically controlled by active transporters that move protons, divalent cations, monovalent counterions, and water into, or out of, the membrane delimited space. As packaged, the adhesive comprises two major, but separated, coacervated components, stored in micrometer-sized modules. The homogeneous granules, based on their morphology, contain a uniformly distributed complex of polybasic proteins and polysulfate. The organization of the heterogeneous granules is more complicated; the polyphosphates (Pc3A/B) are colocated with Mg^{2+} exclusively in spherical subgranules within the heterogeneous granules, surrounded by a uniform matrix containing the polyamines (Pc1/4).[14] The polyphosphate subgranules may be simple (single polyelectrolyte) coacervates formed by the self-condensation of Pc3A/B with Mg^{2+}.[64] A hallmark of coacervates is fluidity; the polyelectrolyte constituent(s) of a coacervate, in general, are free to diffuse throughout the coacervate phase, although their diffusion constants are restricted compared to dilute solution, with the specifics depending on the coacervated system.[65−67] Direct measurement of mucin diffusivity within secretory granules of live cells demonstrated that secretory granule contents, at least in some cell types, are stored in a fluid state that fits the definition of a complex coacervate,[68] although it should be noted that several condensed forms of secreted products are possible in nature, as exemplified by the crystalline core of proinsulin granules.[69]

Interfacial Adhesion. When applied to a substrate, the two major types of complex coacervate modules fuse together and evolve within seconds into a dab of foamy glue. Individual granules are no longer apparent in the final structure (Figure 3B−D), but the separate coacervates undergo limited mixing,[11] creating a coacervate within coacervate structure. With regard to wet interface adhesion, the list of functional groups, phosphates (phosphoserines), primary amines (lysine), aromatic hetercyclic amines (histidine), quanidinium (arginine), and catechols (DOPA), that can participate in adhesion to the mineral substrate now includes sulfate groups contributed by the sulfated polysaccharide. The distinct chemistry of each of these ionizable groups provides a diverse range of mechanisms for combinatorial bonding to fouled natural surfaces, as would any well-adapted, or designed, underwater adhesive.[46] Consistent with a useful role in interfacial adhesion, sulfated polysaccharides have been identified in other marine bioadhesives.[48,70,71]

Adhesive Setting. Small changes in solution conditions that cross the boundary conditions for complex coacervation, as stated earlier, can drive further dehydration, insolubilization, and solidification of the coacervated complexes.[34] The substantial pH change in the surrounding medium, and demembranization (by an unknown mechanism), accompanying secretion into seawater could induce osmotic swelling and differential insolubilization of the separate complex coacervates. The kinetics and pathway of pH triggered reactions are likely to be complex because the adhesive is strongly and inhomogeneously buffered by the polyelectrolyte constituents. Judging from the contrast in the BSE images (Figure 4), the well-defined shell of the pores likely originated from the simple coacervate subgranules, and consists of polyphosphoproteins complexed with Mg^{2+}/Ca^{2+}. Swelling of the subgranules would be resisted by a cross-linked network of counter polyelectrolytes, and hardening of the shell by insolubilization of the polyphosphate and Mg^{2+}/Ca^{2+} as the pH increases.[35] The fluid-filled bubbles in the hardened glue were mostly spherical, which suggested either there was no shear or compressive deformation during their formation, or, they are resilient structures within a deformable matrix that returned to the spherical shape. Exchange of polyelectrolytes at the interface between the two types of coacervated granules could contribute to insolubilization, as another mechanism that contributes to the setting (solidification) reaction.

Covalent Curing. The covalent curing mechanism is built-in; each modular adhesive packet, both homogeneous and heterogeneous granules, contains catechol oxidase. The enzyme remains active long after the bioadhesive has cured. There is ample precedent in nature of dark, quinone-tanned materials formed by cosecreted phenoloxidases.[72] "Autoquinone tanning" of mussel byssal threads and adhesive plaques by a cosecreted catechol oxidase was first proposed by Smyth, in 1954, after he directly demonstrated catechol oxidase activity in the mussel foot enzyme gland, the source of the byssal thread cuticle, by incubating fixed and sectioned mussel foot tissue in an aqueous catechol solution.[73] Later extraction of an active catechol oxidase from whole byssal threads was consistent with the enzyme being a cosecreted component of the final structure.[74] The role of the catechol oxidase in mussel byssal thread and adhesive plaque curing has not been pursued to a definitive conclusion. DOPA is also prone to spontaneous, nonenzymatic oxidation to dopaquinone in aerated seawater, which would subvert the catechol's role in interfacial adhesion, while promoting quinonic cross-linking. The inherent DOPA lability has led to a series of recent hypotheses to explain how the spontaneous oxidation of peptidyl-DOPA is prevented, or reversed, in the mussel byssus. These include locally reduced redox potential of peptidyl-DOPA due to neighboring hydrophobic residues,[75] pH-dependent formation of Fe(III) coordination complexes,[76] and cosecretion of a thiol-rich

protein (Mfp-6) to reduce peptidyl-dopaquinone back to peptidyl-DOPA.[77]

Why does *P. californica* go to the trouble of copackaging catechol oxidase with the structural components of its bioadhesive if DOPA oxidation and subsequent cross-linking is spontaneous in seawater? This is an especially pertinent question if indeed mussels go to metabolic lengths to prevent, and even reverse, spontaneous DOPA oxidation. In nature, high speed curing of underwater bioadhesives to withstand loading as rapidly as possible would be highly adaptive in turbulent habitats. *P. californica* bonds new sandgrains to its tube in less than 30 s,[2] and mussels form and deploy new byssal threads in less than a minute.[78] The rate of uncatalyzed DOPA oxidation is probably much too slow, even in aerated seawater, to reliably and homogeneously cross-link poorly mixed bioadhesive components. This is evident from synthetic mussel-inspired materials in which spontaneous oxidation of pendant catechols is too slow to be useful. Instead, the materials are thoroughly mixed with stoichiometric oxidants (usually sodium periodate) during application to initiate covalent cross-linking, resulting in gelation on a time scale of minutes.[79,80] In contrast to auto-oxidation, preorganization of modular bioadhesives with catechol oxidase packaged within each micrometer-sized adhesive packet would provide rapid, efficient, and spatially homogeneous cross-linking throughout the adhesive, even with limited mixing of the modules. And of further advantage, catechol oxidase stored and secreted with O_2 in the active site (the oxy state), would be primed to immediately oxidize two L-DOPA residues, maximizing the initial rate of quinonic cross-linking.

Enzymes provide specificity. A second advantage of copackaging catechol oxidase in the adhesive granules could be specific cross-linking through a subset of DOPA side chains. Substrate specificities of the type 3 copper proteins are determined by substrate access to identical bicopper active sites, and access is controlled by specific residues, or domains, proximate to the active site.[81] To illustrate, hemocyanins are type 3 copper proteins with virtually identical binuclear Cu active sites as phenoloxidases, yet they do not catalyze either phenol hydroxylation or diphenol oxidation because their active sites are inaccessible to either type of substrate. Instead, hemocyanins function as oxygen transporters. Following this logic, it is conceivable that access of peptidyl-DOPA to the catechol oxidase active site is determined by interactions between residues surrounding the enzyme active site and the amino acids adjacent to the DOPA residues. In this scheme, quinonic cross-linking is enzyme specified and nonrandom; only specific peptidyl-DOPA residues would be rapidly oxidized enzymatically to spatially direct ordered network formation during the curing process.

If catechol oxidase initiates covalent curing of the bioadhesive after secretion, the catechol oxidase itself must be activated during or shortly after secretion. The *P. californica* catechol oxidase pro-enzyme contains, in addition to a secretion signal peptide, a predicted pro-peptide cleavage site at residue 95, which is preceded by a low complexity, unstructured, 31 residue polycationic region rich in arginine residues (Figure 6). Proteolytic activation of latent tyrosinases is common in nature. In arthropods, as a well-studied example, extracellular latent phenoloxidases are proteolytically activated as the end result of a cascade of serine proteinases initiated by tissue damage, or the presence of specific compounds of microbial origin.[82] As part of an innate immune system, the activated phenoloxidases catalyze the deposition of melanin to seal wound sites or encapsulate pathogens. As another example, the latent catechol oxidase from the mussel enzyme gland was activated by limited proteolysis.[74] It is therefore reasonable to suspect the *P. californica* catechol oxidase may be proteolytically activated by removal of the predicted propeptide during or shortly after secretion. However, a more novel activation mechanism is suggested by the high positive charge density of the *P. californica* catechol oxidase propeptide. Perhaps the enzyme is electrostatically inactivated (or activated) by association of the polycationic N-terminal region with the polyanionic components of the secretory granules, or by association with phospholipids in the secretory granule membrane. Activation of the enzyme may be effected by exchange and rearrangement of electrostatic associations during secretion and granule lysis in seawater. Numerous reports of activation of latent plant catechol oxidases by anionic detergents, such as sodium dodecyl sulfate, that bind at specific sites of the enzymes provide ample empirical evidence that electrostatic interactions can reversibly switch the enzymes on and off.[83−85] Coupled to a regulatory function, the highly charged *P. californica* propeptide could also play a role in electrostatically condensing the latent catechol oxidase into the adhesive granules during complex coacervation.

As a final speculative rationalization for cosecretion of catechol oxidase with the adhesive, it is conceivable that the active enzyme is the species specific settlement cue recognized by gregarious *P. californica* larvae. Glass beads removed from laboratory reconstructed tubes containing spots of glue, like those shown in Figure 9, will induce settlement and metamorphosis of cultured planktonic larvae.[3] The aromatic compound 2,6-di-*tert*-butyl-4-methyphenol was shown to strongly induce metamorphosis, which led the authors to suggest the compound is a homologue of a natural aromatic inducer derived from the peptidyl-DOPA in the adhesive. In the scenario proposed here, larvae may probe the surface with an aromatic catechol oxidase substrate. In close proximity to conspecific tubes, the glue embedded catechol oxidase would oxidize the probe compound into a quinonic signal for settlement and metamorphosis.

Conclusion. The *P. californica* underwater bioadhesive is packaged in preorganized modules as two distinct sets of oppositely charged polyelectrolytes. The bioadhesive is initially fluid but rapidly insolubilizes when the two coacervated parts interact and are exposed to seawater. Both types of module are preloaded with a latent catechol oxidase, primed for rapid oxidation of peptidyl-DOPA to initiate formation of a homogeneously cross-linked matrix with minimal mixing of the preorganized modules. The heterogeneous subgranules swell to become divalent cation-stabilized, polyphosphate shells surrounding water-filled pores, some open and most closed. The end result is tough and resilient underwater bonds formed with an energy-absorbing, water-filled adhesive foam. Like manmade bubble wrap used to protect delicate cargoes, the bubbles of the adhesive could deform elastically or plastically at lower loads, or rupture and collapse at higher loads, to dampen the peak load on the joint by dissipating impact energy. At high strain rates, pressure induced flux of water through open pores in the foam would provide additional viscous dissipation of impact energy.[86] Further study of the worm's ingenious adaptations may shed light on design principles for creating self-initiating, fluid-filled foam adhesives underwater from water-soluble macro-precursors.

■ ASSOCIATED CONTENT

Supporting Information

SDS-PAGE of isolated granules with and without protease treatment. This material is available free of charge via the Internet at http://pubs.acs.org.

■ AUTHOR INFORMATION

Corresponding Author

*E-mail: rstewart@eng.utah.edu. Tel.: 801-581-8581.

Notes

The authors declare no competing financial interest.

■ ACKNOWLEDGMENTS

The authors are grateful to Dr. Greta Faccio for helpful tyrosinase discussions, and to Sadee Hansen and Joe Passman for assistance with SEM. This work was supported by the National Science Foundation (DMR-0906014) and the Office of Naval Research (N000141010108).

■ REFERENCES

(1) Dubois, S.; Barillé, L.; Cognie, B.; Beninger, P. G. *Mar. Ecol.: Prog. Ser.* **2005**, *301*, 159−171.
(2) Stevens, M. J.; Steren, R. E.; Hlady, V.; Stewart, R. *Langmuir* **2007**, *23*, 5045−5049.
(3) Jensen, R. A.; Morse, D. E. *J. Chem. Ecol.* **1990**, *16*, 911−930.
(4) Kirtley, D. W.; Tanner, W. F. *J. Sediment. Res.* **1968**, *38*, 73−78.
(5) Noernberg, M. A.; Fournier, J.; Dubois, S.; Populus, J. *Estuarine, Coastal Shelf Sci.* **2010**, *90*, 93−102.
(6) Le Cam, J.-B.; Fournier, J.; Etienne, S.; Couden, J. *Estuarine, Coastal Shelf Sci.* **2011**, *91*, 333−339.
(7) Dubois, S.; Reti re, C.; Olivier, F. D. R. *J. Mar. Biol. Assoc. U. K.* **2002**, *82*, 817−826.
(8) Stewart, R.; Weaver, J.; Morse, D.; Waite, J. *J. Exp. Biol.* **2004**, *207*, 4727−4734.
(9) Endrizzi, B.; Stewart, R. *J. Adhes.* **2009**, *85*, 546−559.
(10) Zhao, H.; Sun, C.; Stewart, R. J.; Waite, J. H. *J. Biol. Chem.* **2005**, *280*, 42938−42944.
(11) Wang, C. S.; Stewart, R. J. *J. Exp. Biol.* **2012**, *215*, 351−361.
(12) Becker, P. T.; Lambert, A.; Lejeune, A.; Lanterbecq, D.; Flammang, P. *Biol. Bull.* **2012**, *223*, 217−225.
(13) Vovelle, J. *Arch. Zool. Exp. Gen.* **1965**, *106*, 1−187.
(14) Wang, C. S.; Svendsen, K. K.; Stewart, R. J. *Biol. Adhes. Syst.* **2010**, 169−179.
(15) Tamarin, A.; Lewis, P.; Askey, J. *J. Morphol.* **1976**, *149*, 199−221.
(16) Flammang, P. *Echinoderm Stud.* **1996**, *5*, 1−60.
(17) Cyran, N.; Klepal, W.; Byern, von, J. *J. Mar. Biol. Assoc. U. K.* **2011**, *91*, 1499−1510.
(18) Jensen, R. A.; Morse, D. E. *J. Comp. Physiol., B.* **1988**, *158*, 317−324.
(19) Rzepecki, L. M.; Waite, J. H. *Mol. Mar. Biol. Biotechnol.* **1993**, *2*, 255−266.
(20) Waite, J.; Tanzer, M. *Science* **1981**, *212*, 1038.
(21) Heo, J.; Kang, T.; Jang, S. G.; Hwang, D. S.; Spruell, J. M.; Killops, K. L.; Waite, J. H.; Hawker, C. J. *J. Am. Chem. Soc.* **2012**, *134*, 20139−20145.
(22) Chung, H.; Grubbs, R. H. *Macromolecules* **2012**, *45*, 9666−9673.
(23) Sparks, B. J.; Hoff, E. F. T.; Hayes, L. P.; Patton, D. L. *Chem. Mater.* **2012**, *24*, 3633−3642.
(24) Holowka, E.; Deming, T. *Macromol. Biosci.* **2010**, *10*, 496−502.
(25) Nishida, J.; Kobayashi, M.; Takahara, A. *J. Polym. Sci., Part A: Polym. Chem.* **2012**, *51*, 1058−1065.
(26) Matos-Perez, C. R.; White, J. D.; Wilker, J. J. *J. Am. Chem. Soc.* **2012**, *134*, 9498−9505.
(27) Brubaker, C. E.; Messersmith, P. B. *Langmuir* **2012**, *28*, 2200−2205.
(28) Bré, L. P.; Zheng, Y.; Pêgo, A. P.; Wang, W. *Biomater. Sci.* **2013**, *1*, 239−253.
(29) Waite, J.; Jensen, R.; Morse, D. *Biochemistry* **1992**, *31*, 5733−5738.
(30) Solomon, E. I.; Sundaram, U. M.; Machonkin, T. E. *Chem. Rev.* **1996**, *96*, 2563−2606.
(31) Olivares, C.; Solano, F. *Pigm. Cell Melanoma Res.* **2009**, *22*, 750−760.
(32) Klabunde, T.; Eicken, C.; Sacchettini, J. C.; Krebs, B. *Nat. Struct. Biol.* **1998**, *5*, 1084−1090.
(33) Shao, H.; Bachus, K. N.; Stewart, R. J. *Macromol. Biosci.* **2009**, *9*, 464−471.
(34) Shao, H.; Stewart, R. *Adv. Mater.* **2010**, *22*, 729−733.
(35) Stewart, R. J.; Wang, C. S.; Shao, H. *Adv. Colloid Interface Sci.* **2011**, *167*, 85−93.
(36) Kaur, S.; Weerasekare, G. M.; Stewart, R. J. *ACS Appl. Mater. Interfaces* **2011**, *3*, 941−944.
(37) LEV, R.; SPICER, S. S. *J. Histochem. Cytochem.* **1964**, *12*, 309−309.
(38) Goldstein, J.; Newbury, D. E.; Joy, D. C.; Lyman, C. E.; Echlin, P.; Lifshin, E.; Sawyer, L.; Michael, J. R. *Scanning Electron Microscopy and X-ray Microanalysis*; Springer: New York, 2003.
(39) Niku-Paavola, M. L.; Raaska, L. *Mycol. Res.* **1990**, *94*, 27−31.
(40) Gasparetti, C.; Nordlund, E.; Jänis, J.; Buchert, J.; Kruus, K. *Biochim. Biophys. Acta* **2012**, *1824*, 598−607.
(41) Arias, M. E.; Arenas, M.; Rodríguez, J.; Soliveri, J.; Ball, A. S.; Hernández, M. *Appl. Environ. Microbiol.* **2003**, *69*, 1953−1958.
(42) Zufelato, M. S.; Lourenço, A. P.; Simões, Z. L. P.; Jorge, J. A.; Bitondi, M. M. G. *Insect Biochem. Mol. Biol.* **2004**, *34*, 1257−1268.
(43) Faure, D.; Bouillant, M.; Bally, R. *Appl. Environ. Microbiol.* **1995**, *61*, 1144−1146.
(44) Walker, J. R. L.; McCallion, R. F. *Phytochemistry* **1980**, *19*, 373−377.
(45) Alexander, J. E.; Corcoran, E. F. *Limnol. Oceanogr.* **1967**, 236−242.
(46) Stewart, R. J.; Ransom, T. C.; Hlady, V. *J. Polym. Sci., Part B: Polym. Phys.* **2011**, *49*, 757−771.
(47) Vitarello Zuccarello, L. *Tissue Cell.* **1981**, *13*, 701−713.
(48) Smith, A. M.; Callow, J. A. In *Biological Adhesives*; Smith, A. M., Callow, J. A., Eds.; Springer: Berlin, 2006, 63−78.
(49) Odling, K.; Albertsson, C.; Russell, J.; MÅlrtensson, L. *J. Exp. Biol.* **2006**, *209*, 956.
(50) Reggio, H.; Dagorn, J. C. *J. Cell Biol.* **1978**, *78*, 951−957.
(51) Bungenberg de Jong, H. G. In *Colloid Science*; Kruyt, H. R., Ed. Elsevier Publishing Company, Inc.: New York, 1949; Vol. *II*, pp 431−482.
(52) Spruijt, E. *Strength, Structure and Stability of Polyelectrolyte Complex Coacervates*; Wageningen University: Wageningen, The Netherlands, 2012.
(53) Gummel, J.; Cousin, F.; Boué, F. *J. Am. Chem. Soc.* **2007**, *129*, 5806−5807.
(54) Veis, A. *Adv. Colloid Interface Sci.* **2011**, *167*, 2−11.
(55) Gelbart, W. M.; Bruinsma, R. F.; Pincus, P. A.; Parsegian, V. A. *Phys. Today* **2000**, *53*, 38.
(56) Priftis, D.; Tirrell, M. *Soft Matter* **2012**, *8*, 9396.
(57) Priftis, D.; Laugel, N.; Tirrell, M. *Langmuir* **2012**, *28*, 15947−15957.
(58) Kayitmazer, A.; Shaw, D.; Dubin, P. *Macromolecules* **2005**, *38*, 5198−5204.
(59) Kayitmazer, A.; Seyrek, E.; Dubin, P.; Staggemeier, B. *J. Phys. Chem. B* **2003**, *107*, 8158−8165.
(60) Weinbreck, F.; De Vries, R.; Schrooyen, P.; de Kruif, C. *Biomacromolecules* **2003**, *4*, 293−303.
(61) Antonov, M.; Mazzawi, M.; Dubin, P. *Biomacromolecules* **2009**, *11*, 51−59.
(62) Spruijt, E.; Sprakel, J.; Stuart, M.; Gucht, J. *Soft Matter* **2010**, *6*, 172−178.
(63) Chollakup, R.; Smitthipong, W.; Eisenbach, C. D.; Tirrell, M. *Macromolecules* **2010**, *43*, 2518−2528.

(64) Silva, M.; Franco, D.; C de Oliveira, L. *J. Phys. Chem. A* **2008**, *112*, 5385−5389.
(65) Weinbreck, F.; Rollema, H.; Tromp, R.; de Kruif, C. *Langmuir* **2004**, *20*, 6389−6395.
(66) Kayitmazer, A.; Bohidar, H.; Mattison, K.; Bose, A.; Sarkar, J.; Hashidzume, A.; Russo, P.; Jaeger, W.; Dubin, P. *Soft Matter* **2007**, *3*, 1064−1076.
(67) Kausik, R.; Srivastava, A.; Korevaar, P. A.; Stucky, G.; Waite, J. H.; Han, S. *Macromolecules* **2009**, *42*, 7404−7412.
(68) Perez-Vilar, J.; Mabolo, R.; McVaugh, C.; Bertozzi, C.; Boucher, R. *J. Biol. Chem.* **2006**, *281*, 4844.
(69) Michael, J.; Carroll, R.; Swift, H. H.; Steiner, D. F. *J. Biol. Chem.* **1987**, *262*, 16531−16535.
(70) Tanur, A. E.; Gunari, N.; Sullan, R. M. A.; Kavanagh, C. J.; Walker, G. C. *J. Struct. Biol.* **2010**, *169*, 145−160.
(71) Flammang, P.; Michel, A.; Cauwenberge, A.; Alexandre, H.; Jangoux, M. *J. Exp. Biol* **1998**, *201* (Pt 16), 2383−2395.
(72) Waite, J. H. *Biol. Bull.* **1992**, *183*, 178−184.
(73) Smyth, J. D. *Q. J. Microsc. Sci.* **1954**, *3*, 139−152.
(74) Waite, J. H. *J. Mar. Biol. Assoc. U. K.* **1985**, *65*, 359−371.
(75) Wei, W.; Yu, J.; Broomell, C.; Israelachvili, J. N.; Waite, J. H. *J. Am. Chem. Soc.* **2013**, *135*, 377−383.
(76) Barrett, D. G.; Fullenkamp, D. E.; He, L.; Holten-Andersen, N.; Lee, K. Y. C.; Messersmith, P. B. *Adv. Funct. Mater.* **2012**, *23*, 1111−1119.
(77) Yu, J.; Wei, W.; Danner, E.; Ashley, R. K.; Israelachvili, J. N.; Waite, J. H. *Nat. Chem. Biol.* **2011**, *7*, 586−588.
(78) Waite, J. *Results Probl. Cell Differ.* **1992**, 27−54.
(79) Lee, B.; Dalsin, J.; Messersmith, P. *Biomacromolecules* **2002**, *3*, 1038−1047.
(80) Brubaker, C.; Kissler, H.; Wang, L.; Kaufman, D.; Messersmith, P. *Biomaterials* **2010**, *31*, 420−427.
(81) Ginsbach, J. W.; Kieber-Emmons, M. T.; Nomoto, R.; Noguchi, A.; Ohnishi, Y.; Solomon, E. I. *Proc. Natl. Acad. Sci. U.S.A.* **2012**, *109*, 10793−10797.
(82) Cerenius, L.; Söderhäll, K. *Immunol. Rev.* **2004**, *198*, 116−126.
(83) Kenten, R. H. *Biochem. J.* **1958**, *68*, 244−251.
(84) Jiménez, M.; García-Carmona, F. *Phytochemistry* **1996**, *42*, 1503−1509.
(85) Pérez-Gilabert, M.; Morte, A.; García-Carmona, F. *Plant Sci.* **2004**, *166*, 365−370.
(86) Gibson, L. J.; Ashby, M. F. *Cellular Solids: Structure and Properties*; Cambridge University Press: New York, 1999.

CHAPTER 5

CONCLUSION

5.1 Summary of sandcastle worm adhesive processing mechanism

Tube-building sabellariid polychaetes have major impacts on the geology and ecology of shorelines worldwide. Sandcastle worms, *Phragmatopoma californica* (Fewkes), live along the western coast of North America. Individual sabellariid worms build tubular shells by gluing together mineral particles with a multipart polyelectrolytic adhesive. Distinct sets of oppositely charged components are packaged and stored in concentrated granules in separate cell types. Homogeneous granules contain sulfated macromolecules as counter-polyanion to polycationic Pc2 and Pc5 proteins, which become major components of the fully cured glue. Heterogeneous granules contain polyphosphoproteins, Pc3A/B, paired with divalent cations and polycationic Pc1 and Pc4 proteins. Both types of granules contain catechol oxidase that catalyzes oxidative cross-linking of L-DOPA. Co-secretion of catechol oxidase guarantees rapid and spatially homogeneous curing with limited mixing of the preassembled adhesive packets. Catechol oxidase remains active long after the glue is fully cured, perhaps providing an active cue for conspecific larval settlement.

The worm adhesive processing mechanism is illustrated in Figure 5.1. The end result is tough and resilient underwater bonds formed with an energy-absorbing, water-

filled adhesive foam. Like manmade bubble wrap used to protectdelicate cargoes, the bubbles of the adhesive could deform elastically or plastically at lower loads, or rupture and collapse at higher loads, to dampen the peak load on the joint by dissipating impact energy. At high strain rates, pressure induced flux of water through open pores in the foam would provide additional viscous dissipation of impact energy. Further study of the worm's ingenious adaptations may shed light on design principles for creating self-initiating, fluid-filled foam adhesives underwater from water-soluble macroprecursors.

5.2 Future direction toward synthetic analogs of the sandcastle glue

The natural sandcastle adhesive is formed from sets of highly charged biomacromolecules. The development of first generation biomimetic underwater adhesives was inspired by the complex coacervation hypothesis that oppositely charged adhesive proteins play a key role in forming the natural adhesive.[1] Complex coacervation is a phenomenon where oppositely charged polyelectrolytes (PEs) associate electrostatically and phase separate into a dense aqueous fluid of concentrated PEs,[2] whereas less dense phase (upper) is depleted of PEs and called the equilibrium phase, or supernatant. The major driving force for condensation of the PEs into the coacervate phase is the gain in translational entropy of small counterions displaced when the macroions associate.[3-5] Complex coacervation occurs only within a narrow range of conditions, which are determined by several parameters such as molar mass, shape, flexibility, ionizable species, and mol% of ionizable groups[6-7] and solution conditions that affect PE charge densities and charge-charge interactions. Hence, for a given set of

PEs, upper and lower critical values of pH and ionic strength define the boundaries of the complex coacervation conditions.[8-10] Outside of these conditions the PEs will be either insoluble precipitates or stable colloidal polyelectrolyte complexes (PECs).

5.3 Complex coacervates as the foundation for wet-field adhesives

Characterization of the sandcastle worm adhesive has provided valuable insights for the design and synthesis of water-borne, underwater adhesive analogs based on complex coacervation. The adhesive complex coacervates may overcome many of the practical and technical challenges of creating adhesives for wet environments, including living tissues. Several important characteristics of this type of adhesive will be listed below.

- Complex coacervate adhesives are water-immiscible and denser than water so they can be delivered under water without dissolving or floating, and displace less dense fluids.[11]
- The ionic sidechains of the coPEs form interfacial bonds with wet substrates in the high salt and pH of the ocean (or physiological fluids).[12]
- The infinitesimal interfacial tension between complex coacervates and water allows them to readily spread on wet surfaces, which maximizes adhesive contact.
- The supramolecular structure of complex coacervates results in lower viscosity than an equivalent concentration of entangled polymers,[13] as well as shear thinning behavior, both of which aid application through narrow gauge cannulae.[14]

• Complex coacervates self-organize in water from pre-polymers so there are no toxic solvents, or exothermic, nor promiscuous polymerization chemistry *in situ.*

• The adhesives can be cured (hardened) into load bearing glues with adjustable working times through chemical and/or photochemical initiation depending on the properties of polymers.

• The synthetic biomimetics have 10-15x the adhesive bond strength of the natural sandcastle worm adhesive.[14]

• The watery bicontinuous structure provides a container for water-soluble components to create complex materials, binary curing mechanism, or to deliver bioactives.

• Their potential as medical adhesives was demonstrated *in vivo* in a live rat calvarial defect model[11] and *ex vivo* with donated fetal membranes.[15] The first generation adhesive complex coacervates demonstrate we are on the right pathway toward practical undersea adhesives. However, so far, only one level of the natural adhesive has been copied. Sandcastle worms may have much more to teach about underwater adhesives. In this study, sandcastle worm utilize two distinct sets of polyelectrolyte condensation, also called coacervate in the coacervate, to form the final glue. These distinct sets of charged biomacromolecules in sandcastle glue suggest a double-networked system, and might give superior mechanical properties than single network crosslinked system. The future objectives of underwater adhesive development, in broad terms, are to recently identified features of the sandcastle worm adhesive into second generation underwater adhesives based on polyelectrolyte condensation.

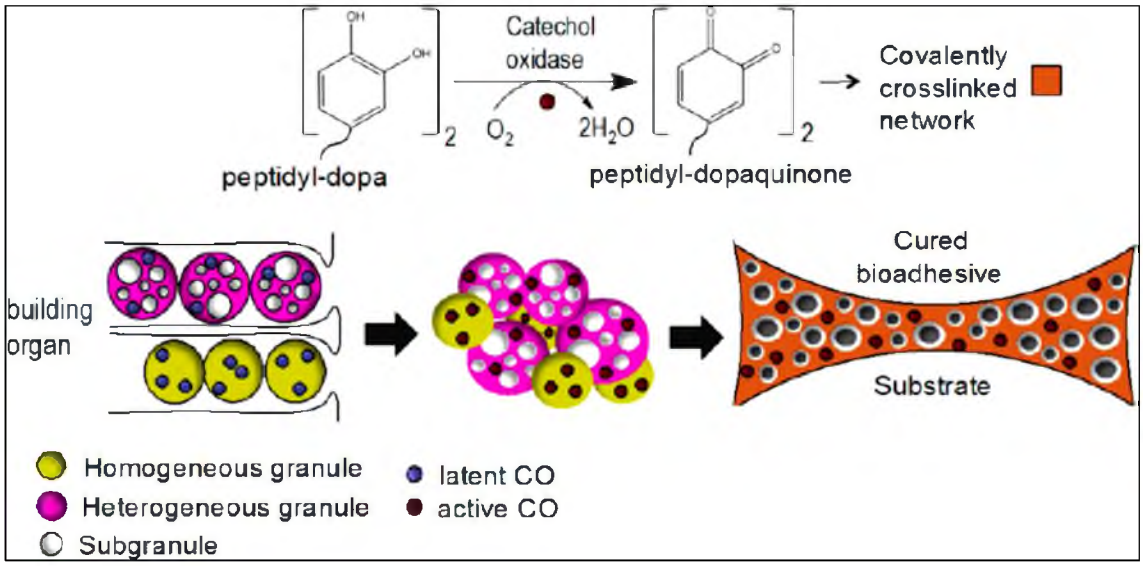

Figure 5.1. Worm adhesive secretion and curing model.

5.4 References

(1) Stewart, Russell J., James C. Weaver, Daniel E. Morse, and J. Herbert Waite. "The tube cement of *Phragmatopoma californica*: a solid foam." *Journal of Experimental Biology* 207, no. 26 (2004): 4727-4734.

(2) Bungenberg de Jong, H. G. "Crystallisation-coacervation-flocculation." *Colloid Science* 2 (1949): 232-258.

(3) Gummel, Jérémie, Fabrice Cousin, and François Boué. "Counterions release from electrostatic complexes of polyelectrolytes and proteins of opposite charge: a direct measurement." *Journal of the American Chemical Society* 129, no. 18 (2007): 5806-5807.

(4) Veis, Arthur. "A review of the early development of the thermodynamics of the complex coacervation phase separation." *Advances in Colloid and Interface Science* 167, no. 1 (2011): 2-11.

(5) Gelbart, William M., Robijn F. Bruinsma, Philip A. Pincus, and V. Adrian Parsegian. "DNA-inspired electrostatics." *Physics Today* 53, no. 9 (2007): 38-44.

(6) Kayitmazer, A. B., D. Shaw, and P. L. Dubin. "Role of polyelectrolyte persistence length in the binding of oppositely charged micelles, dendrimers, and protein to chitosan and poly (dimethyldiallyammonium chloride)."*Macromolecules* 38, no. 12 (2005): 5198-5204.

(7) Kayitmazer, A. B., E. Seyrek, P. L. Dubin, and B. A. Staggemeier. "Influence of chain stiffness on the interaction of polyelectrolytes with oppositely charged micelles and proteins." *The Journal of Physical Chemistry B* 107, no. 32 (2003): 8158-8165.

(8) Weinbreck, F., R. De Vries, P. Schrooyen, and C. G. De Kruif. "Complex coacervation of whey proteins and gum arabic." *Biomacromolecules* 4, no. 2 (2003): 293-303.

(9) Antonov, Margarita, Malek Mazzawi, and Paul L. Dubin. "Entering and exiting the protein– **polyelectrolyte coacervate phase via nonmonoto**nic salt dependence of critical conditions." *Biomacromolecules* 11, no. 1 (2009): 51-59.

(10) Spruijt, Evan, Joris Sprakel, Martien A. Cohen Stuart, and Jasper van der Gucht. "Interfacial tension between a complex coacervate phase and its coexisting aqueous phase." *Soft Matter* 6, no. 1 (2010): 172-178.

(11) Winslow, Brent D., Hui Shao, Russell J. Stewart, and Patrick A. Tresco. "Biocompatibility of adhesive complex coacervates modeled after the sandcastle glue of *Phragmatopoma californica* for craniofacial reconstruction.

"*Biomaterials* 31, no. 36 (2010): 9373-9381.

(12) Stewart, Russell J. "Protein-based underwater adhesives and the prospects for their biotechnological production." *Applied Microbiology and Biotechnology* 89, no. 1 (2011): 27-33.

(13) Weinbreck, Fanny, Roland HW Wientjes, Hans Nieuwenhuijse, Gerard W. Robijn, and Cornelus G. de Kruif. "Rheological properties of whey protein/gum arabic coacervates." *Journal of Rheology* 48, no. 6 (2004): 1215-1228.

(14) Kaur, Sarbjit, G. Mahika Weerasekare, and Russell J. Stewart. "Multiphase adhesive coacervates inspired by the Sandcastle worm." *ACS Applied Materials & Interfaces* 3, no. 4 (2011): 941-944.

(15) Mann, Lovepreet K., Ramesha Papanna, Kenneth J. Moise, Robert H. Byrd, Edwina J. Popek, Sarbjit Kaur, Scheffer CG Tseng, and Russell J. Stewart. "Fetal membrane patch and biomimetic adhesive coacervates as a sealant for fetoscopic defects." *Acta biomaterialia* 8, no. 6 (2012): 2160-2165.